JAERI-M
83-002

BASE INPUT FOR LARGE BREAK LOCA ANALYSIS OF COMMERCIAL PWR WITH PUBLISHED VERSION OF THYDE-P1
(THYDE-P1 SAMPLE CALCULATION RUN 21)

January 1983

Masashi HIRANO and Seiji KOSUGI

日 本 原 子 力 研 究 所
Japan Atomic Energy Research Institute

JAERI-M
83-002

BASE INPUT FOR LARGE BREAK LOCA ANALYSIS OF COMMERCIAL PWR WITH PUBLISHED VERSION OF THYDE-P1
(THYDE-P1 SAMPLE CALCULATION RUN 21)

January 1983

Masashi HIRANO and Seiji KOSUGI

日本原子力研究所
Japan Atomic Energy Research Institute

編集兼発行　日本原子力研究所
印　　刷　日立高速印刷株式会社

Base Input for Large Break LOCA Analysis of Commercial PWR with Published Version of THYDE-P1 (THYDE-P1 Sample Calculation Run 21)

by

Masashi HIRANO and Seiji KOSUGI

Division of Nuclear Safety Evaluation
Tokai Research Establishment

(Received January 6, 1982)

This report describes input data to be used with the THYDE-P1 interim version SV02L03, which has been published through NEA DATA BANK in April, 1982, and its calculated results. The input data consist of three input data sets, one is for steady state and the following transients and the other two are for restarting, and they are successively used for a through calculation of a large break loss-of-coolant accident (LOCA) of a 1,100 MWe commercial pressurized water reactor (PWR) with "best estimate" (BE) options. The major purposes to set up the input data are not only to provide users sample data in publishing THYDE-P1 but also to demonstrate the ability of the published version of THYDE-P1 without any modification to perform a through calculation of a large break LOCA. The results from the present calculation will also be widely utilized as a bench mark in performing sensitivity calculations and further code modifications. In this sense, the input can be called a base input for the published version of THYDE-P1.

This report also contains the results from several sensitivity calculations, which show high capability of the version of THYDE-P1 to analyse large break LOCAs.

Keywords : THYDE-P1, LOCA, Large Break, 1,100 MWe Commercial PWR, Through Calculation, Base Input

公開版ＴＨＹＤＥ－Ｐ１による商用ＰＷＲ
大破断ＬＯＣＡ解析用ベースインプット
（ＴＨＹＤＥ－Ｐ１サンプル計算Run21）

日本原子力研究所東海研究所安全解析部
平野　雅司・小杉　誠司

（１９８３年１月６日受理）

１９８２年４月に，ＮＥＡデータ・バンクを通して公開されたＴＨＹＤＥ－Ｐ１コード（SV02L03）用インプットデータ，及びその計算結果を報告する。本インプットデータは，３個のインプットデータセットにより構成され，１個は，定常及びそれに続く過渡計算用で，他の２個は，再スタート用であり，これらのデータセットで，最適評価モデルによる1,１００MWe商用ＰＷＲ大破断冷却材喪失事故（ＬＯＣＡ）の一貫解析を行う。本インプットデータは，ＴＨＹＤＥ－Ｐ１の公開に際して，利用者にサンプルデータを提供すると共に，公開版ＴＨＹＤＥ－Ｐ１の大破断ＬＯＣＡ一貫解析性能を検証する目的で作成された。また，本解析結果は，今後，感度解析や，コードの修正を実施する際のベンチマークとして広範に利用可能である。その意味から，本インプットデータは，公開版ＴＨＹＤＥ－Ｐ１のベースインプットと呼び得る。

また，本報告では，いくつかの感度解析の結果も含まれており，それらは，公開版ＴＨＹＤＥ－Ｐ１の高い解析性能を示している。

Contents

目　　　次

List of Figures

List of Figures (continued)

List of Figures (continued)

List of Tables

1. Introduction

The THYDE-P1 code[1,2] is a computer code to analyse transient thermal-hydraulic responses of pressurized water reactors (PWRs) to postulated loss-of-coolant accidents (LOCAs). Extensive verification calculations[3-9] have been performed so far and the THYDE-P1 interim version SV02L03 has been published through NEA DATA BANK in April, 1982.

A through calculation of a large break LOCA of a 1,100 MWe 4-loop commercial PWR has been carried out using the published version of THYDE-P1 without any modification not only to provide a complete set of input data being called a base input, which is used as sample data for published THYDE-P1, but also to demonstrate the ability of the code to analyse large break LOCAs. This report contains the description of the set of input data, the base data, and the results from the calculation. The base data consist of three input data sets. The first data set is used for the steady state and the following blowdown analysis until 15 sec and the second and the third data sets are used for restarting from 15 sec until 30 sec and from 30 sec to the end of the problem, respectively. The second and the third data sets are the same except the input data for the time constants of the relaxation model[4-9].

The base input data have been made based on those used in Sample Calculation Run 20[4], which is one of a series of THYDE-P1 verification calculations, where the plant geometrical data are almost identical with the RELAP4/MOD5 sample problem[10]. The present calculation has been performed also as Sample Calculation Run 21. The major models and assumptions applied in Run 21 are summarized as follows:

(1) Double-ended guillotine break at the cold leg,
(2) Discharge coefficient 0.6,
(3) Pump coastdown just after rupture,
(4) "Best estimate" (BE) calculation, and
(5) Two core channel calculation with a single cross flow.

This report also contains the results from several sensitivity calculations using the data which deviates from the base data with respect to pump condition, CHF correlations and a minimum stable film boiling temperature (MSFBT) correlation, for the sake of future usability. As for the MSFBT correlation, a model has been tentatively developed and studied. The calculated results from the pump on and off of a commercial PWR are shown to be qualitatively consistent with the experimental results from LOFT large break experiments L2-3(11) and L2-5(12,13). By applying the present MSFBT model, the history of the cladding surface temperature at high elevation during the reflooding is shown to be markedly improved.

2. Description of Base Input Data

2.1. Usage of Base Input Data

The THYDE-P1 input requirement has been described in detail in Ref.2). There are two kinds of input data sets in THYDE-P1. One is for starting from an initial steady state and another is for restarting from a restart dump point in a previous run. In the base data, the data for restarting are further divided into two data sets. Therefore the base data for the published version of THYDE-P1 consist of three data sets named Data 1, Data 2 and Data 3 :

(1) The first data set Data 1 is used for the steady state and the following blowdown until 15 sec,
(2) The second data set Data 2 is used for restarting from 15 sec to 30 sec, and
(3) The third data set Data 3 is used for restarting from 30 sec to the end of the problem (250 sec).

In the first data set Data 1, the relaxation model for density change is not taken into account for any nodes and mixing junctions. Therefore, an equilibrium model is applied during the period. In the second data set Data 2, the relaxation model is firstly taken into account in order to avoid the large pressure drop due to very rapid vapor condensation at the duct nodes near the ECC injection points. The time constants τ_Ds are set in Data 2 to be 4 sec for the ECC duct nodes and the cold leg nodes from 15 sec after rupture. In Data 3, those for the downcomer and lower plenum nodes are set to be 40 sec and those for the core nodes and upper plenum node are set to be 4 sec and 40 sec, respectively, from 30 sec after rupture. The input data sets Data 1, Data 2 and Data 3 are listed in Appendix A.

2.2. Input Data Presentation

The input data of THYDE-P1 Sample Calculation Run 21, the base data, are made based on those used in THYDE-P Sample Calculation Run 20[4]. The major parts of them are summarized in this subsection.

A nodalization scheme in the present calculation is shown in Fig.2-1. The main parts of the plant are expressed by the following nodes:

Average core channel	Nodes 23 to 28
Hot core channel	Nodes 29 to 34
Lower plenum	Node 22
Upper plenum	Node 37
Downcomer	Node 21
S.G. Secondary	Nodes 46 and 47
Accumulator	Nodes 48 and 49
Pressurizer	Node 45
Upperhead	Node 38.

The geometrical data and loss coefficients for each node are shown in Tables 2-1 and 2-2, respectively.

(1) Steam Generator Data

U-tube pitch	3.0×10^{-2} m
Number of U-tubes of one unit	3265
Initial secondary system pressure	62atm
Initial specific enthalpy of feedwater	222 kcal/kg
Initial feedwater mass flow rate	474.0 kg/sec
Initial subcooled water level	4.0 m
Initial void fraction of saturated region	0.95

Initial heat flux

Node No.	Heat flux (kcal/m.sec)
14	65.65
15	49.24
16	41.03

The feedwater is assumed to be shut off at 0.4 sec after LOCA initiation.

(2) Core Data

The core is divided radially into two channels, i.e. an average channel and a hot bundle average channel. The radial peaking factor of the hot channel is assumed to be a value of 1.30. The input data are shown as follows:

Initial heat flux and number of fuel rods

	Hot channel region		Average channel region	
	node no.	heat flux (kcal/m.sec)	node no.	heat flux (kcal/m.sec)
initial heat flux	29	non-heated	23	non-heated
	30	203.0	24	156.0
	31	304.0	25	234.0
	32	304.0	26	234.0
	33	203.0	27	156.0
	34	non-heated	28	non-heated
number of rod	200		39170	

Reactor thermal power	3,479 MWt
Fuel length	3.66 m
Plenum gas volume	1.235×10^{-5} m
Clad outer diameter	1.0732×10^{-2} m
Clad thickness	6.187×10^{-4} m
Pellet diameter	9.3146×10^{-3} m
Fuel rod pitch	1.42×10^{-2} m,

where the last four values are those at a full power operating condition.

(3) Pressurizer Data

Cross-sectional area 3.58 m

Height	15.56 m
Stand pipe length	0.1 m
Initial subcooled water level	9.0 m
Initial void fraction of saturated region	0.99

(4) ECCS Data

Accumulator data

Initial water volume	23.3 m
Initial nitrogen volume	10.0 m
Specific enthalpy of water	30 kcal/kg
Initial pressure	44 atm

Pumped injection data

Specific enthalpy of water	30 kcal/kg for each loop
Mass flow rate	220 kg/sec for each loop

(5) Container pressure

Time(sec)	0.0	7.5	15.0	30.0	1000.0
Pressure(atm)	1.0	2.7	4.0	4.0	4.0

(6) Time constants of relaxation model for density change

After 15 sec:
4 sec for the duct nodes 7, 8, 9, 10, 18, 19, 20, 41, 42, 43 and 44, and
4 sec for all the mixing junctions.

After 30 sec:
40 sec for the nodes 8, 21(downcomer), 22(lower plenum) and 37(upper plenum),
4 sec for all the core nodes 23 to 36, and
10 sec for all the other nodes and all the mixing junctions.

2.3. Deviation from Run 20

The deviation of the base input data from those used in Run 20 is summarized in this subsection.

(1) The values of diameter and length for pump nodes are modified in order to avoid the large pressure drops at the pump nodes during the early stage of the blowdown.

(2) The temperature coefficients in the reactivity data BB17 of the sample calculation Run 20 are greater by a factor of about twenty than those of the RELAP4/MOD5 sample problem(10). These data are revised based on the RELAP4/MOD5 sample problem.

(3) The pump trip index is altered from pump rotor locking into pump coastdown.

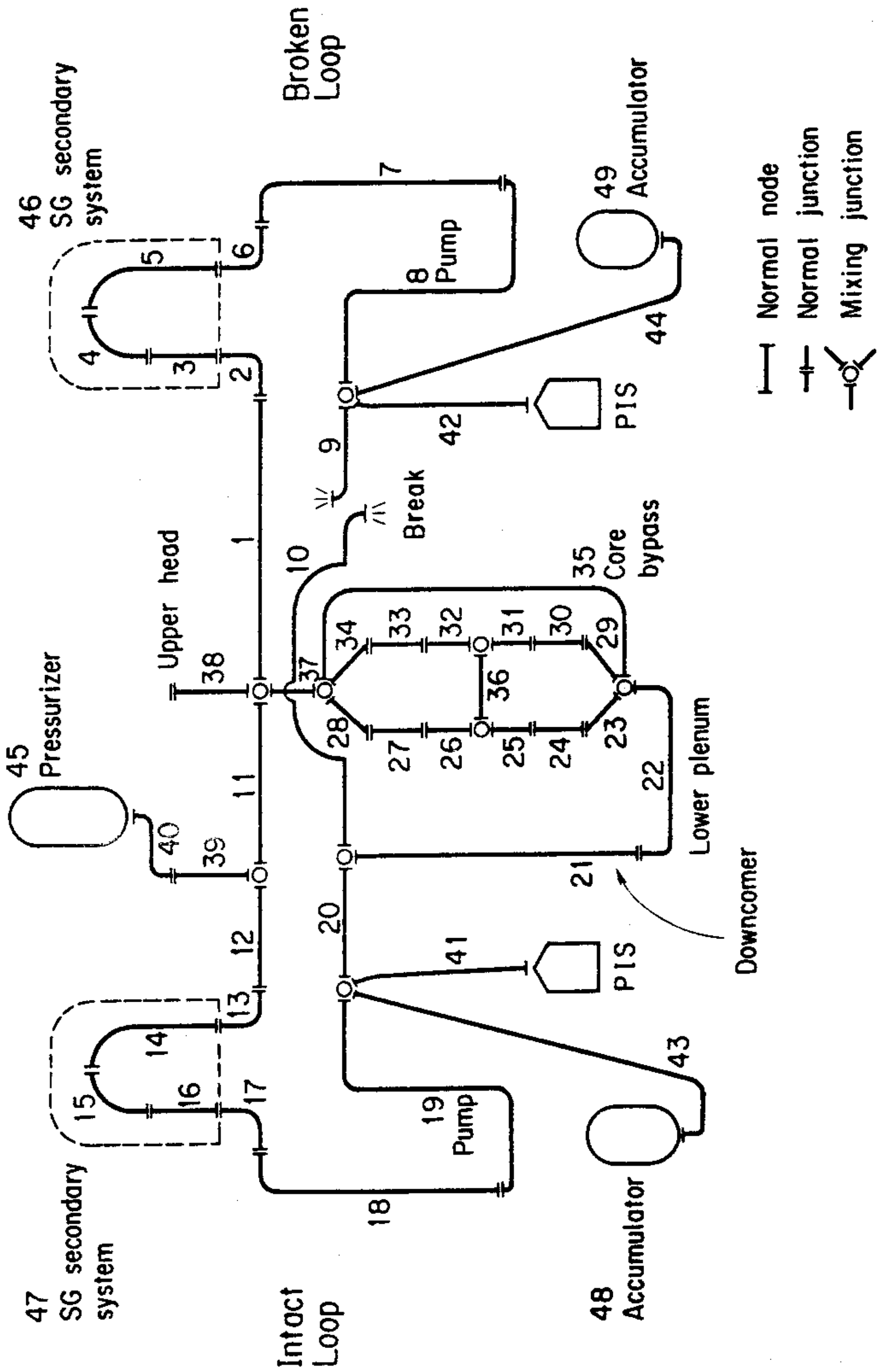

Fig.2-1 Nodalization of base input data

Table 2-1 **Node geometrical data**

Node No.	Description	Flow Area A (m^2)	Node Length L (m)	Node Volume V (m^3)
1	Broken loop hot leg	0.4266	5.240	2.235
2	SG inlet plenum	2.8953	1.665	4.821
3	SG U-tube	0.9952	5.000	4.976
4	SG U-tube	0.9952	5.460	5.434
5	SG U-tube	0.9952	10.460	10.410
6	SG outlet plenum	2.8953	1.665	4.821
7	Broken loop cold leg	0.4865	7.340	3.571
8	Pump	0.4266	12.412	2.379
9	Broken loop cold leg	0.3837	2.825	1.084
10	Broken loop cold leg	0.3837	3.130	1.201
11	Intact loop hot leg	1.2798	2.000	2.560
12	Intact loop hot leg	1.2798	3.240	4.147
13	SG inlet plenum	8.6859	1.665	14.462
14	SG U-tube	2.9856	5.460	14.928
15	SG U-tube	2.9856	5.460	16.301
16	SG U-tube	2.9856	10.460	31.229
17	SG outlet plenum	8.6859	1.665	14.462
18	Intact loop cold leg	1.4594	7.340	10.712
19	Pump	0.5750	12.412	7.137
20	Intact loop cold leg	1.2798	5.955	6.855
21	Downcomer	2.7435	7.248	19.885
22	Lower plenum	4.8578	6.075	29.511
23	non-Active core in average	4.3552	0.230	1.002
24	Active core in average	4.3552	0.800	3.484
25	Active core in average	4.3552	0.800	3.484
26	Active core in average	4.3552	0.800	3.484
27	Active core in average	4.3552	0.800	3.484
28	non-Active core in average	4.3552	0.230	1.002
29	non-Active core in hot	0.0222	0.230	5.11-3
30	Active core in hot	0.0222	0.800	1.78-2
31	Active core in hot	0.0222	0.800	1.78-2
32	Active core in hot	0.0222	0.800	1.78-2
33	Active core in hot	0.0222	0.800	1.78-2
34	non-Active core in hot	0.0222	0.230	5.11-3
35	Core bypass	0.2419	3.660	0.885
36	Core cross area	9.079-4	0.100	9.08-5
37	Upper plenum	9.2941	4.341	40.346
38	Upper head	3.8568	3.658	14.108
39	Pressurizer surge line	0.0661	15.00	0.992
40	Pressurizer surge line	0.0661	14.30	0.945
41	Pumped injection duct	0.2192	12.00	2.630
42	Pumped injection duct	0.0731	12.00	0.877
43	Accumulator duct	0.1161	120.00	13.932
44	Accumulator duct	0.0387	120.00	4.644

Table 2-2 Loss coefficients of nodes

Node No.	K	K^{Af}	K^{Ar}	K^{Ef}	K^{Er}
1	0.023	0.043	0.084	0.0	0.0
2	0.021	3.73	1.97	0.0	0.0
3	0.011	0.033	0.048	0.0	0.0
4	0.008	0.0	0.0	0.0	0.0
5	0.017	0.0	0.0	0.033	0.048
6	0.030	0.0	0.0	3.73	1.97
7	0.019	0.042	0.077	0.0	0.0
8	0.303	0.273	0.367	0.203	0.203
9	3.958	0.055	0.015	0.0	0.0
10	0.019	0.0	0.0	0.0	0.0
11	0.024	0.043	0.083	0.0	0.0
12	0.028	0.0	0.0	0.0	0.0
13	0.013	3.73	1.97	0.0	0.0
14	0.025	0.033	0.048	0.0	0.0
15	0.021	0.0	0.0	0.0	0.0
16	0.027	0.0	0.0	0.033	0.048
17	0.029	0.0	0.0	3.73	1.97
18	0.022	0.042	0.077	0.0	0.0
19	3.961	0.055	0.015	0.203	0.203
20	0.011	0.0	0.0	0.0	0.0
21	1.032	0.0	0.0	0.0	0.0
22	1.398	0.0	0.0	0.0	0.0
23	6.416	0.74	0.74	0.0	0.0
24	6.161	0.0	0.0	0.0	0.0
25	6.072	0.0	0.0	0.0	0.0
26	6.218	0.0	0.0	0.0	0.0
27	6.045	0.0	0.0	0.0	0.0
28	6.737	0.0	0.0	0.0	0.0
29	5.295	1.284	2.482	0.0	0.0
30	5.642	0.0	0.0	0.0	0.0
31	5.570	0.0	0.0	0.0	0.0
32	5.574	0.0	0.0	0.0	0.0
33	4.662	0.0	0.0	0.0	0.0
34	6.104	0.76	0.34	0.0	0.0
35	47.857	0.77	0.83	0.87	0.78
36	12.354	0.0	0.0	0.0	0.0
37	2.08-2	0.0	0.0	0.0	0.0
38	5.0	1.491+4	1.491+4	0.0	0.0
39	5.0	0.41	0.87	0.0	0.0
40	5.0	0.0	0.0	0.0	0.0
41	10.0	0.0	0.0	0.0	0.0
42	10.0	0.0	0.0	0.0	0.0
43	10.0	0.109	0.049	0.0	0.0
44	10.0	0.109	0.049	0.0	0.0

3. Results and Discussions from Base Calculation, Run 21

In this section, the calculated results from Run 21 are presented along with the brief discussions on them. The chronology of events is shown in Table 3-1. The other calculated results from Run 21 than those shown in this section are presented in Appendix B without explanation.

3.1. Pressure Transient

The pressures calculated at pressurizer and the intact loop hot leg are shown in Fig. 3-1-1. The hot leg pressure shows that the end of blowdown is about 30 sec after rupture. The calculated SG primary system and secondary system pressures of the intact and broken loop loops are shown in Figs. 3-1-2 and 3-1-3, respectively. As shown in these figures, the maximum pressure at the SG secondary system of the broken loop is higher than that of the intact loop and the depressurization rate of the SG secondary system is also higher in the broken loop than in the intact loop.

3.2. Fuel and Core

The calculated cladding surface temperatures of the average and hot channels are shown in Figs. 3-2-1 and 3-2-2, respectively. The fuel center temperatures are presented in Figs. 3-2-3 and 3-2-4. Rewetting phenomenon during the early portion of the blowdown observed in the LOFT large break experiments(11) is calculated to occur only at the bottom of the core as shown in Figs. 3-2-1 and 3-2-2. The cladding surface temperature at the middle of the hot channel reaches a peak at about 50 sec during the very early stage of the reflooding, and then rapidly decreases owing to the effects of ECC water. The mass fluxes at the core inlet and outlet are shown in Figs. 3-2-5 and 3-2-6, respectively. From the figures, it is found that the core flow has large effects on the behavior of the cladding surface temperature. The core flow becomes almost stagnant at 30 sec and then the surface temperatures increase gradually until the reflooding begins. After the reflooding starts, the core nodes become successively quenched from the lower part to the upper one. The quenching in the hot channel is delayed in comparison with the average channel. The time when all the core nodes in the average channel become quenched is about 170 sec and in the case of the hot channel the time is about 230 sec. The behavior of the cladding surface temperature in the uppermost node seems to be unrealistic in that the quench does not occur even when the surface temperature decreases below 300 C. This point will be discussed later in Subsec. 4.3 .

The histories of the calculated heat transfer coefficients at the average and hot channels are shown in Figs.3-2-7 and 3-2-8, respectively.

3.3. Downcomer and Lower Plenum

Figure 3-3-1 shows the mass fluxes at the inlet and the outlet of the downcomer. At about 47 sec, ECC water begins to enter into the downcomer and after that the flows remain almost positive. The calculated equilibrium densities at the downcomer and the lower plenum are shown in Fig. 3-3-2. It shows that the equilibrium states at the downcomer and the lower prelum become subcooled almost simultaneously at about 50 sec. Fig. 3-3-3 shows the differential pressure through the downcomer, which indicates the collapsed water level of the node. The figure shows the non-equilibrium mixture density of the downcomer gradually approaches to the equilibrium value according to the relaxation model. The time when the downcomer is actually filled with subcooled water is about 200 sec after rupture.

3.4. Break

The histories of the break pressures are presented in Figs. 3-4-1. Figures 3-4-2 and 3-4-3 show the break flows of the hot leg side and the cold leg side, respectively. Figure 3-4-4 shows the equilibrium coolant qualities at the break points. The Figures 3-4-2 and 3-4-3 indicate that the hot leg side of the break flow remains positive throughout the problem. At the hot leg side, on the other hand, the reverse flow occurs twice at about 70 sec and 110 sec, which is due to the rapid system depressurization caused by ECC injection.

3.5. ECC Injection

The mass fluxes and coolant temperatures at the ECC ducts are shown in Figs. 3-5-1 and 3-5-2, respectively. The accumulator at the intact loop is actuated at about 15 sec and terminated at about 70 sec. The pumped injections to the intact and broken loops are actuated by trips at about 25 sec simultaneously with a constant mass flow rate of 220 kg/sec.

3.6. Reflooding

The calculated differential pressure through the core is shown in Fig. 3-6-1. The figure shows that the total amount of mass accumulation in the core increases rather rapidly during the early portion of the reflooding but decreases or remains almost constant during the later portion. The calculated differential pressures through the intact loop, through the SG side of the broken loop and through the vessel side of the broken loop are shown in Figs. 3-6-2, 3-6-3 and 3-6-4, respectively. Differential pressures through the intact loop and the broken loop (hot leg side) have similar trends to each other but the former is larger than the latter. The reason is that the mass flow rate through the broken loop is higher than that through the intact loop especially during the early portion of the reflooding as shown in Fig. 3-6-5.

The reason for the negative values of the differential pressure through the vessel side of the broken loop cold leg (see Fig. 3-6-4) is that the reverses flows are calculated to occur due to the system depressurization.

Table 3-1 Chronology of events

Time (sec)	Events
0.01	Rupture took place.
0.01	Pumps were tripped off.
0.15	Voiding started at top of hot channel.
0.22	Voiding started at intact loop hot leg.
0.3	Voiding started at upperhead.
0.4	SG feed waters were tripped off.
3.5	Voiding started at lower plenum.
9.0	Accumulator injection to broken loop started.
16.0	Accumulator injection to intact loop started.
22.0	Pressurizer emptied.
22.5	Pumped injections started by trips.
47.0	ECC water started to penetrate downcomer(end of bypass).
48.0	Reflooding started(bottom of core recovery).
63.0	Accumulator injection to broken loop ended.
66.0	Accumulator injection to intact loop ended.
170.0	Reflooding ended at average channel.
230.0	Reflooding ended at hot channel.

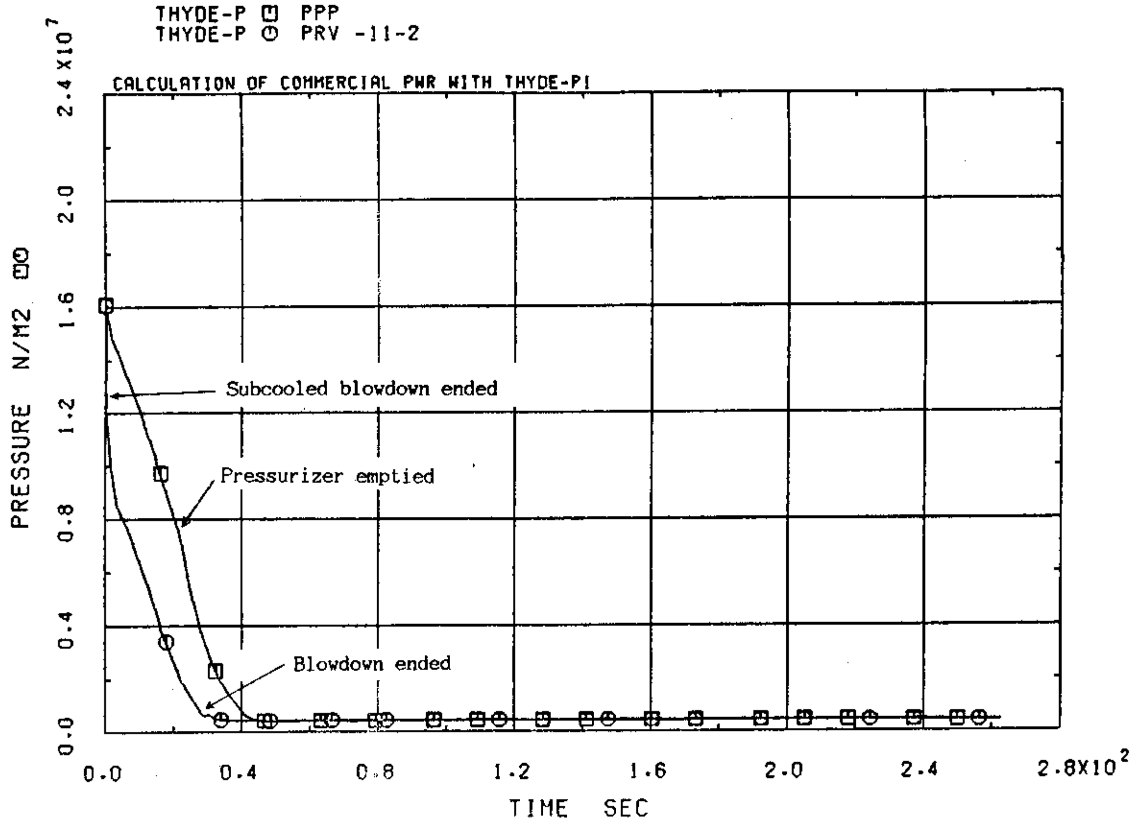

Fig.3-1-1 Intact loop hot leg and pressurizer pressures

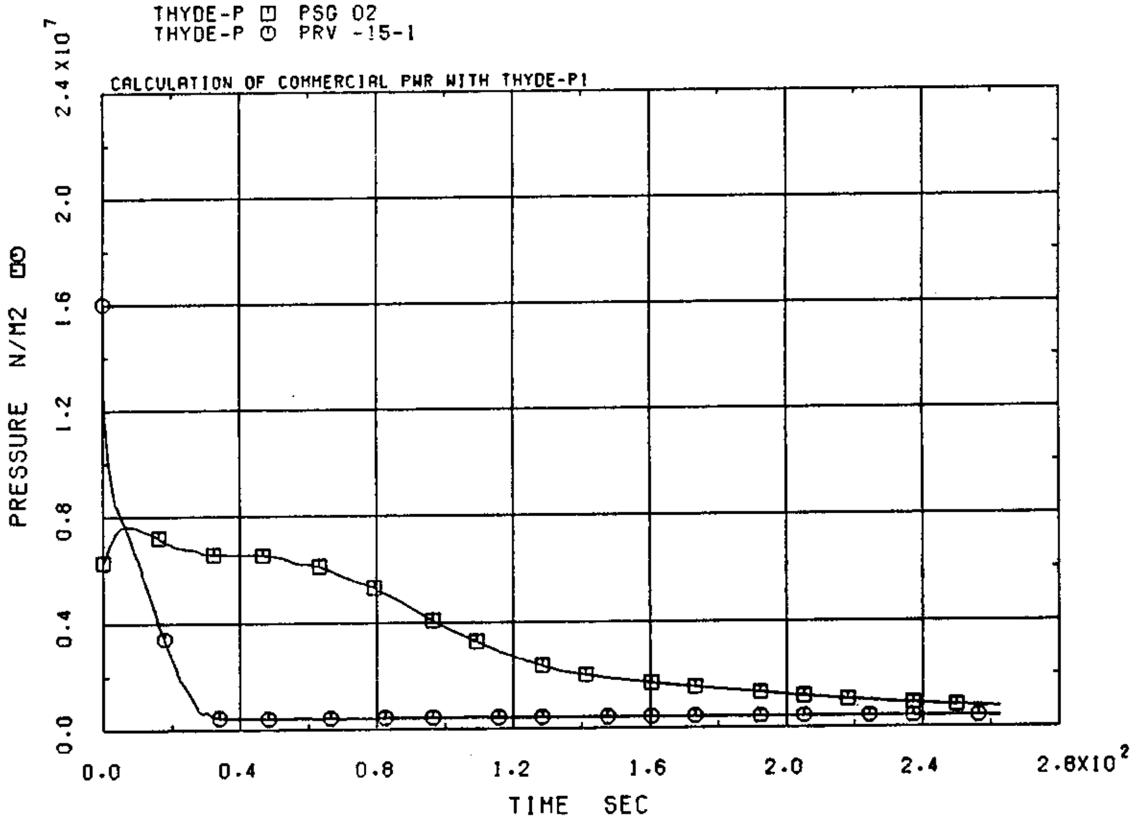

Fig.3-1-2 SG primary and secondary pressures at intact loop

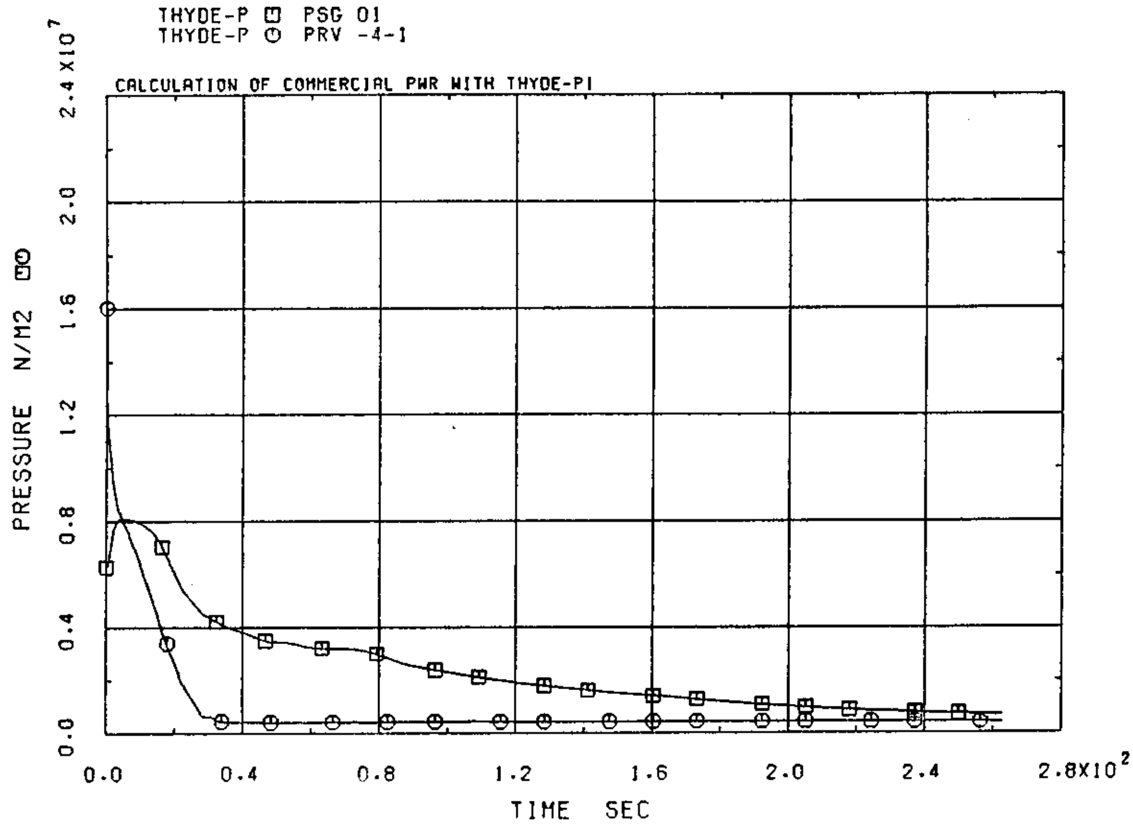

Fig.3-1-3 SG primary and secondary pressures at broken loop

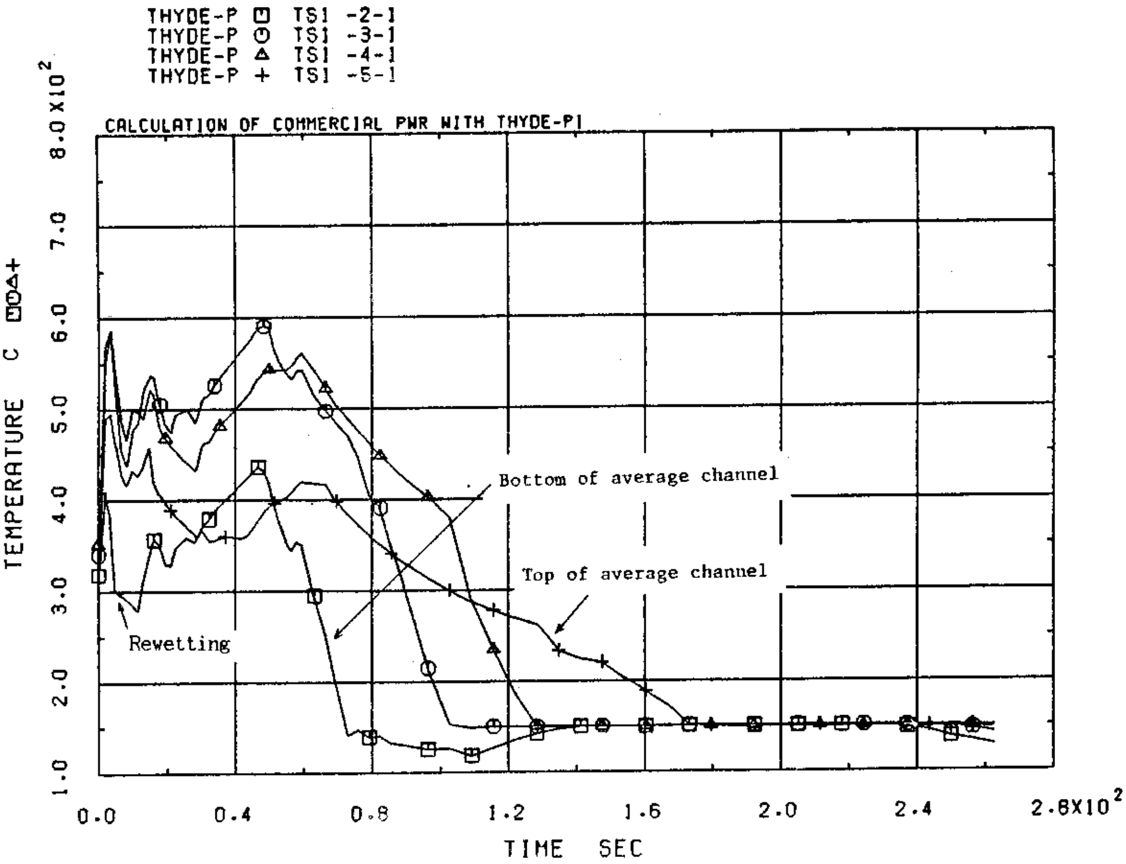

Fig.3-2-1 Cladding surface temperatures in average channel

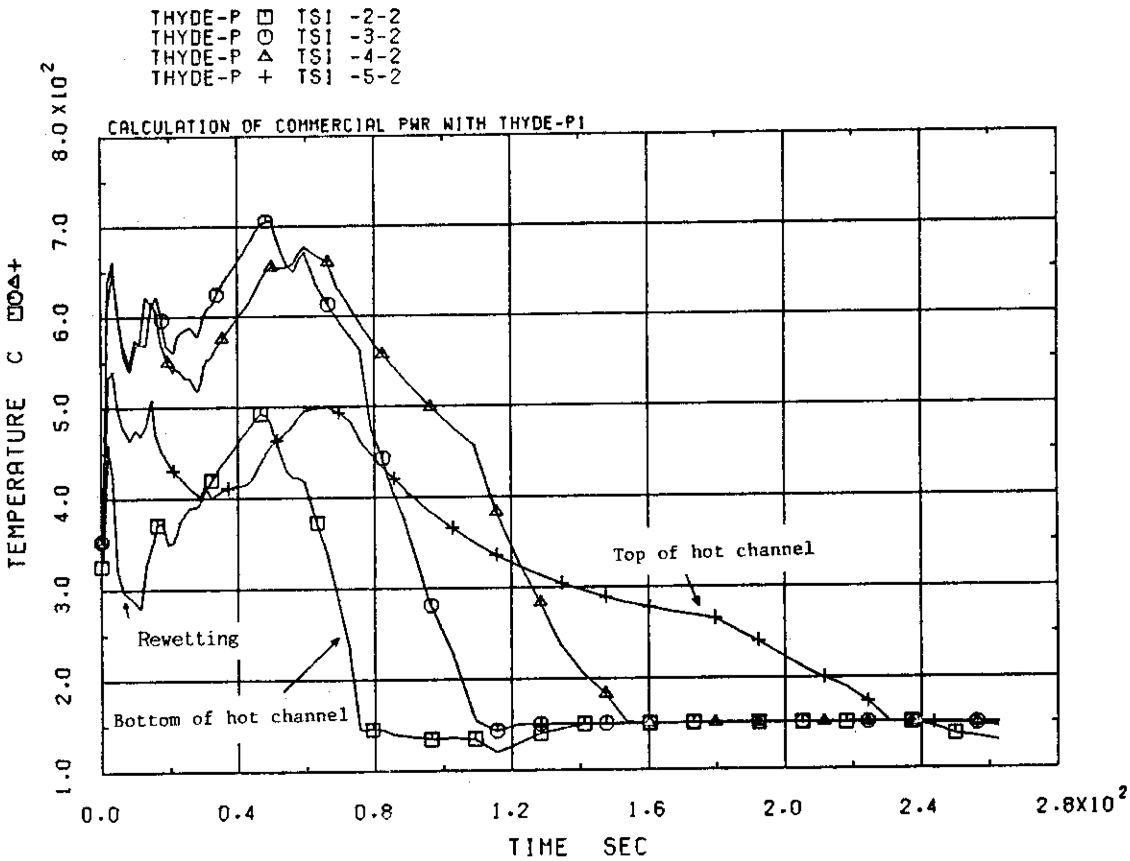

Fig.3-2-2 Cladding surface temperatures in hot channel

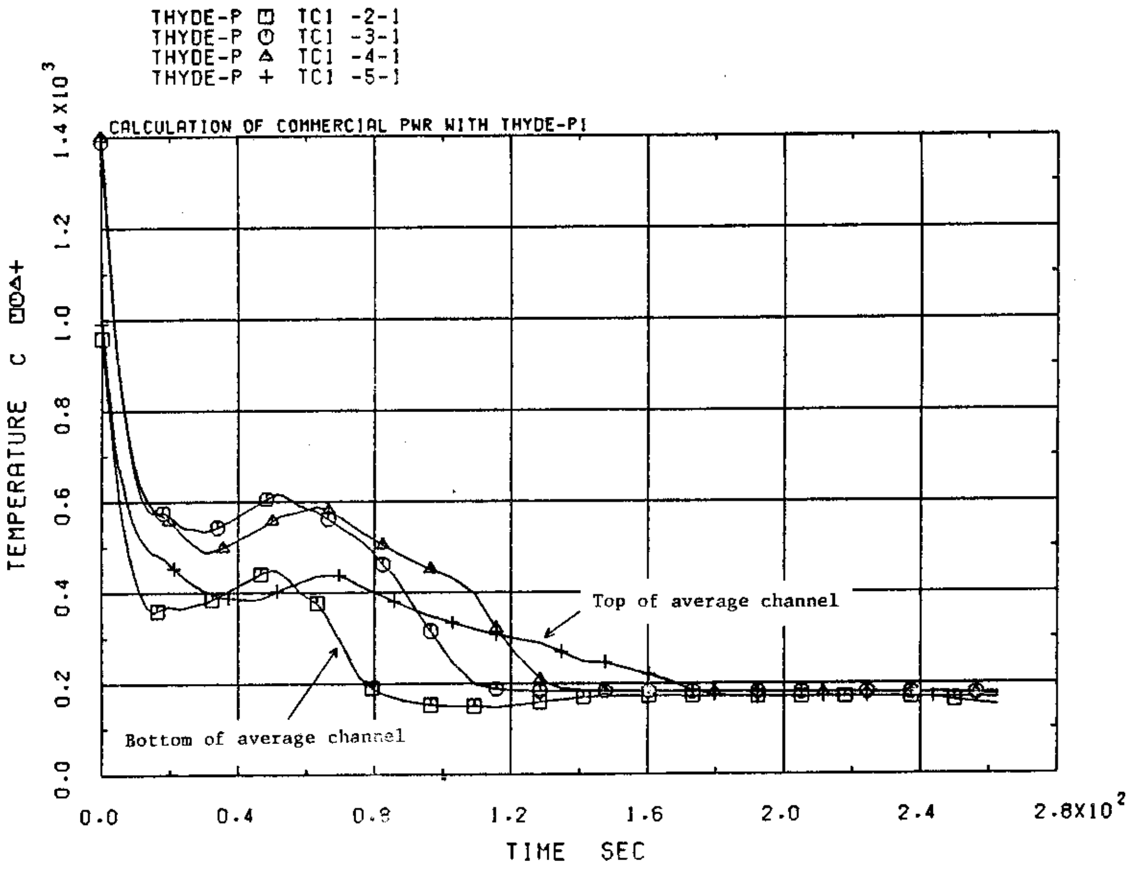

Fig.3-2-3 Fuel centre temperatures in average channel

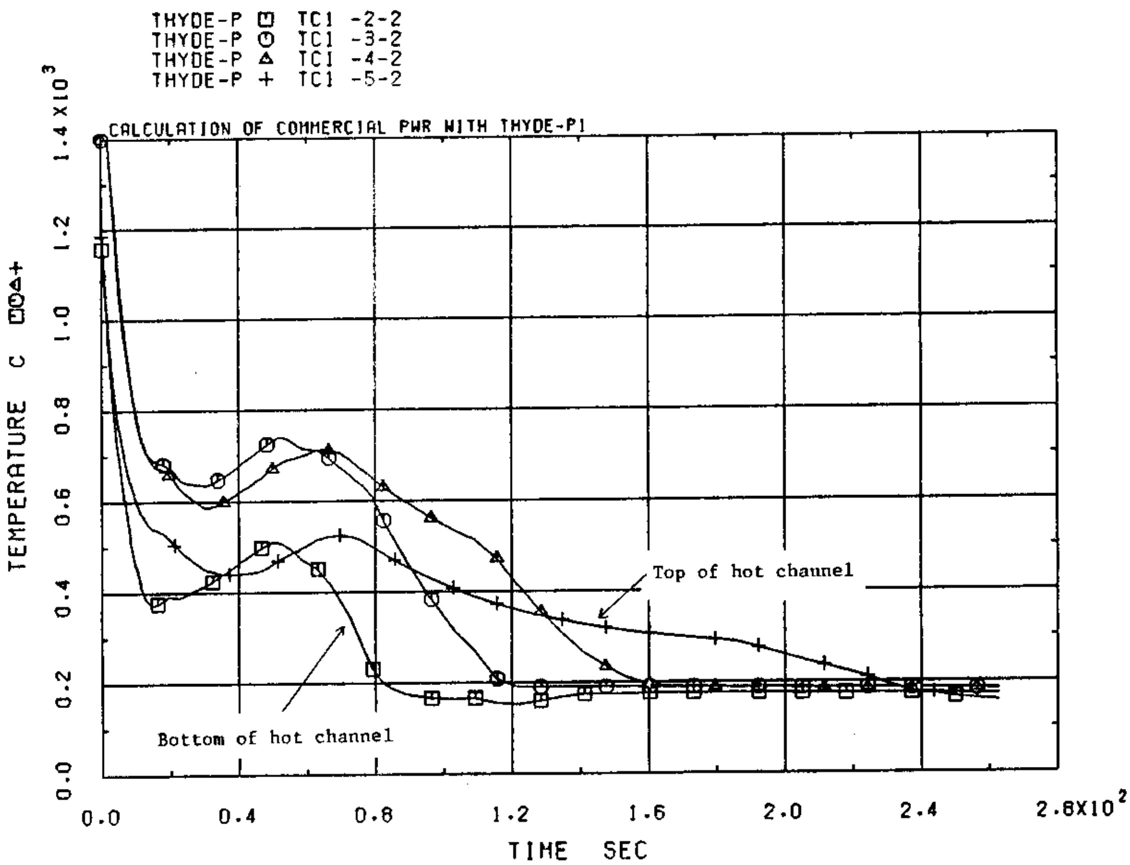

Fig.3-2-4 Fuel centre temperatures in hot channel

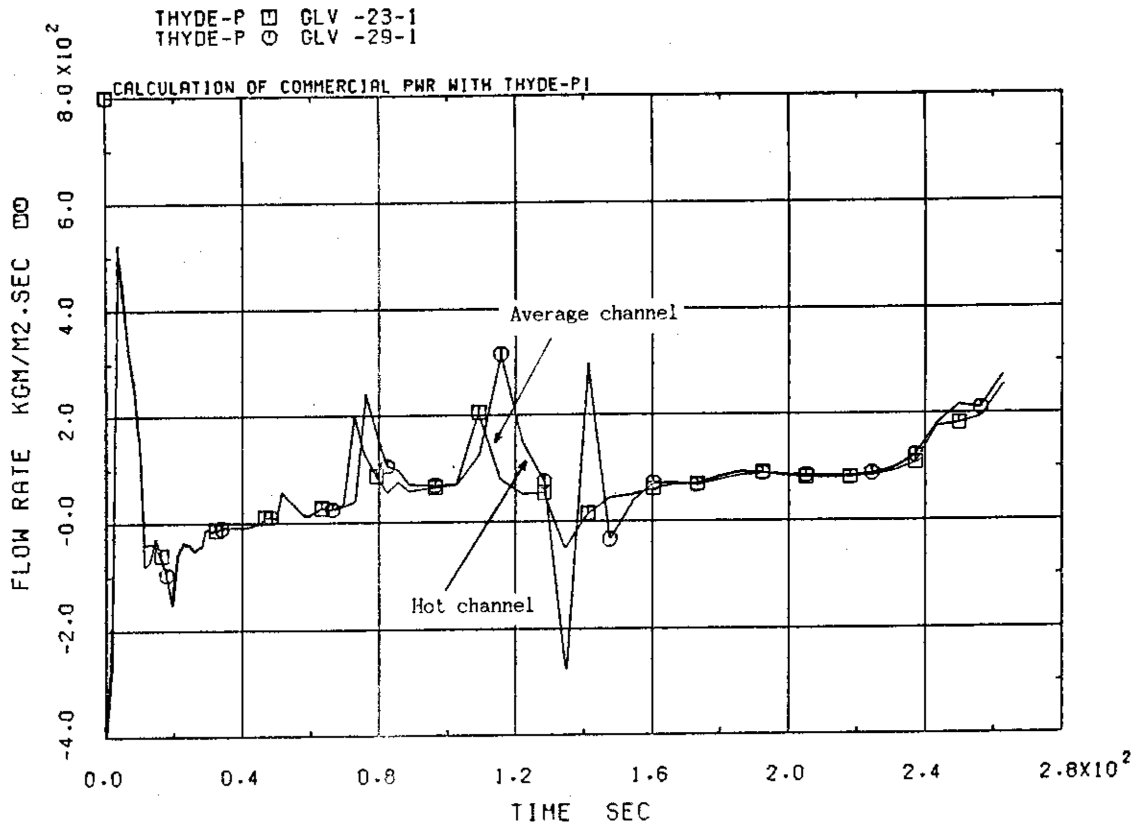

Fig.3-2-5 Core inlet flows

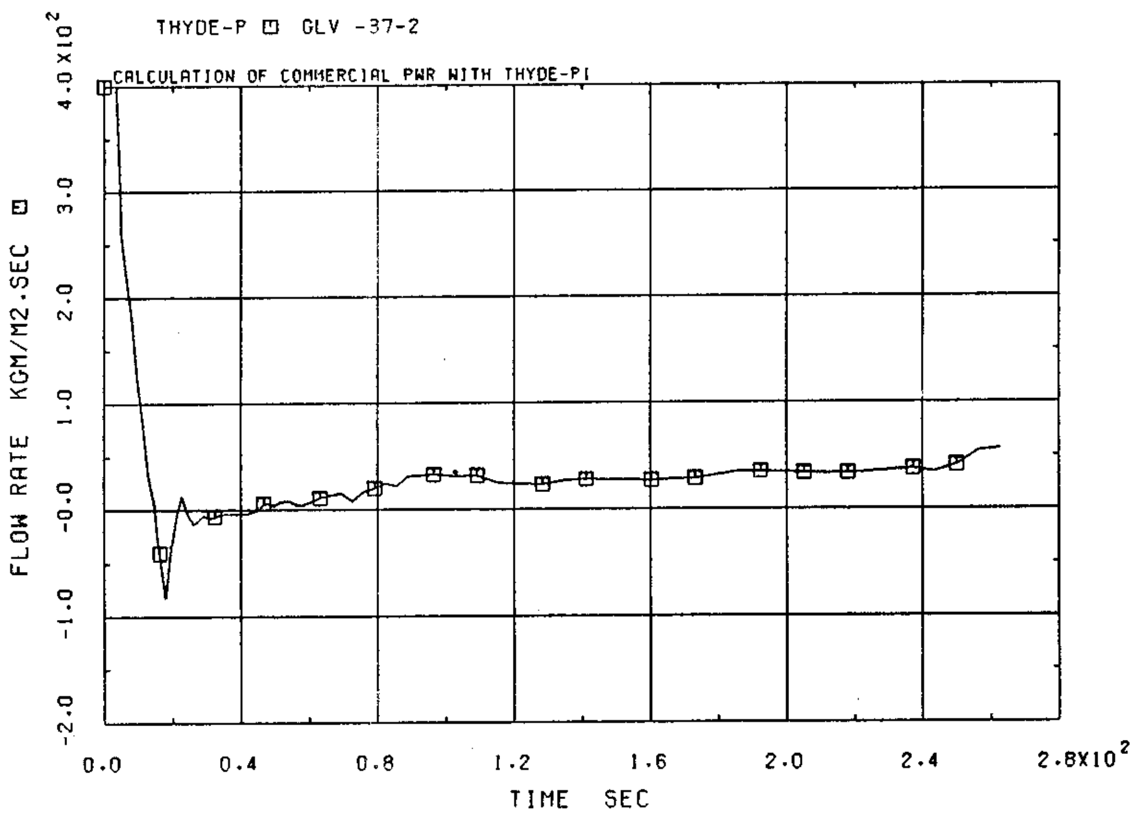

Fig.3-2-6 Core outlet flow

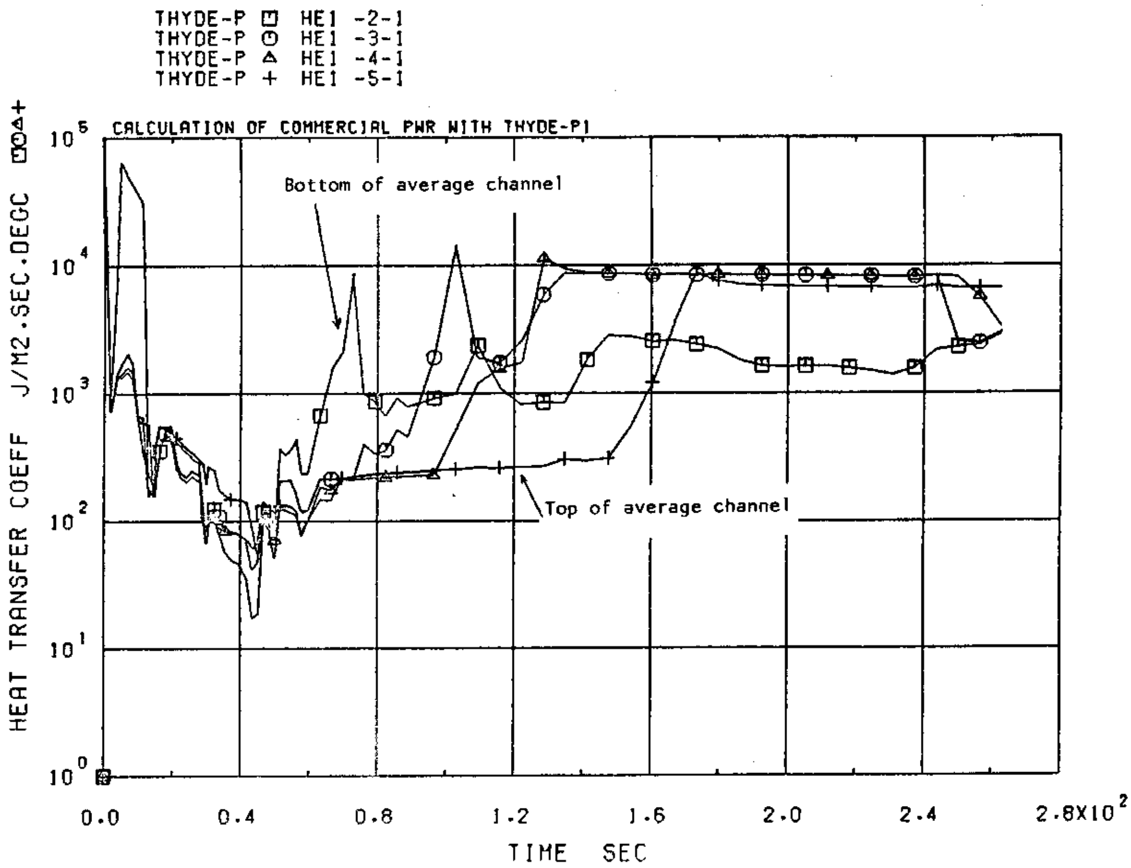

Fig.3-2-7 Heat transfer coefficients in average channel

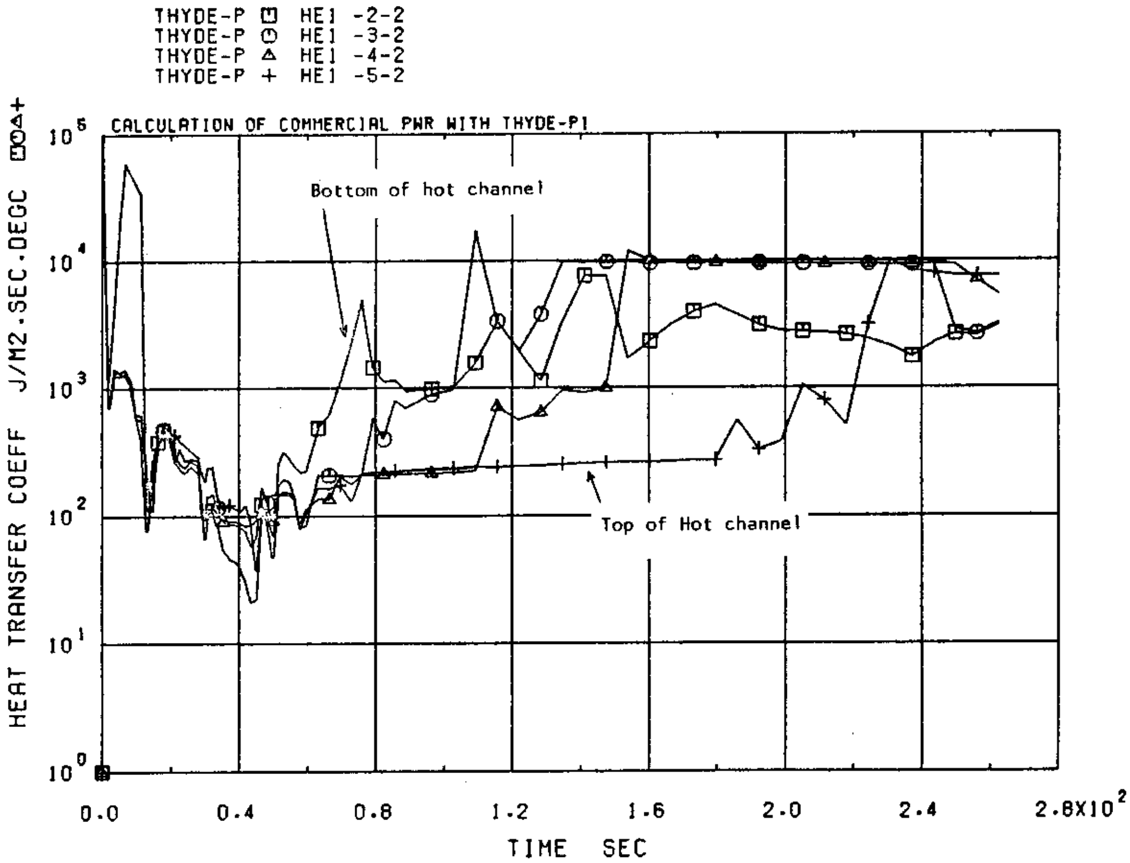

Fig.3-2-8 Heat transfer coefficients in hot channel

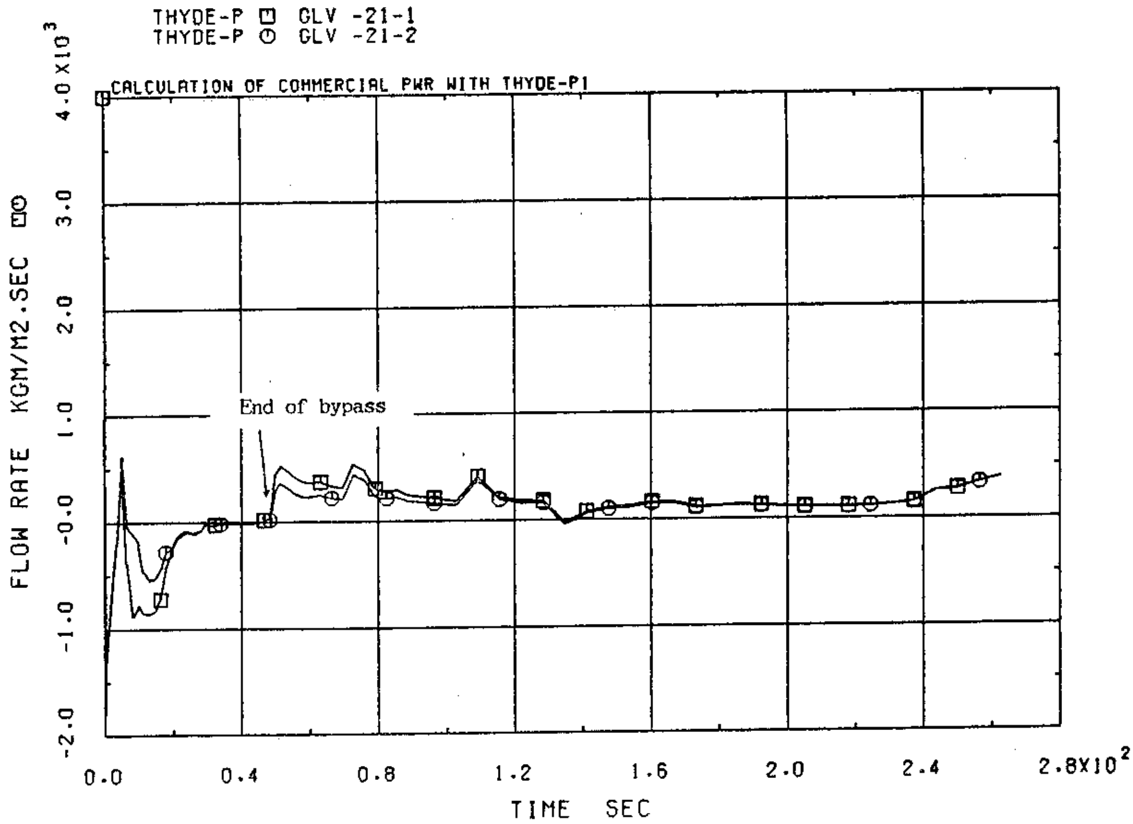

Fig.3-3-1 Mass fluxes at inlet and outlet of downcomer

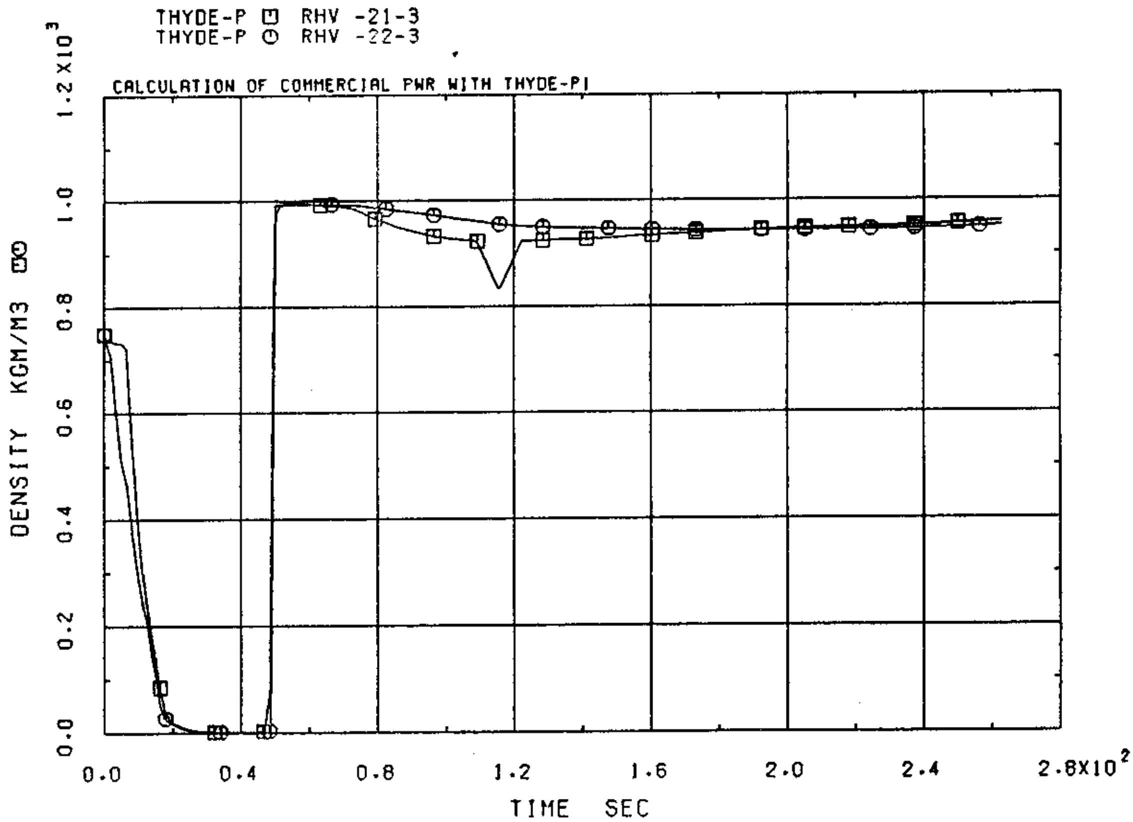

Fig.3-3-2 Equilibrium node average densities at downcomer and

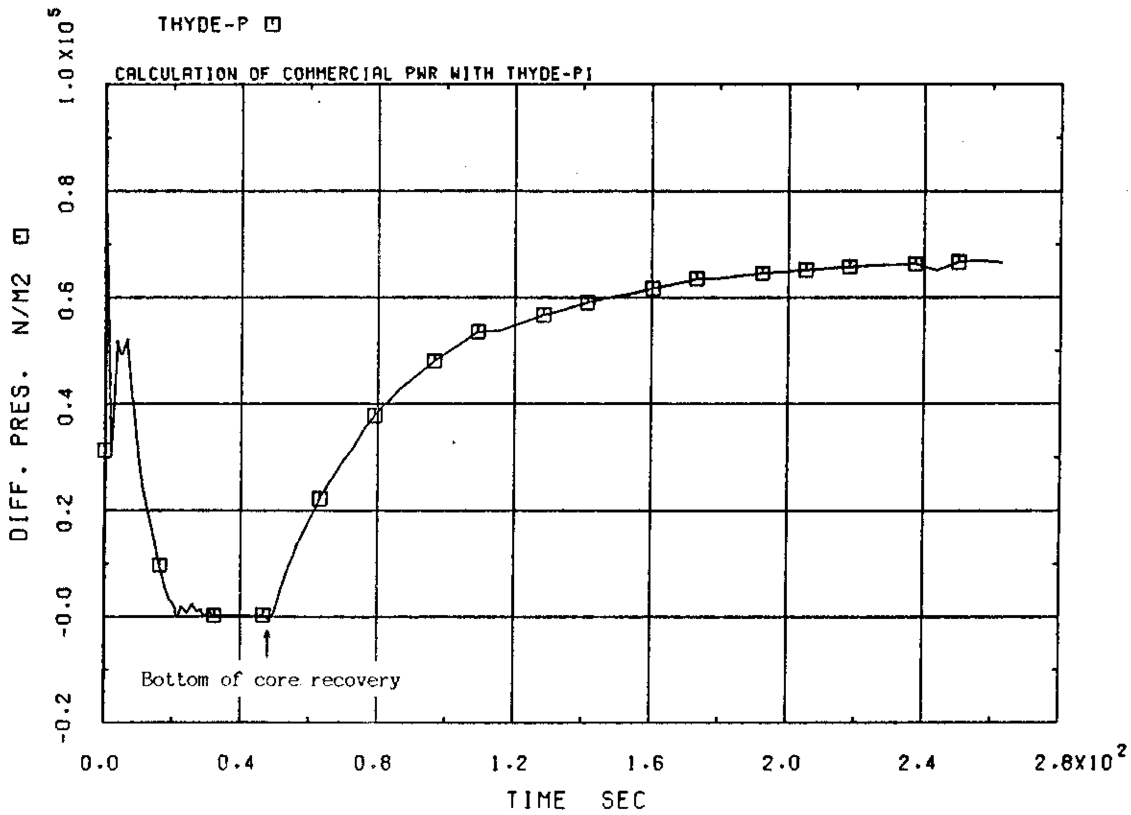

Fig.3-3-3 Differential pressure through downcomer

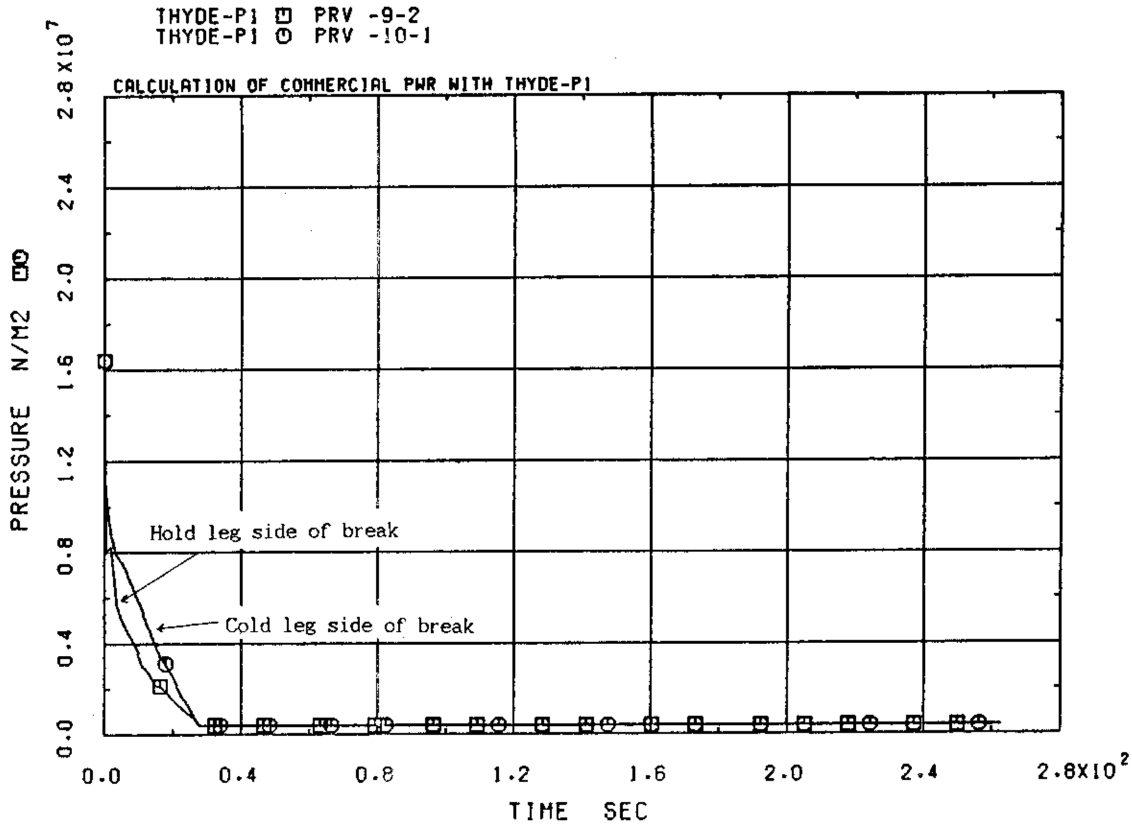

Fig.3-4-1 Pressures at break point

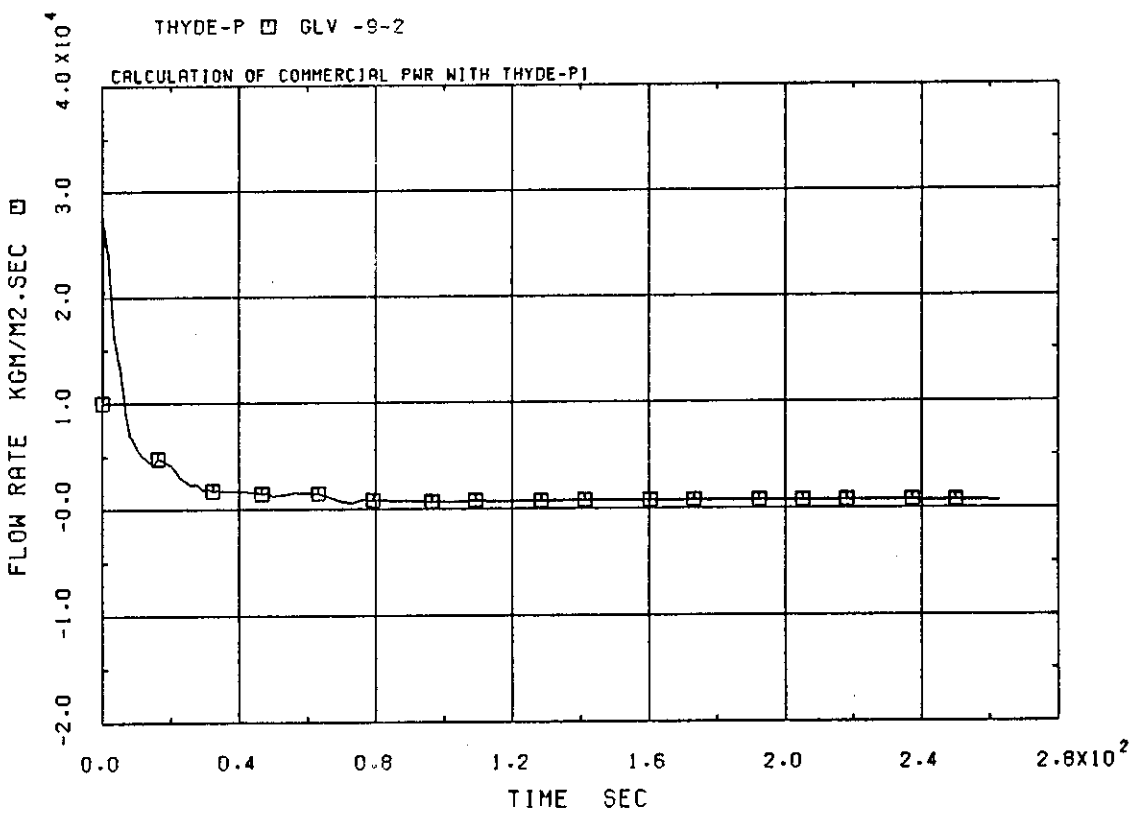

Fig.3-4-2 Hot leg side of break flow

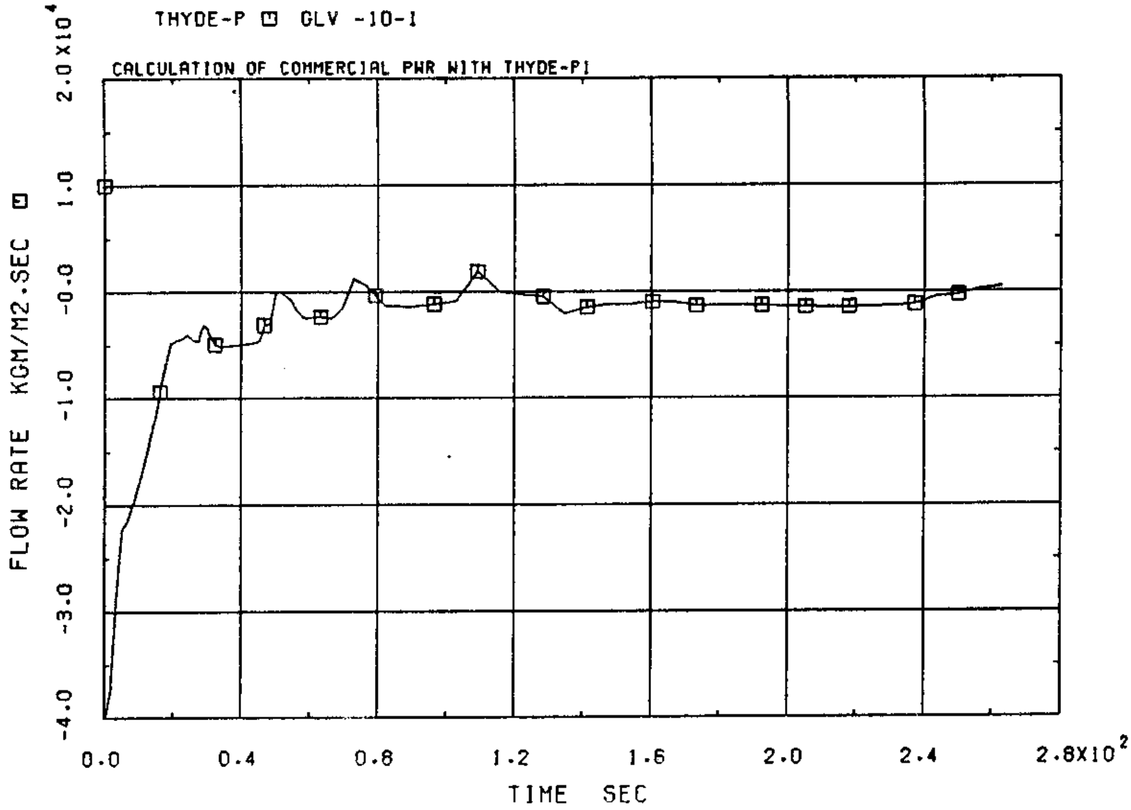

Fig.3-4-3 Cold leg side of break flow

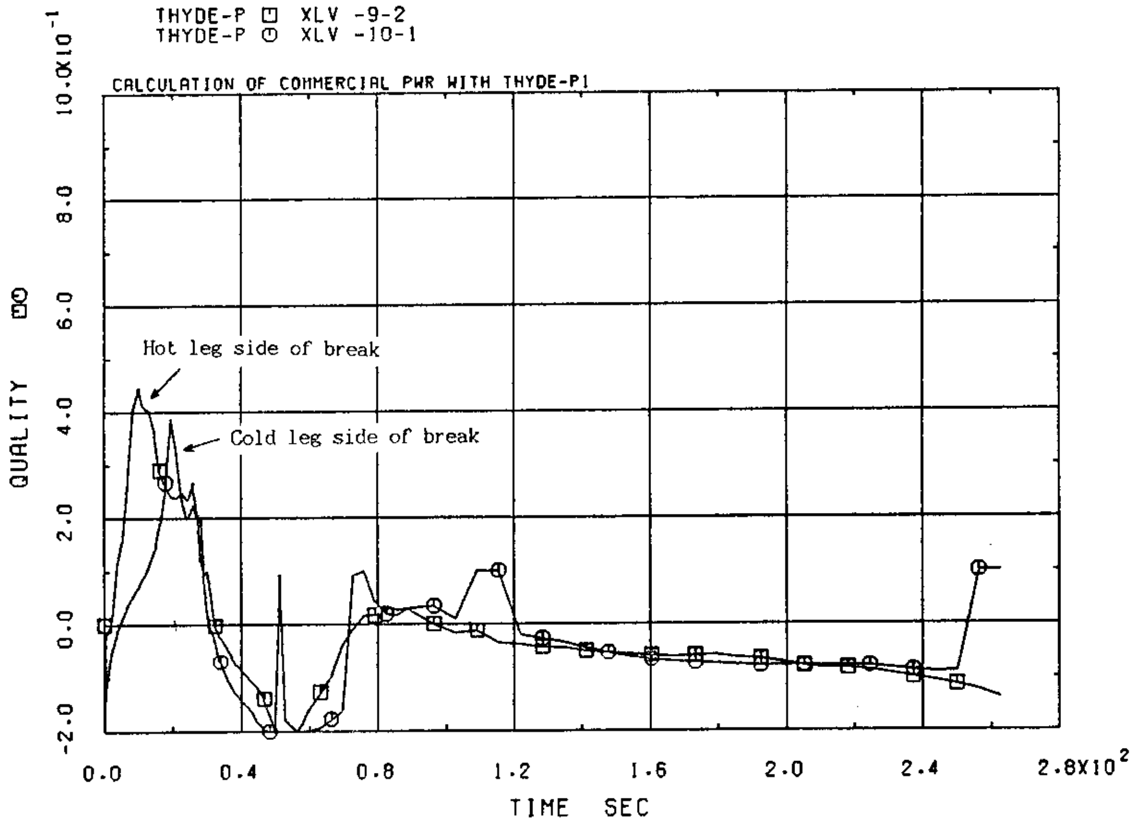

Fig.3-4-4 Equilibrium coolant qualities at break points

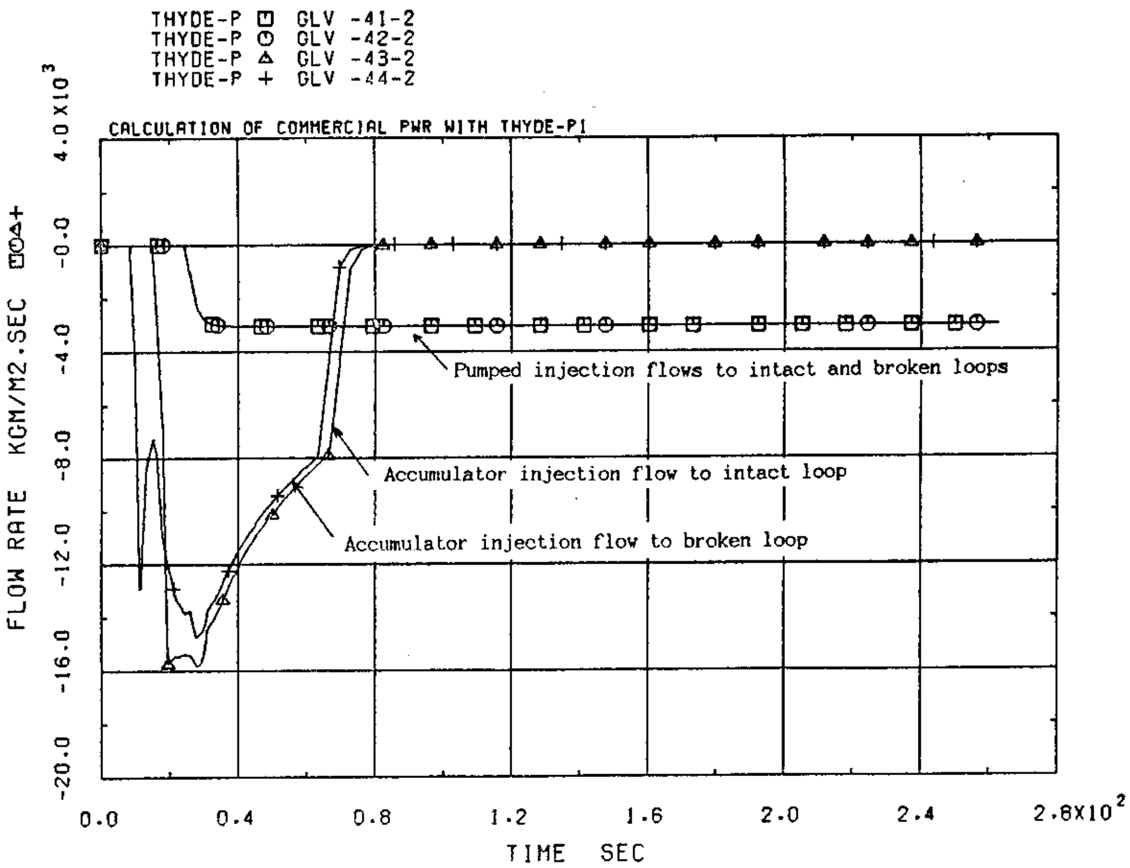

Fig.3-5-1 ECC injection mass fluxes

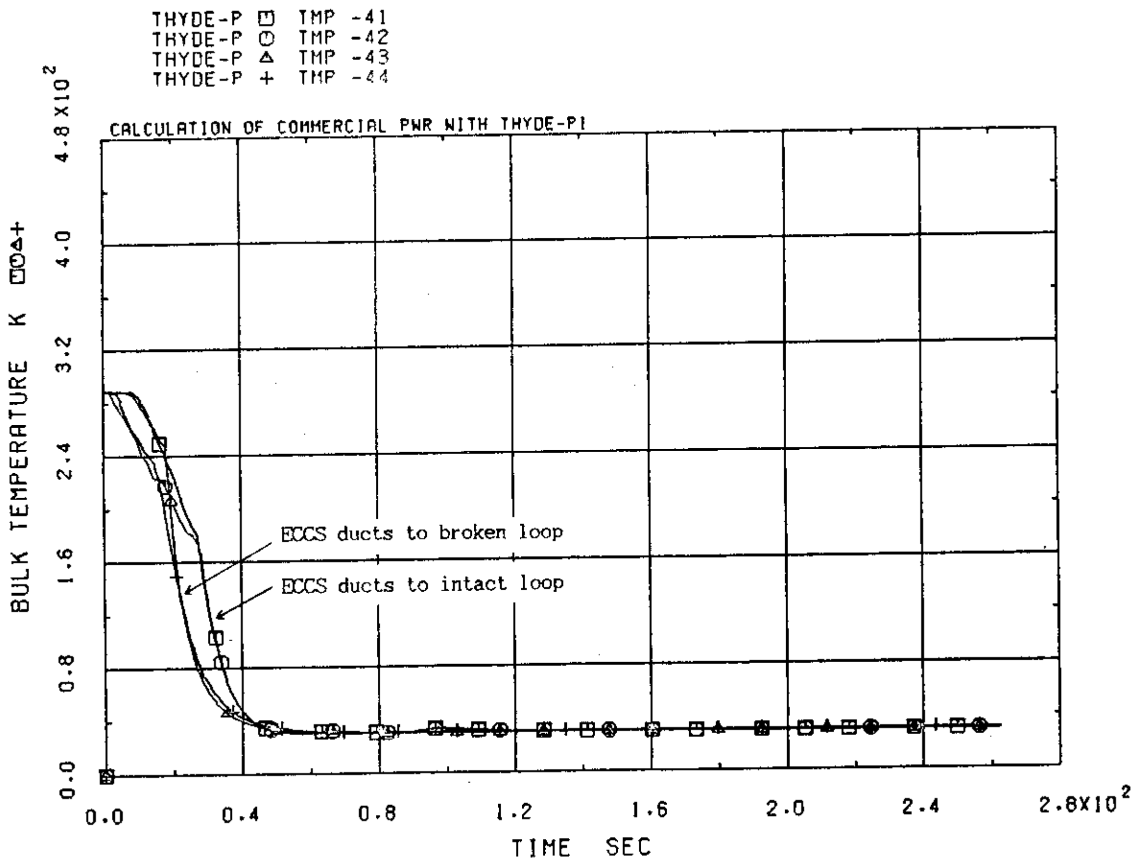

Fig.3-5-2 Coolant temperatures at ECC injection ducts

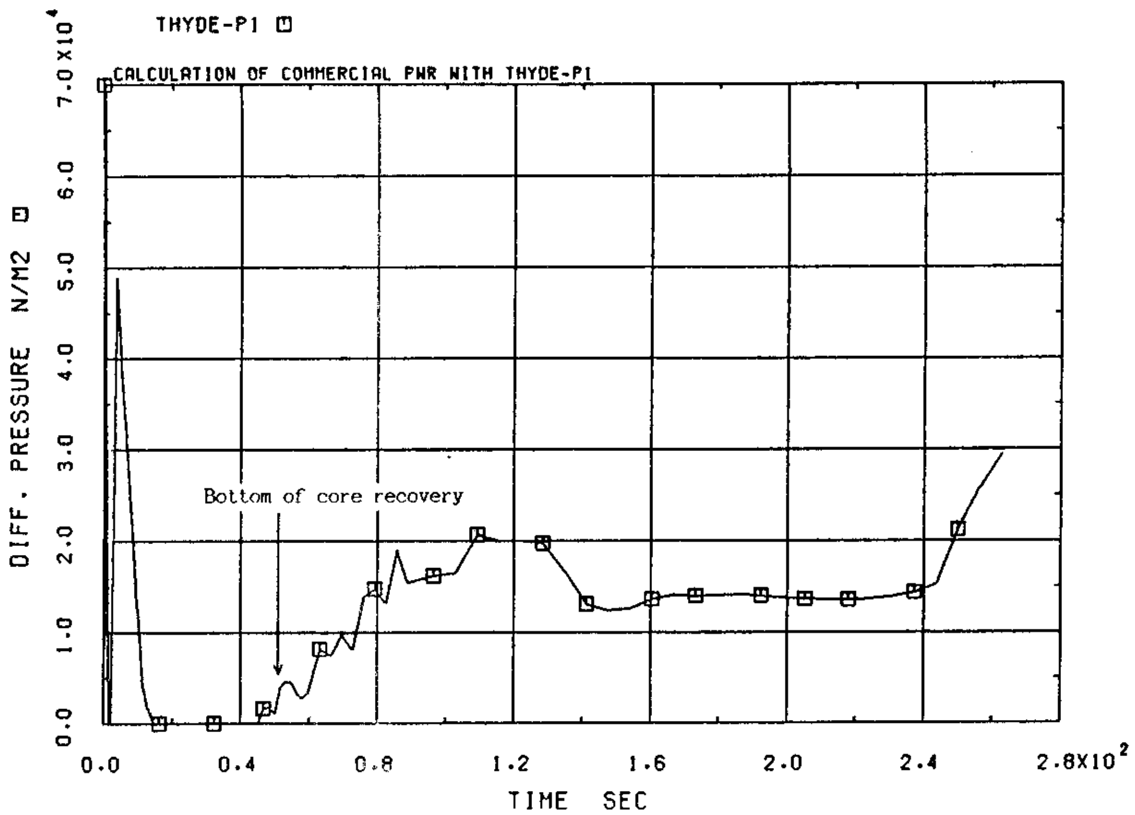

Fig.3-6-1 Differential pressure through core

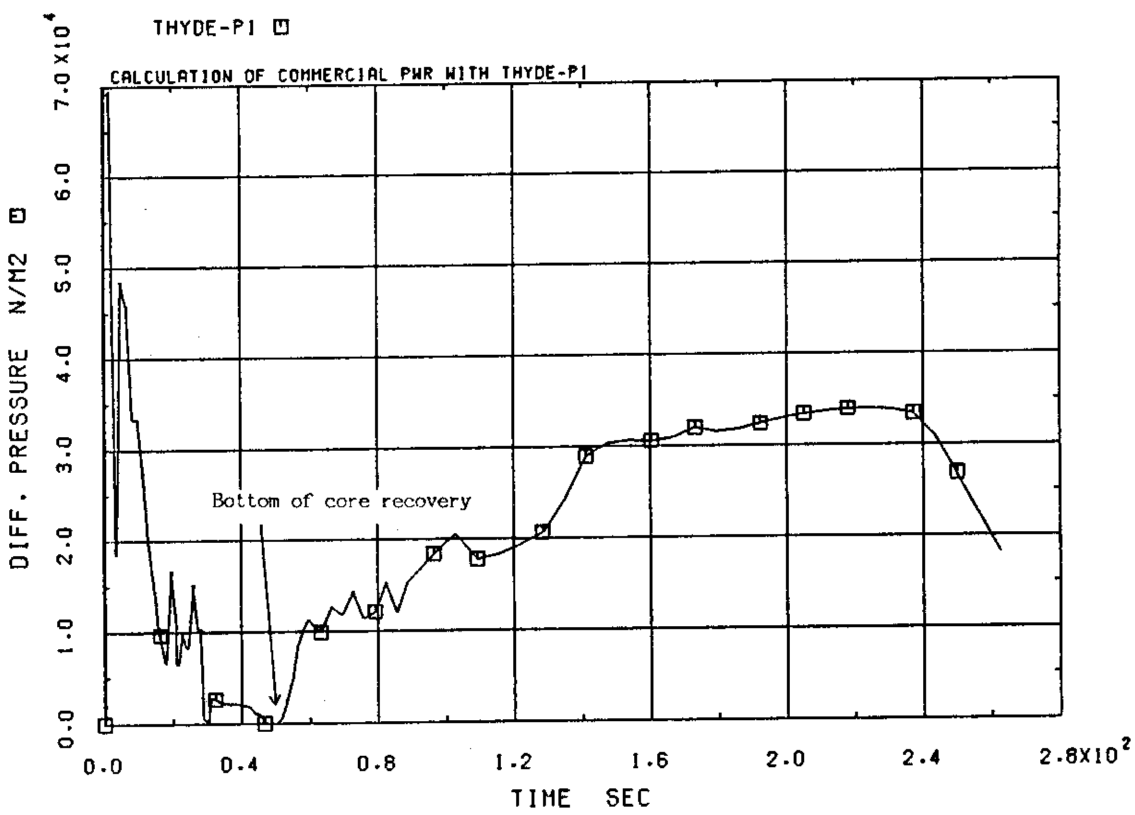

Fig.3-6-2 Differential pressure through intact loop

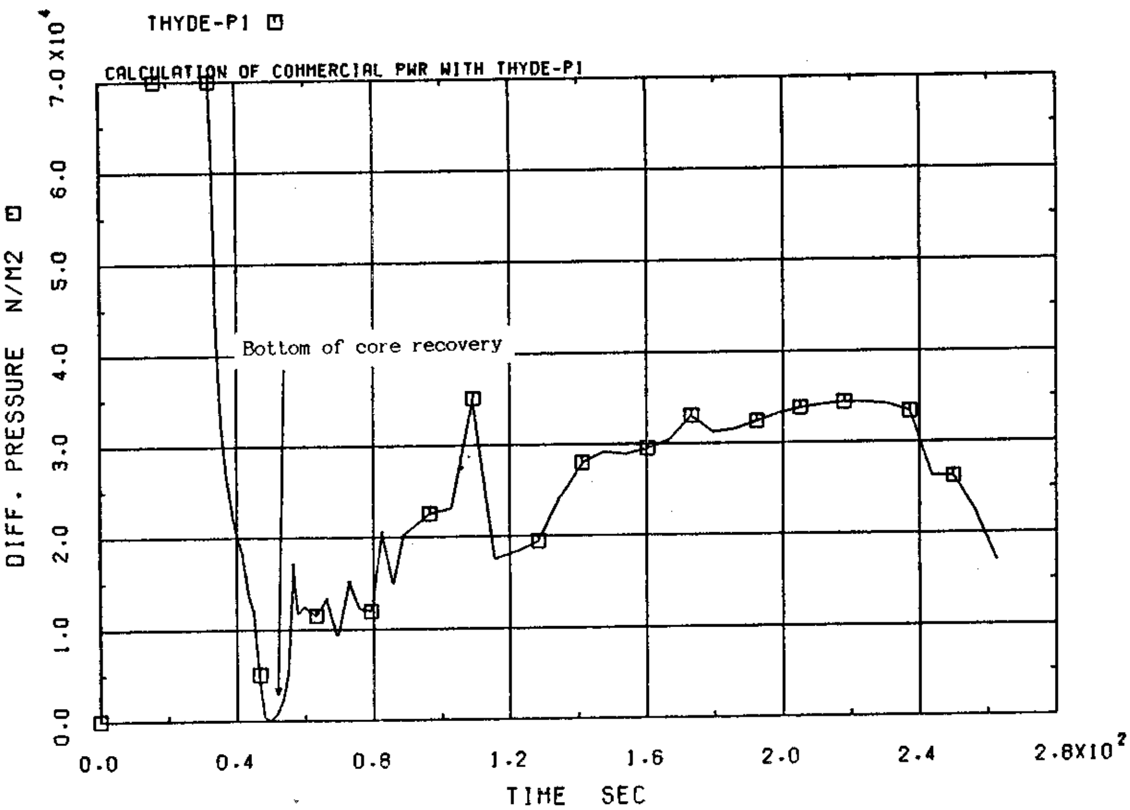

Fig.3-6-3 Differential pressure through broken loop

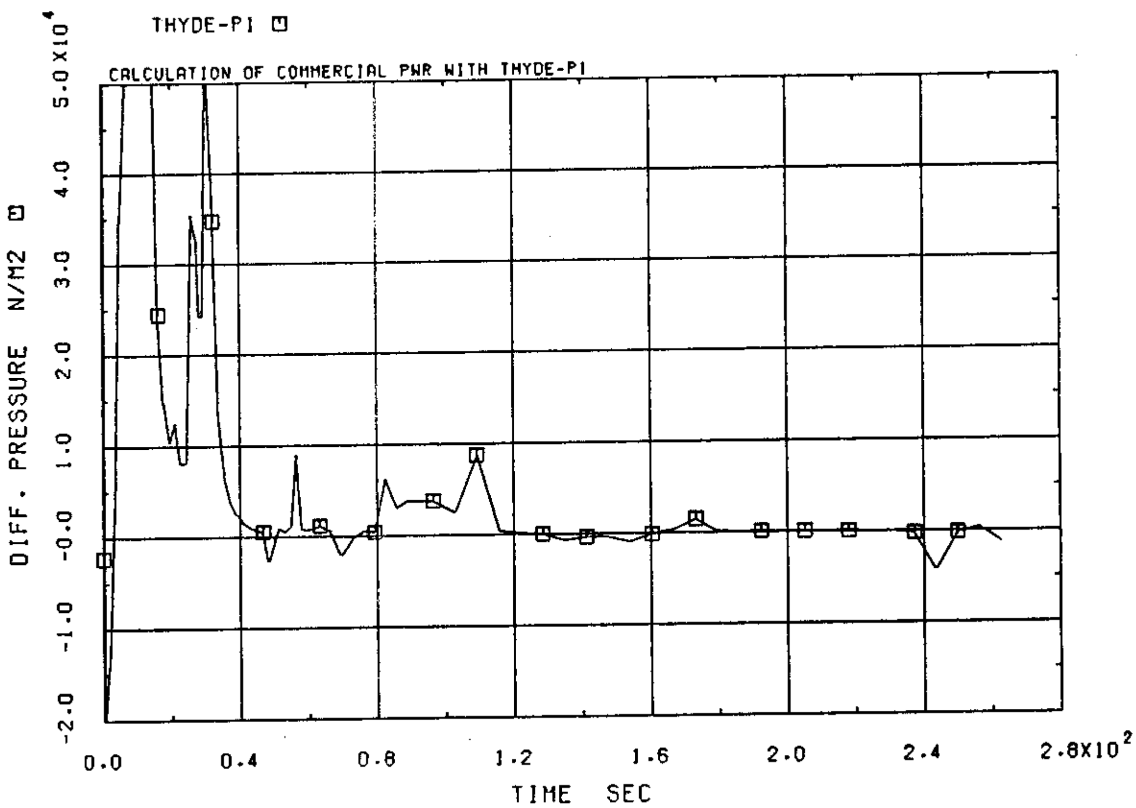

Fig.3-6-4 Differential pressure through broken loop cold leg

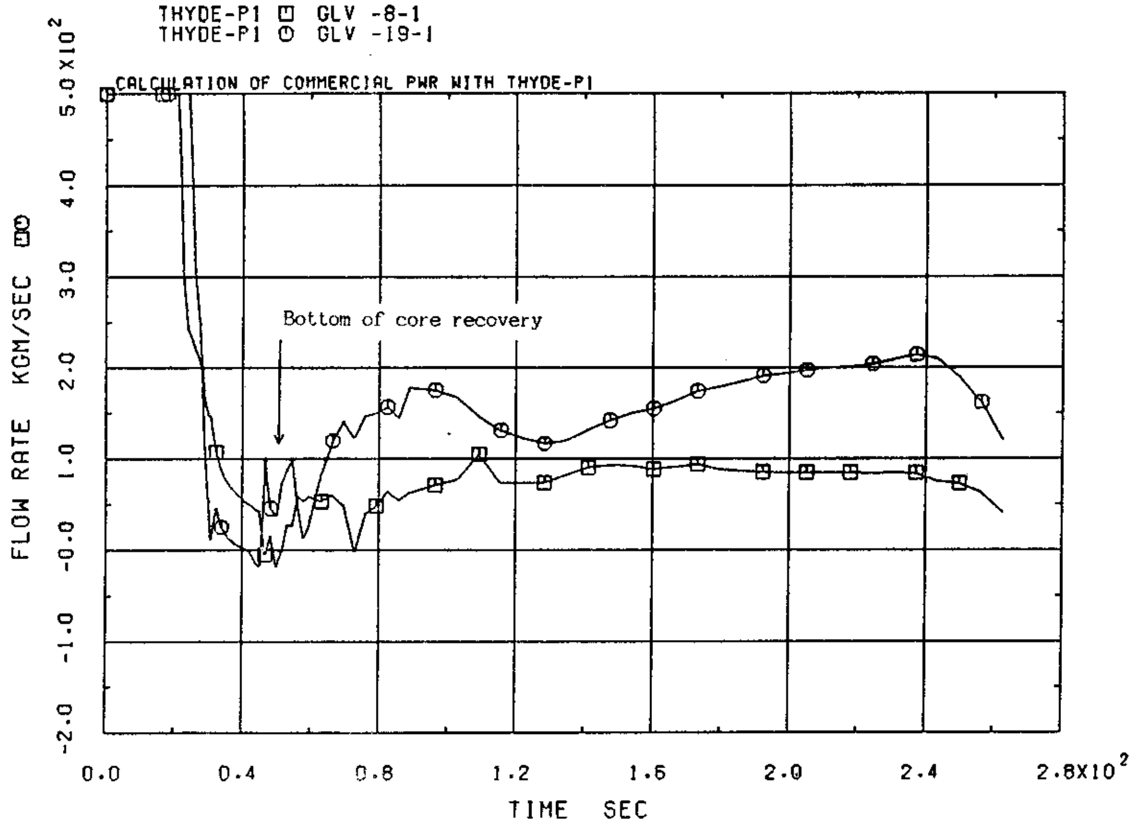

Fig.3-6-5 Mass flow rates through hot legs of intact and broken loops

4. Sensitivity Calculations

In this section, the results from three kinds of sensitivity calculations are presented: the pump operational conditions, CHF correlations and a minimum stable film boiling temperature (MSFBT) correlation. The first two sensitivity studies have been performed with the published version of THYDE-P1 without modification. In the last sensitivity study, however, a model has been developed and tentatively implemented into the code.

4.1. Pump On and Off

Two additional calculations with different pump conditions from Run 21 have been performed as an example of sensitivity calculations utilizing the base input data. Pump coastdown just after scram is assumed to occur in Run 21. In the additional calculations, however, pump running with a constant speed and pump rotor locking just after scram are assumed.

Fig. 4-1-1 shows the experimental cladding surface temperatures at the middle of the core in the pump on and off cases of the LOFT experiments, L2-3(11) and L2-5(12,13). Experiment L2-3 simulated a large break LOCA of a commercial PWR and the primary coolant pumps were running throughout the experiment. Experiment L2-5 was conducted under almost the same conditions as those in Experiment L2-3 except the pump condition, where an atypically fast pump coastdown was simulated. As shown in Fig 4-1-1, early rewetting was observed in Experiment L2-3 but was not observed in L2-5 due to the effects of the primary coolant pump condition. Although quantitative comparisons between the results from the LOFT experiments and those from the present sensitivity calculations have less meaning, qualitative ones may be useful to verify the system responses of THYDE-P1 to the pump conditions.

Figures. 4-1-2, 4-1-3, 4-1-4 and 4-1-5 show the normalized pump speeds, the pump heads, the normalized pump hydraulic torques, and the normalized pump volumetric flows, respectively. In the pump locking case, the pump speed is made to rapidly decrease to be zero just after scram with a time constant 0.05 sec. Fig. 4-1-6 shows the calculated cladding surface temperatures at the middle of the core. Early core-wide rewetting is calculated to occur in the pump running case but is not in the other two pump conditions. These results are qualitatively consistent with the LOFT experimental results. Fig. 4-1-7 shows the core inlet flows. The core inlet flow until 15 sec is highest in the pump running case and the lowest in the pump locking case. It is clearly shown in this figure that the positive core flow recovery in the pump running case brings about the early rewetting.

Figs. 4-1-8 and 4-1-9 shows the hot leg side and cold leg side of the break flows. The effects of the pump condition to the hot leg side of the break flow seem to be small but those to the cold leg side of the break flow are considerable. In the case of pump rotor locking, the cold leg side of the break flow is considerably smaller than that in the other two cases.

Fig. 4-1-10 shows the calculated pressure transients. The pressures in the pump running case and the coastdown case are similar to each other. Because of the early rewetting, the pressure is calculated to be higher in the pump running case or the coastdown cace than in the pump locking case until 15 sec. These results are also consistent with the LOFT experimental results(13). The reason why the the pressure after 15 sec is calculated to be higher in the pump locking case than in the other cases is due to the effects of the break flow.

4.2. CHF Correlations

In THYDE-P1, there are three and two options for the CHF calculation under a forced convection condition and a pool flow condition, respectively, as follows:

For the forced convection condition,

(1) The Biasi correlation(20),

(2) The GE correlation(21) and

(3) RELAP4 type correlation(19) (interpolation of the CHF values calculated using the B&W2(22), Barnett(23) and modified Barnnet(24) correlations), and

For the pool flow condition,

(1) Interpolation by a mass flux G between the CHF values evaluated at $G = G_{min}$ (= 273 kg/m^2/sec) and 67.9 kcal/m^2/sec, and

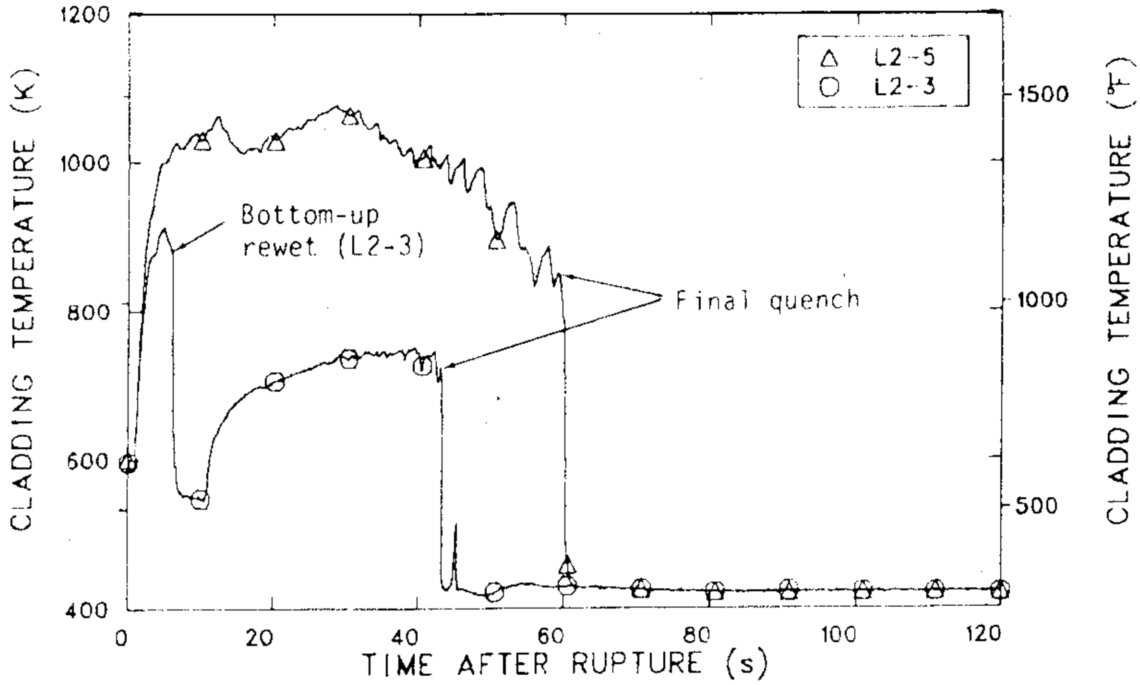

Fig.4-1-1 Experimental cladding surface temperatures in LOFT Large Break Experiments L2-3 and L2-5

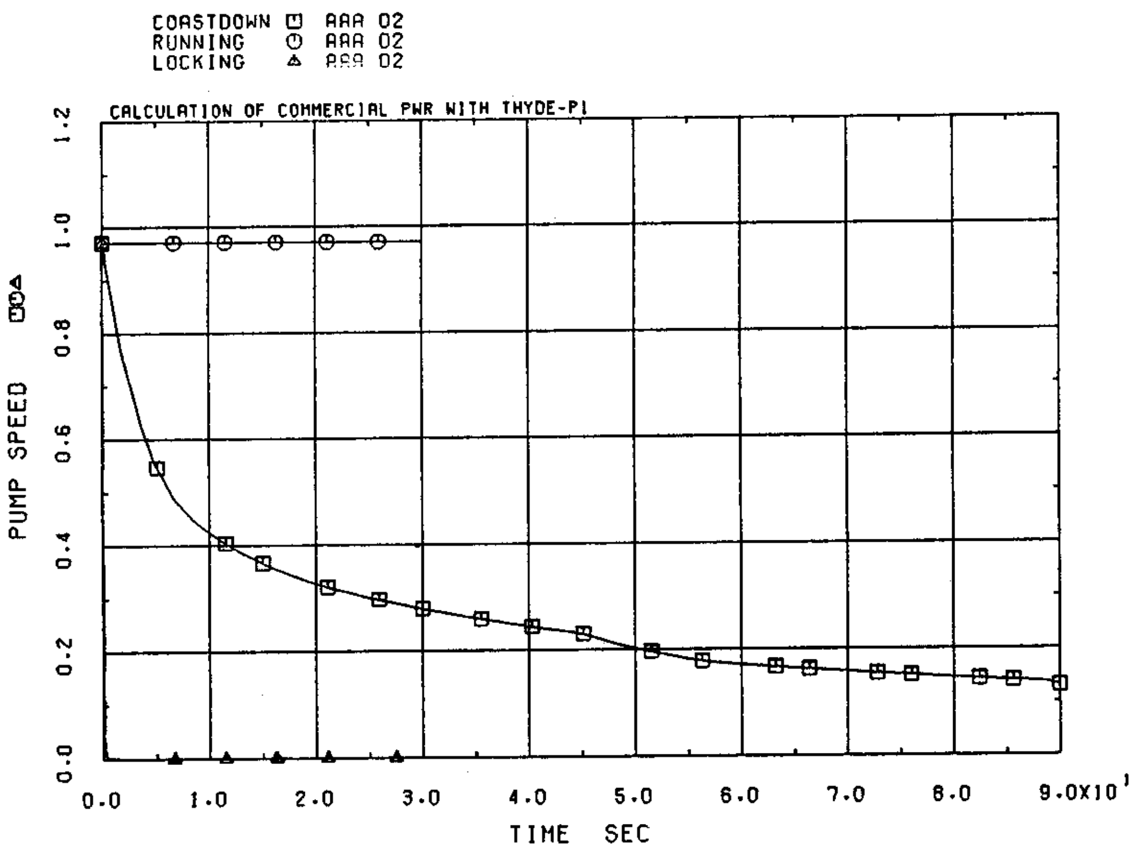

Fig.4-1-2 Normalized pump speeds

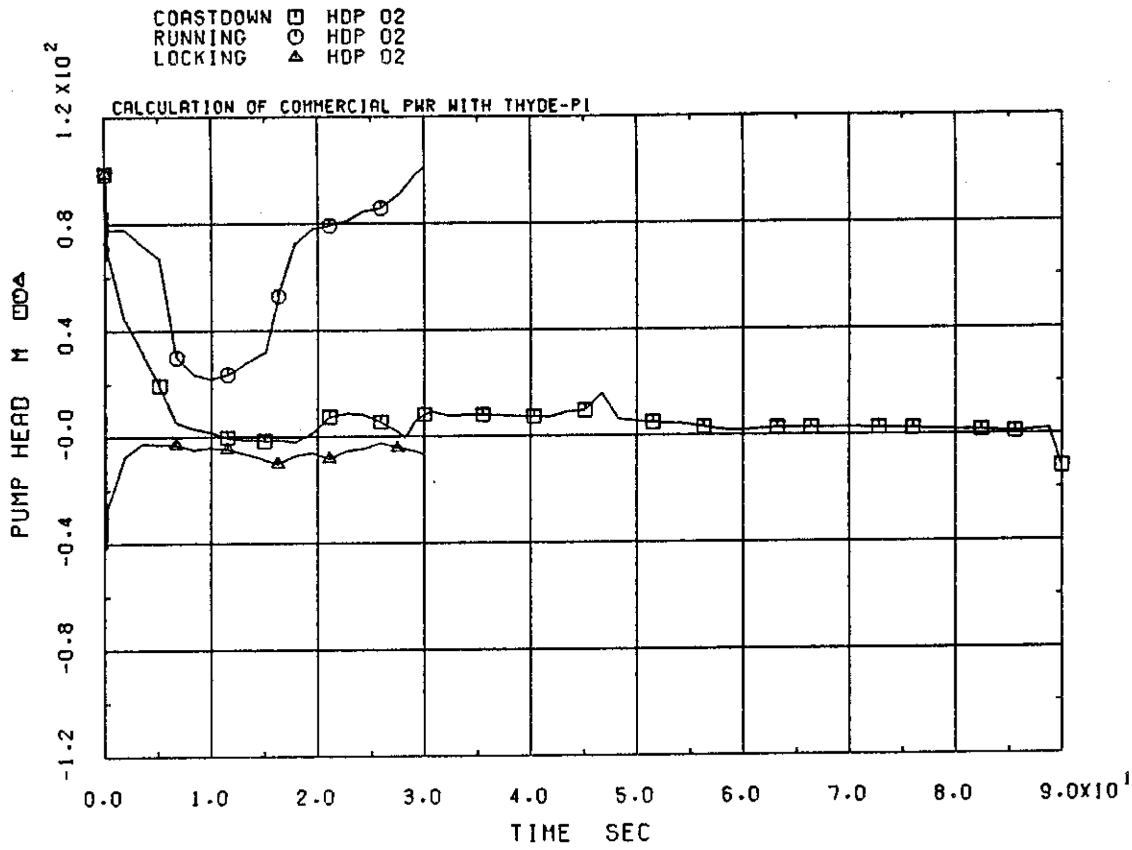

Fig.4-1-3 Pump heads

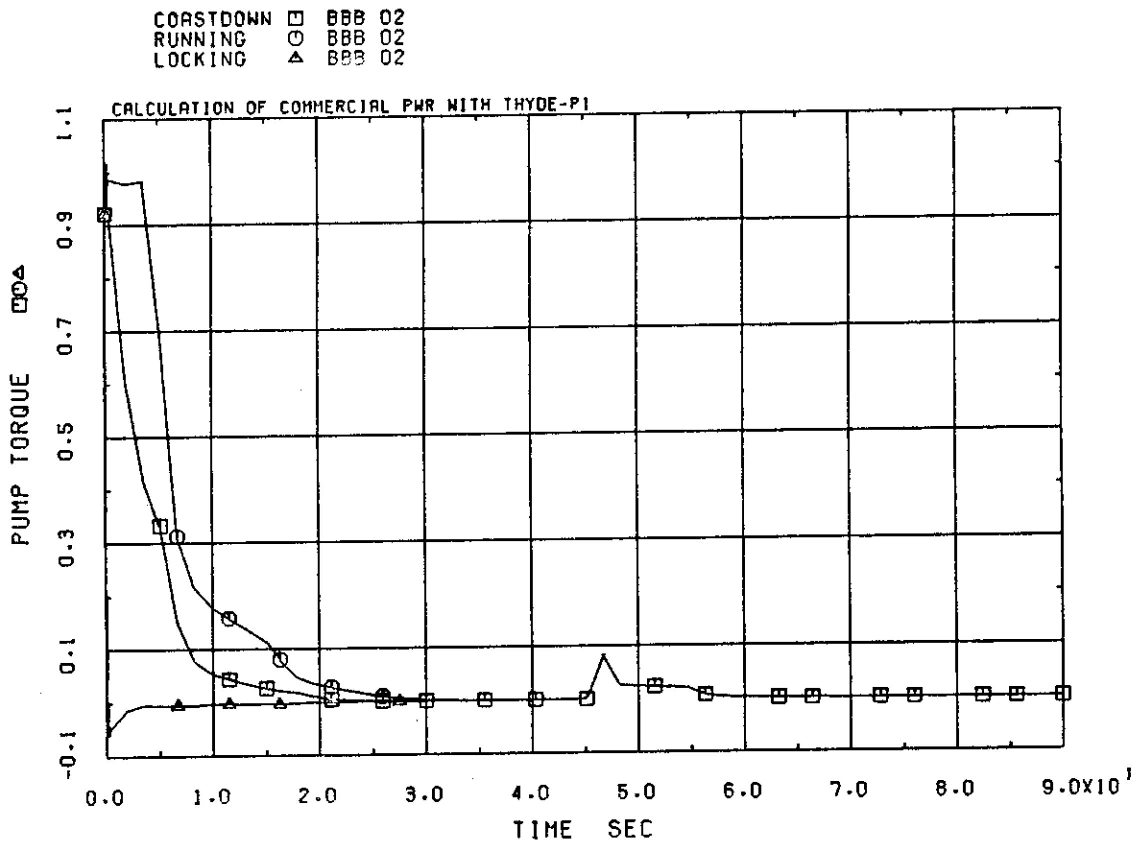

Fig.4-1-4 Normalized pump hydraulic torques

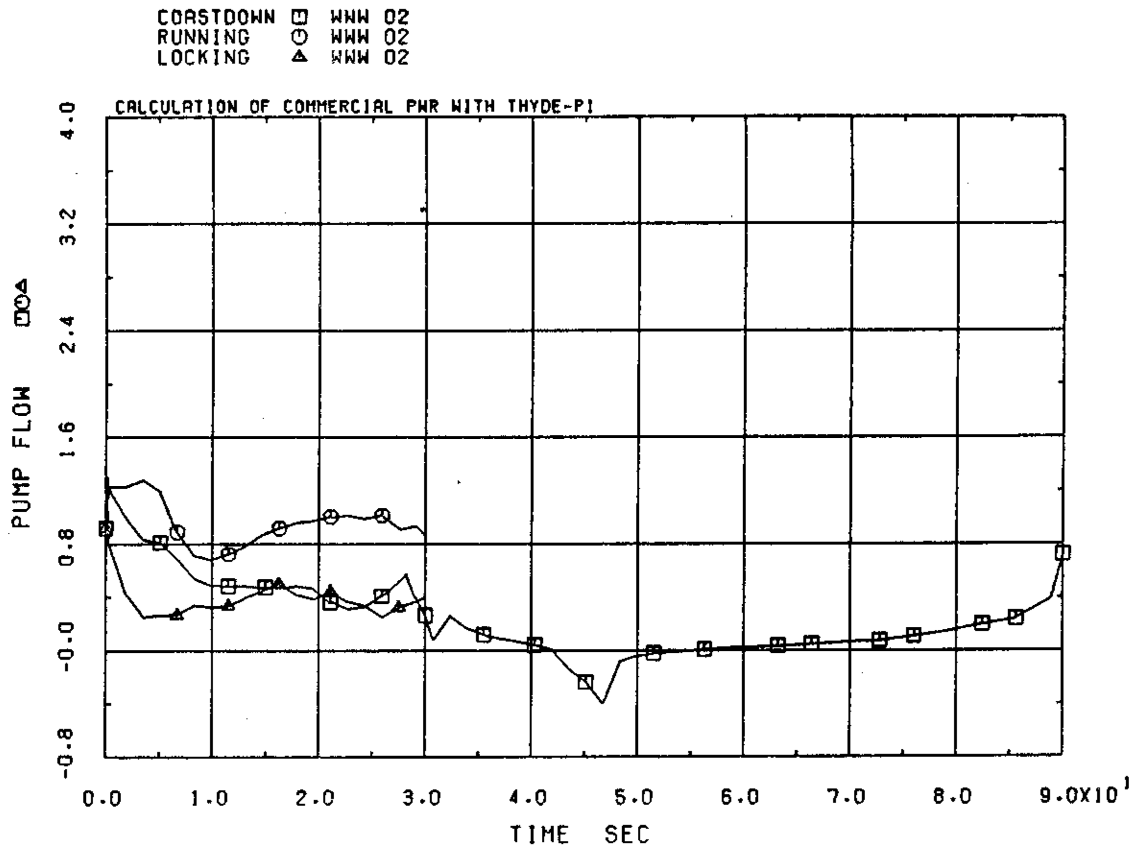

Fig.4-1-5 Normalized pump flows

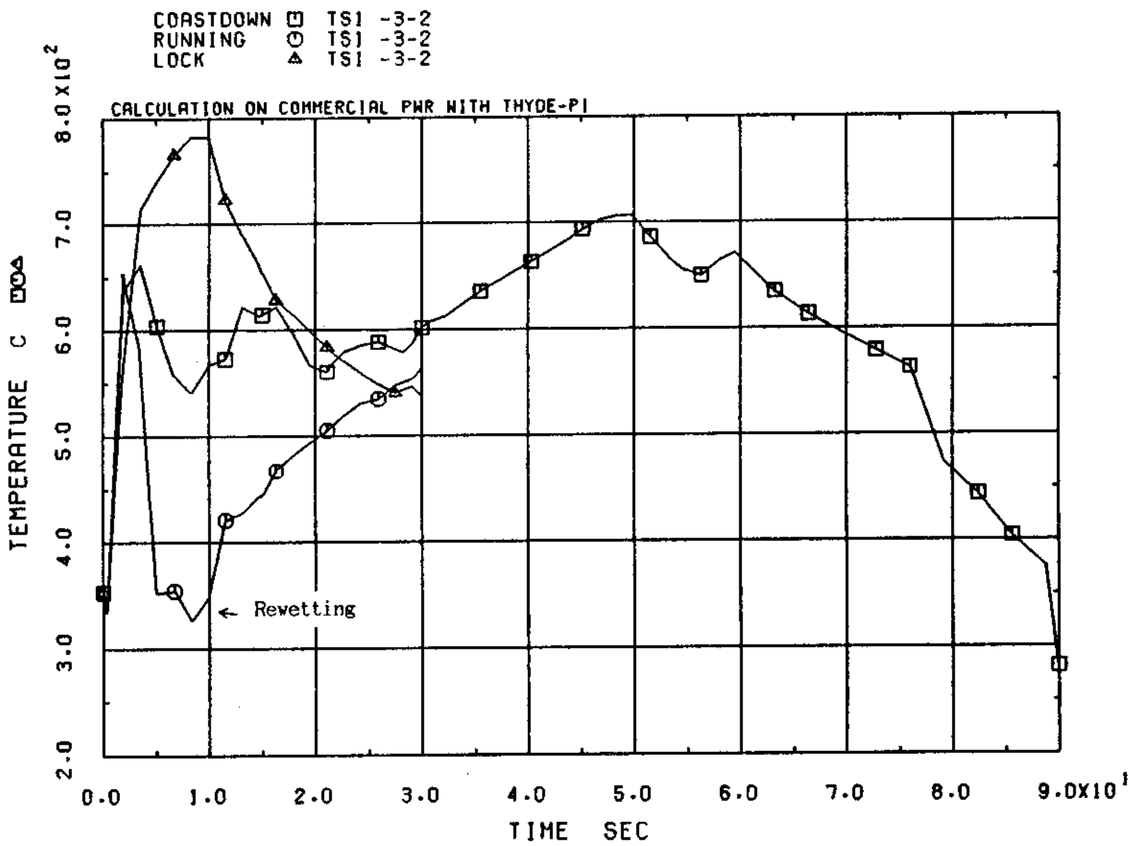

Fig.4-1-6 Cladding surface temperatures at middle of hot channel

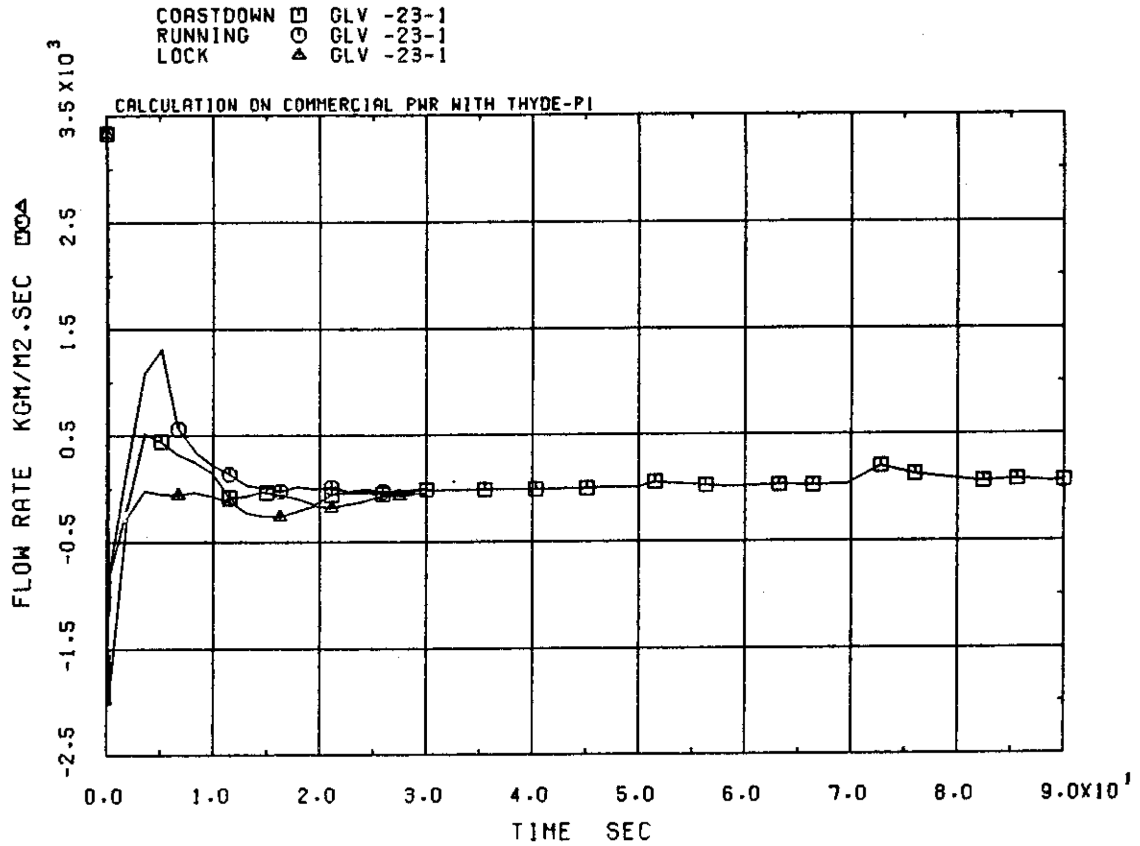

Fig.4-1-7 Core inlet mass fluxes

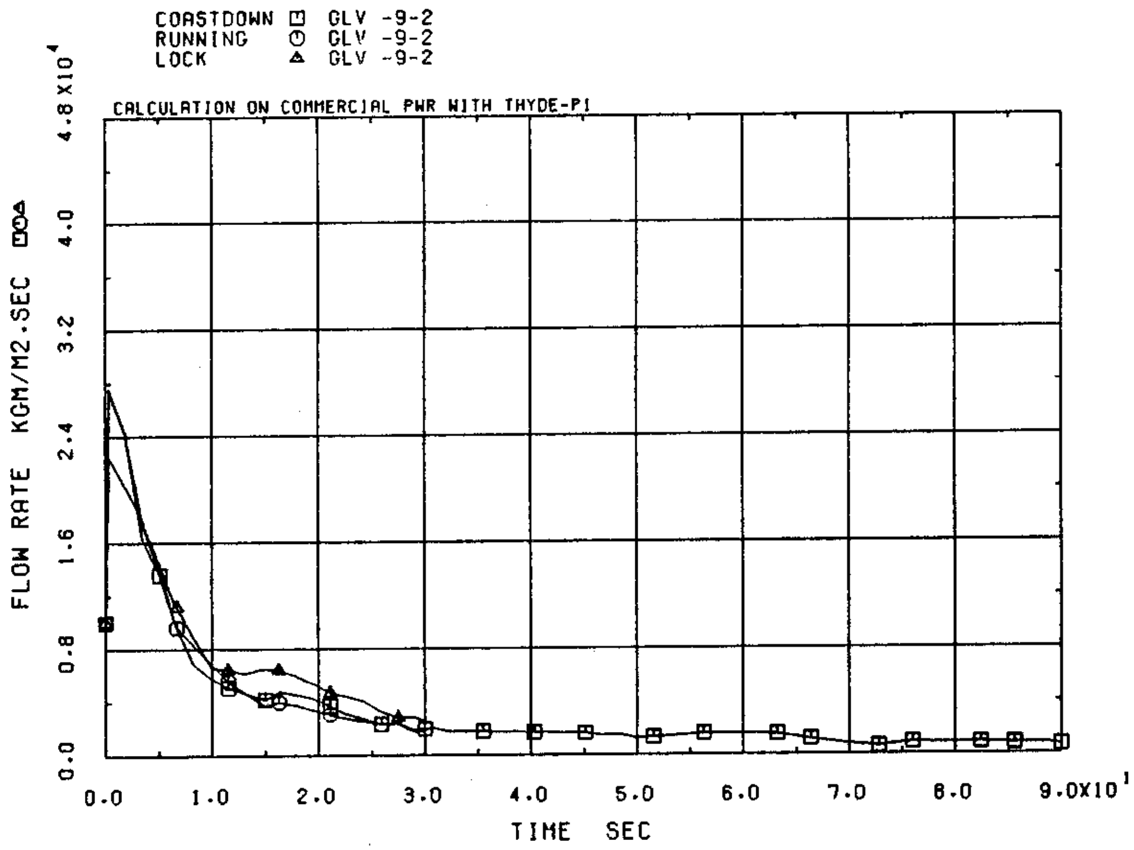

Fig.4-1-8 Hot leg side of break flows

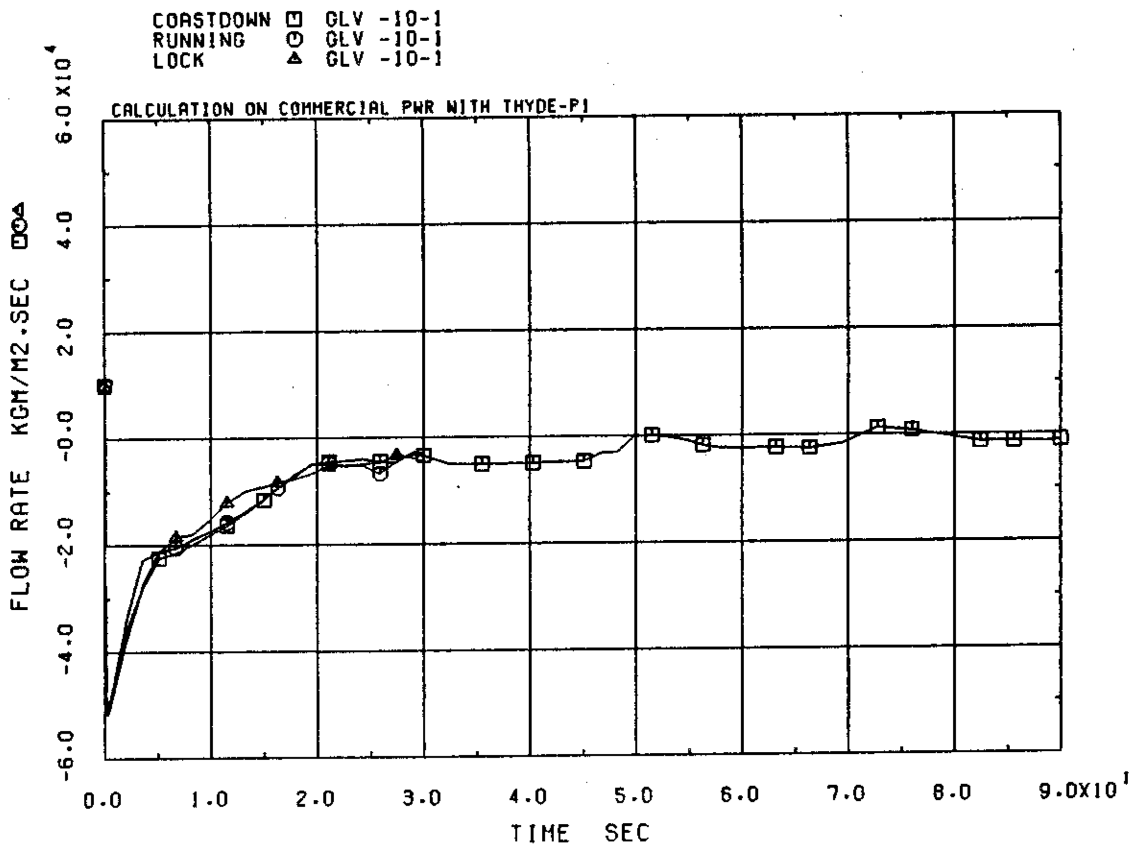

Fig.4-1-9 Cold leg side of break flows

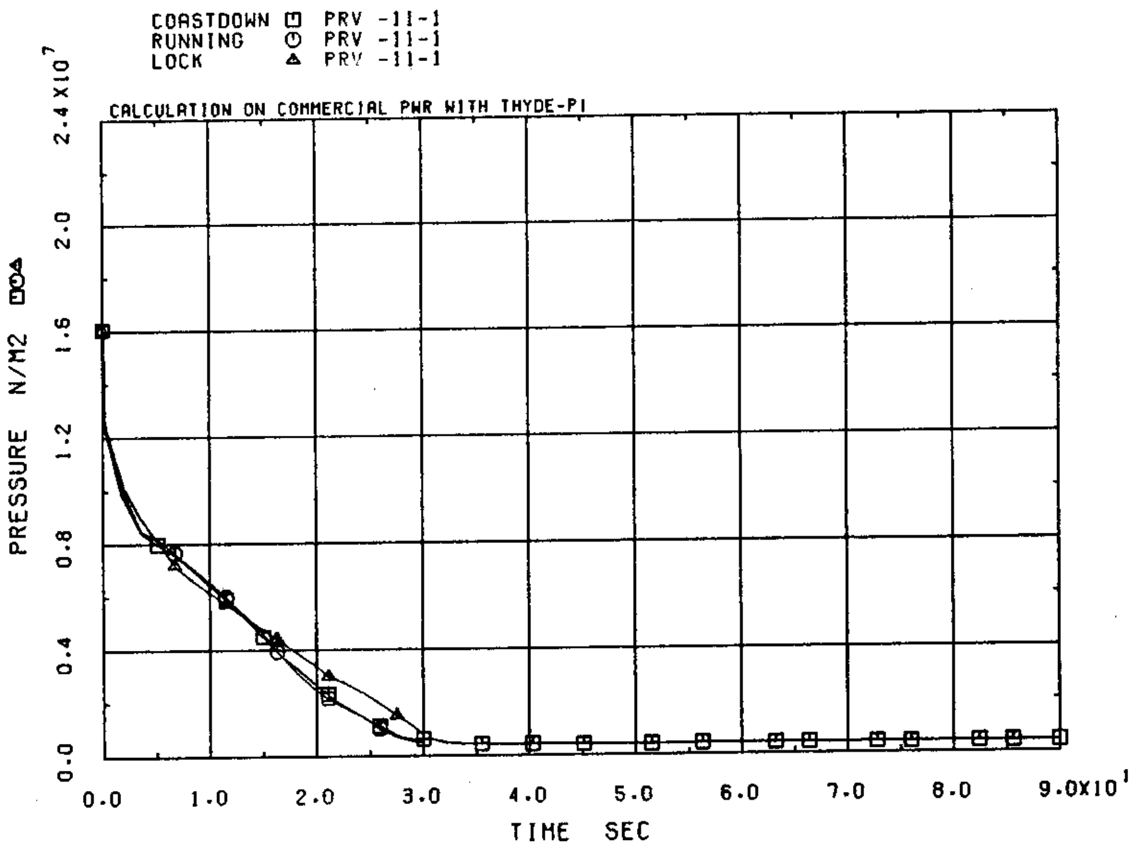

Fig.4-1-10 Intact loop hot leg pressures

(2) Modified Zuber[25] correlation.

In the base case calculation, Run 21, the options (3) and (1) are selected for the forced convection condition and the pool flow condition, respectively. In the additional calculation, however, the options (1) and (2) are selected.

The comparisons of the cladding surface temperatures, the fuel centre temperatures and the heat transfer coefficients between the base case calculation and the additional calculation are shown in Figs. 4-2-1, 4-2-2 and 4-2-3, respectively. The differences in the two calculations do not seem considerable.

4.3 Minimum Stable Film Boiling Temperature Model

In the published version of THYDE-P1, an empirical correlation for minimum stable film boiling temperature (MSFBT) is not implemented. Since in THYDE-P1, quenching is caused only when the quality of a core node under consideration decreases below 0.1, the quenching time at the higher elevation is considerably delayed. In order to improve this point, a model has been tentatively implemented and studied. In the present MSFBT model, the quenching is also assumed to occur when the cladding surface temperature decreases below MSFB temperature T_{MSFB}. Therefore this model is expected to improve the histories of the cladding surface temperatures at the higher elevation and of the quench front.

In the present model, in order to apply the MSFBT, two types of boiling curves are assumed to exist for DNB and quenching separately as shown later. It should be noted that the model may be regarded as temporary and oppotune.

T_{MSFB} is defined to be the wall temperature which is required to maintain film boiling. In this analysis, T_{MSFB} was obtained based on the same formula as TRAC-P1A[14]. For low pressures, the classic film boiling instability analysis has been successfuly used by Berenson[15] to predict this temperature. Henry[16] modified that analysis to account for surface effects:

$$T_{MINHB} = T_{MINB} + 0.42(T_{MINB}-T_l)\left[\frac{h_{lg}}{(c_p)_w DT_{MINB}}\frac{((k\rho c_p)_l)^{1/2}}{((k\rho c_p)_w)^{1/2}}\right]^{0.6} \qquad (4\text{-}3\text{-}1)$$

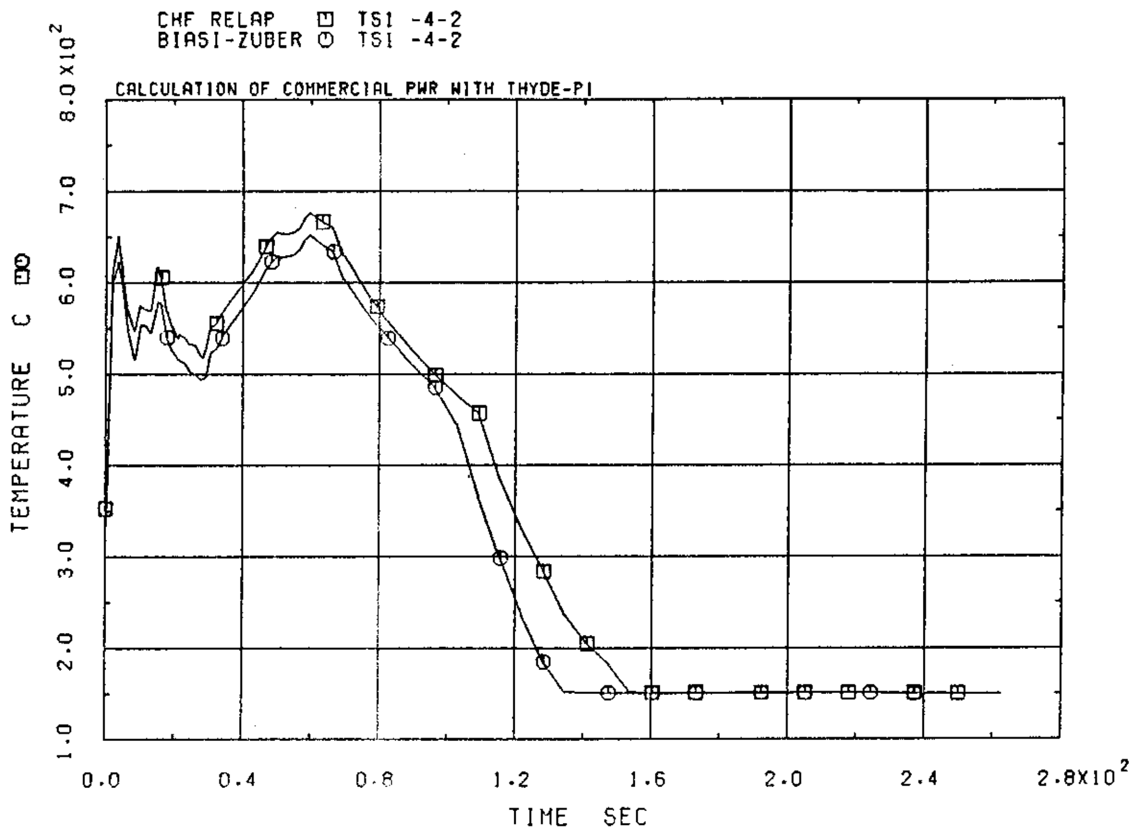

Fig.4-2-1 Cladding surface temperatures at middle of hot channel

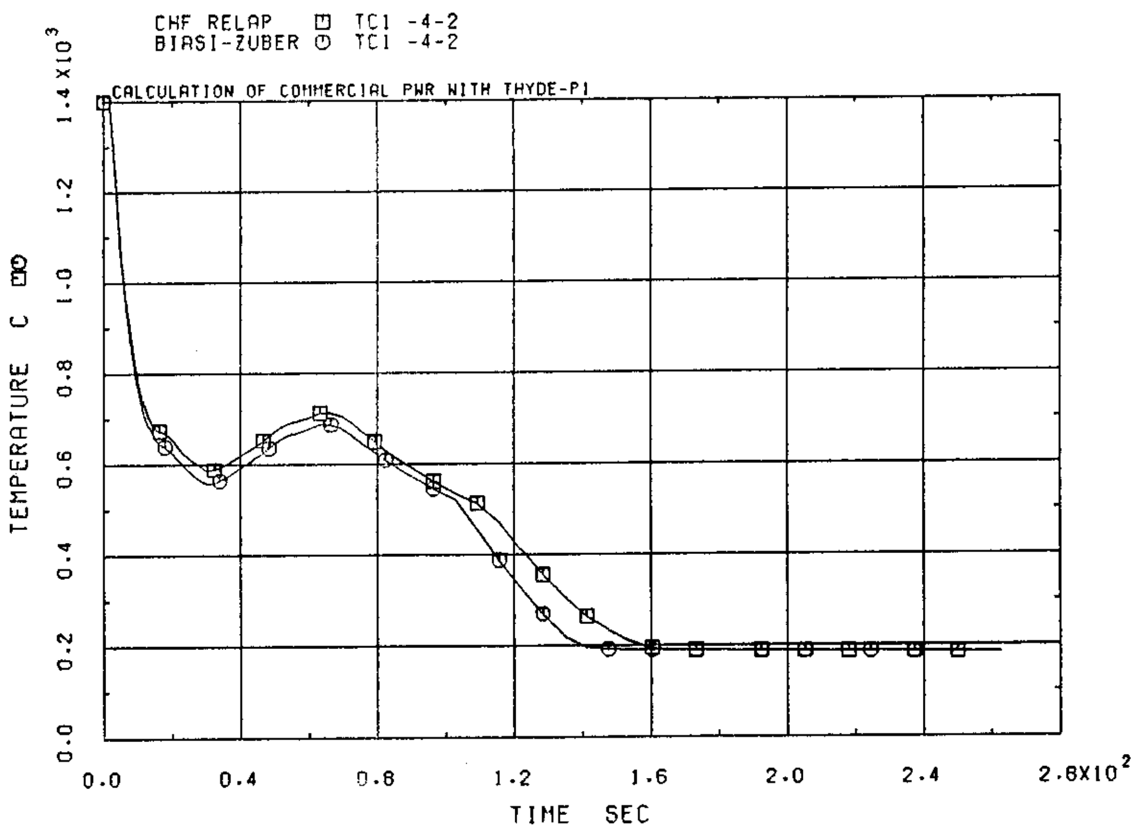

Fig.4-2-2 Fuel centre temperatures at middle of hot channel

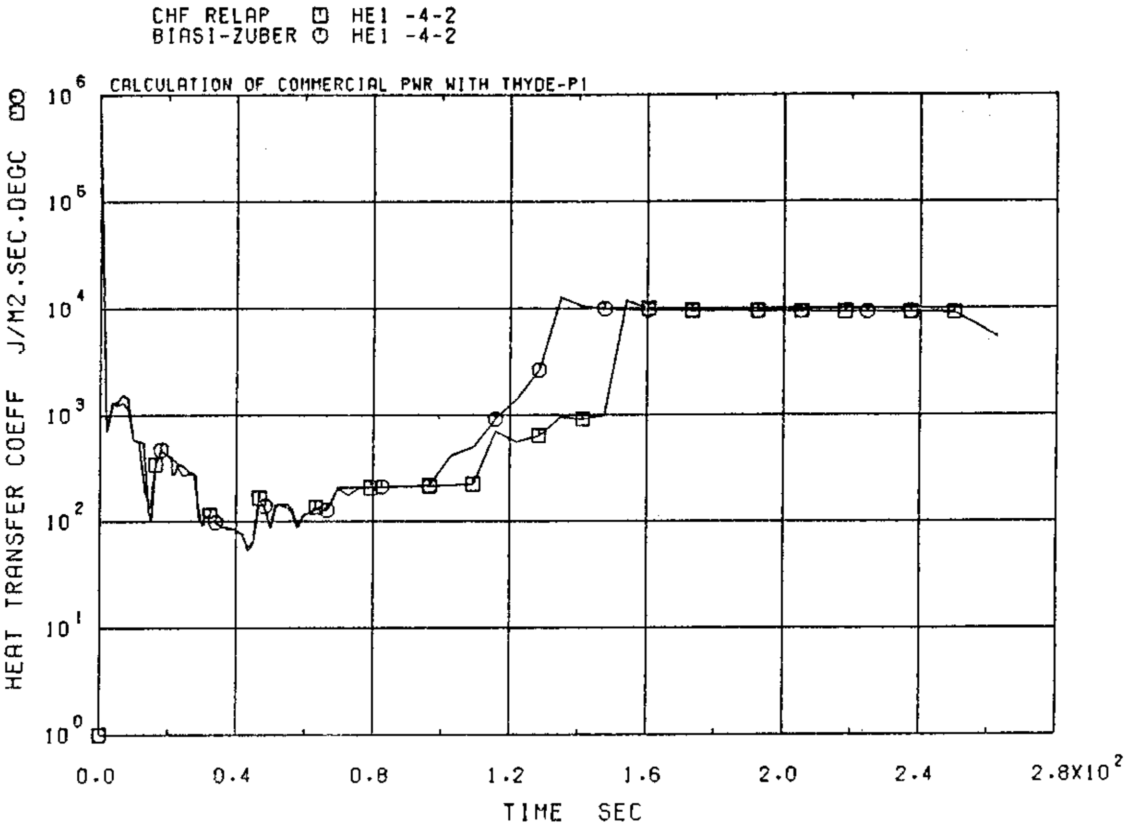

Fig.4-2-3 Heat transfer coefficients at middle of hot channel

and

$$T_{MINB} = T_s + 0.127\frac{\rho_l h_{lg}}{k_g}\left[\frac{g(\rho_l-\rho_g)}{\rho_l+\rho_g}\right]^{2/3}\left[\frac{\sigma}{g(\rho_l-\rho_g)}\right]^{1/2}\left[\frac{\mu_g}{g(\rho_l-\rho_g)}\right]^{1/3} \qquad (4\text{-}3\text{-}2)$$

where

T_l ; liquid temperature

T_s ; saturation temperature

ρ ; density

Cp ; specific heat at constant pressure

k ; thermal conductivity

h_{lg} ; latent heat of vaporization

g ; acceleration due to gravity

σ ; surface tension

μ ; viscosity.

At higher pressures, the homogeneous nucleation mechanism[17] seems to dominate. Bjornard and Griffith[18] recommended Henry's modification to the Berenson formula also for the homogeneous nucleation phenomena:

$$T_{MINHN} = T_{HN} + (T_{HN}-T_l)\left[\frac{(k\rho C_p)_{liquid}}{(k\rho C_p)_{wall}}\right]^{1/2} \qquad (4\text{-}3\text{-}3)$$

where T_{HN} is the homogeneous nucleation temperature. It is a weak function of pressure and varies from 307 C at atmospheric pressure to the critical temperature (374 C) at the critical pressure for water. The larger value is used in Eq.(4-3-3). The minimum of Eqs.(4-3-1) and (4-3-3) was chosen as T_{MSFB} in this analysis.

A boiling curve can be divided into three major regions according to the wall superheat. These are the pre-CHF (wet wall), transition boiling (alternating wet and dry walls) and film boiling (dry wall) regions. As shown in Fig. 4-3-1, it is assumed in the present analysis that there are two curves in the transition region. The curve (1) is applied to the transition from the nucleate boiling to the post-CHF (DNB). The curve (2) is used for the transition from the post-CHF to the nucleate boiling (quenching)[26]. When the curve of type (2) is also applied to DNB, DNB may not be calculated to occur. We now introduce a index I whose values correspond to the type of the above curves : when the index I = 1 (or 2), the curve (1) (or (2)) is adopted. The index I is determined as follows. At first I is set to be 0 for the steady state. When the wall temperature becomes larger than T_{MSFB}, or when the heat transfer mode of a core node under consideration becomes the superheated vapor mode, I is altered from 0 to 1. Then I is set to be 0 again if the heat transfer mode goes back to the nucleate boiling mode.

The results from the calculation with MSFBT model are compared in Figs. 4-3-2 to 4-3-4 with those from the base case calculation where the MSFBT model is not applied. As has been expected, the effects of the MSFBT model are remarkable for the histories of the cladding surface temperatures at the higher nodes (see Fig. 4-3-4). When this model is taken into account, the quenching occurs during the early stage of the reflooding at the upper core nodes. On the other hand, this model has rather small effects on the bottom flooding (see Figs. 4-3-2 and 4-3-3).

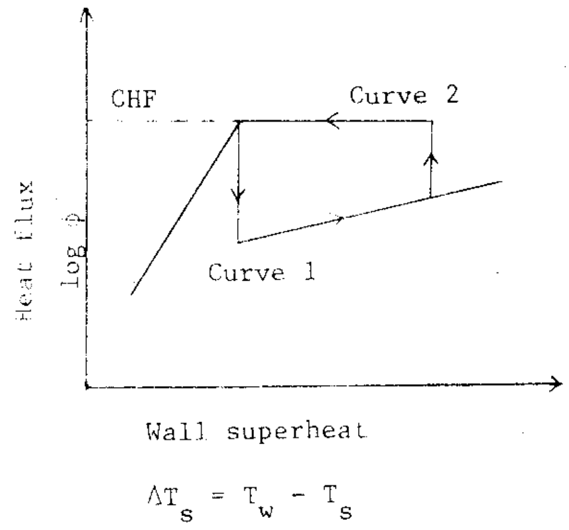

Fig. 4-3-1 Boiling curve in present MSFBT model

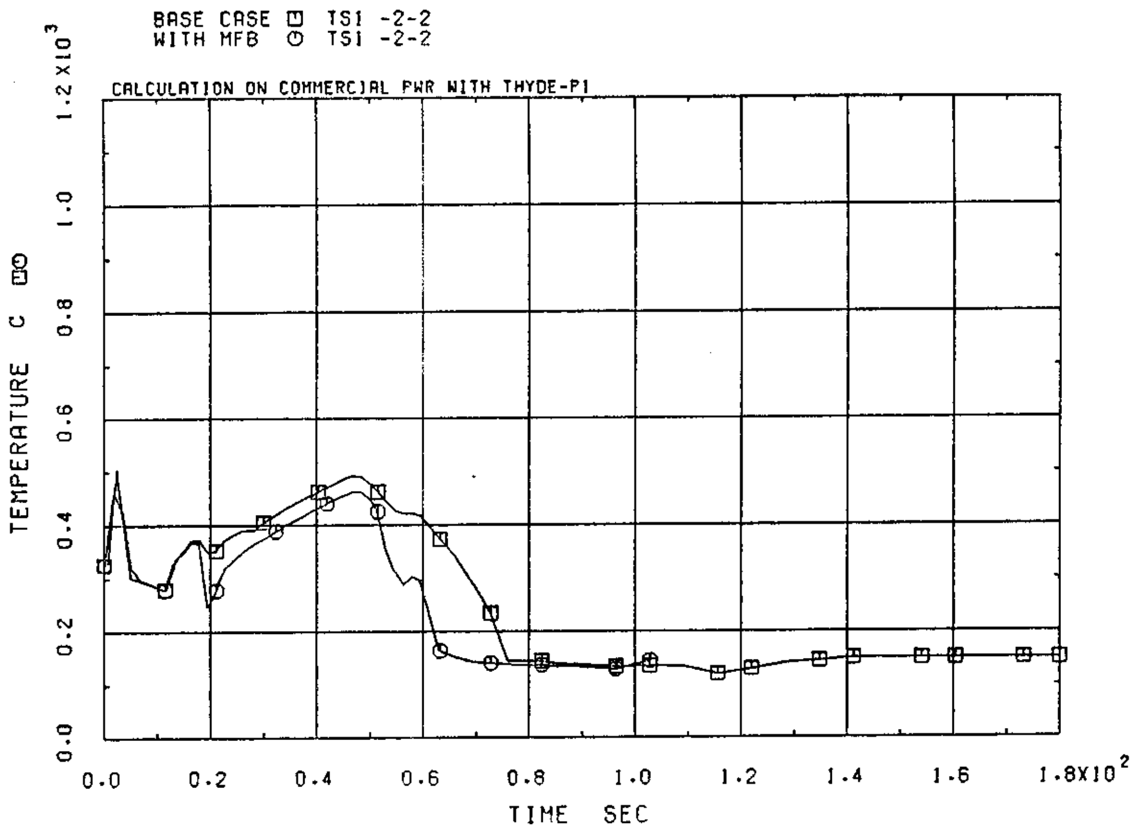

Fig.4-3-2 Cladding surface temperatures at bottom of hot channel

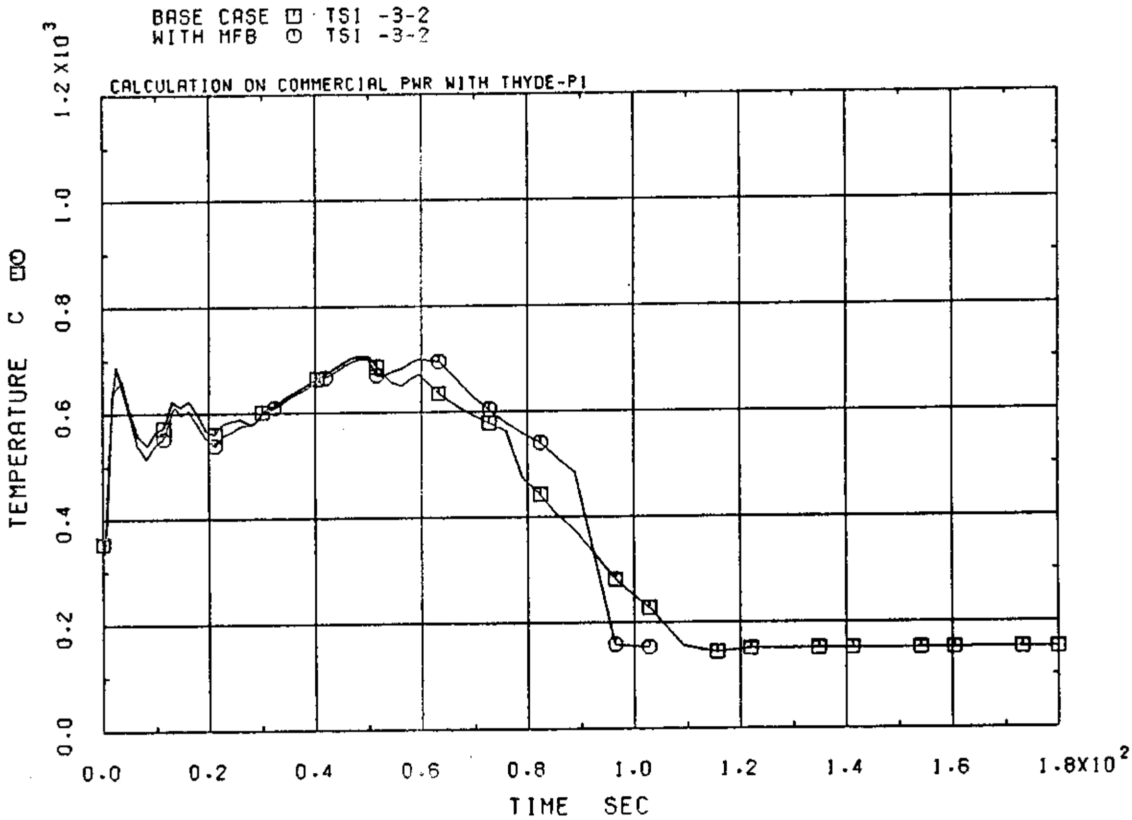

Fig.4-3-3 Cladding surface temperatures at middle of hot channel

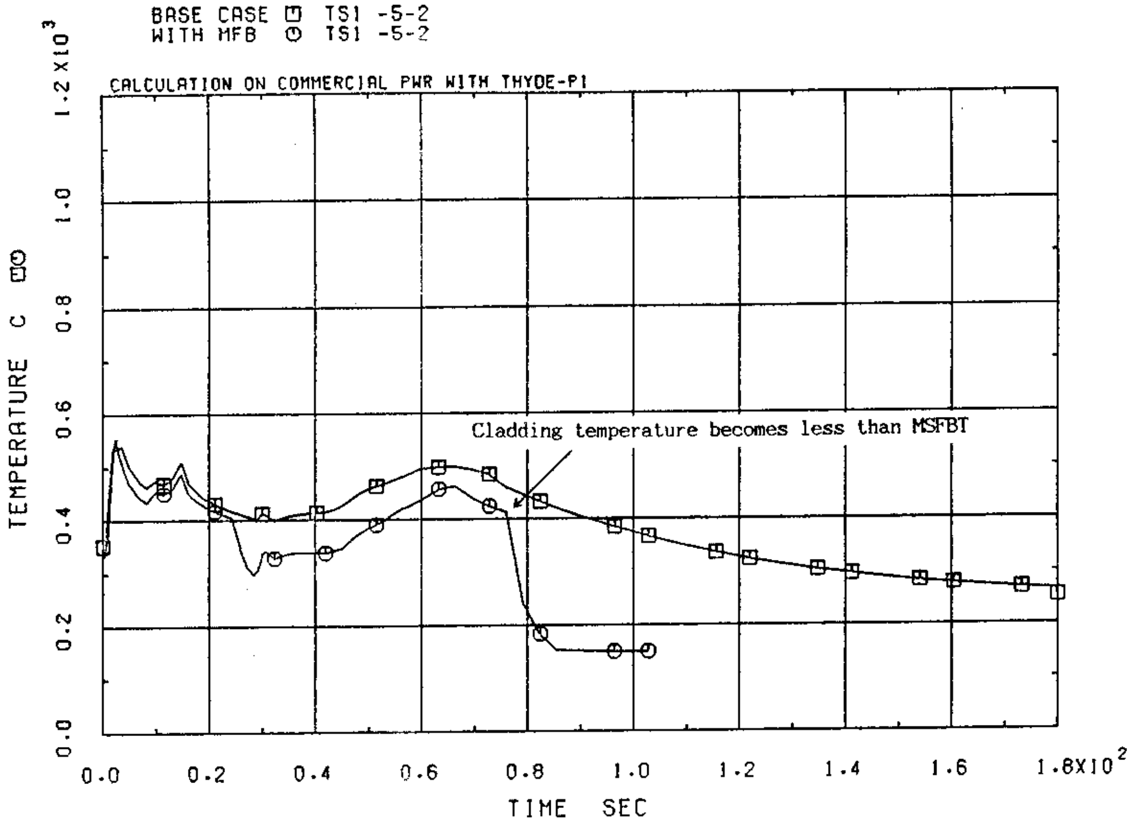

Fig.4-3-4 Cladding surface temperatures at top of hot channel

5. Conclusion

In this report, the base input for a postulated large break LOCA of a commercial PWR to be used with the published version of THYDE-P1 (SV02L03), and its calculated results have been presented. The present work has been done in order to provide users sample input data sets which can be used for a through calculation without any code modification. In the present calculation using the base input, the caldding surface temperature reached a peak of about 700°C at 50 sec after rupture, during the early portion of the reflooding. The core was reflooded at about 230 sec after rupture.

This base input has also been used as a bench mark for the sensitivity calculations (pump on and off, and selection of the CHF correlations) and a model development (a minimum stable film boiling temperature (MSFBT) model). In the sensitivity calculations for the pump operational conditions, the results were shown to be qualitatively consistent with those observed in the LOFT large break experiments. As a result from applying the present MSFBT model, quenching characteristics at high elevation were shown to be markedly improved. Such a usage of the base input has been found to be very useful and expected to be widely done.

Acknowledgement

The authors would like to express their sincere thanks to the members of Nuclear Safety Code Development Labolatory, especially to Mr. M. Akimoto, for his valuable discussions to carry out the present work.

In the present work, the SPLPLOT-1 program, which has been developed by Mr. K. Muramatsu in the labolatory, was used to plot the calculated results. The authers are also grateful to him for his appropriate suggestions.

5. Conclusion

In this report, the base input for a postulated large break LOCA of a commercial PWR to be used with the published version of THYDE-P1 (SV02L03), and its calculated results have been presented. The present work has been done in order to provide users sample input data sets which can be used for a through calculation without any code modification. In the present calculation using the base input, the caldding surface temperature reached a peak of about 700°C at 50 sec after rupture, during the early portion of the reflooding. The core was reflooded at about 230 sec after rupture.

This base input has also been used as a bench mark for the sensitivity calculations (pump on and off, and selection of the CHF correlations) and a model development (a minimum stable film boiling temperature (MSFBT) model). In the sensitivity calculations for the pump operational conditions, the results were shown to be qualitatively consistent with those observed in the LOFT large break experiments. As a result from applying the present MSFBT model, quenching characteristics at high elevation were shown to be markedly improved. Such a usage of the base input has been found to be very useful and expected to be widely done.

Acknowledgement

The authors would like to express their sincere thanks to the members of Nuclear Safety Code Development Labolatory, especially to Mr. M. Akimoto, for his valuable discussions to carry out the present work.

In the present work, the SPLPLOT-1 program, which has been developed by Mr. K. Muramatsu in the labolatory, was used to plot the calculated results. The authers are also grateful to him for his appropriate suggestions.

References

(1) Asahi, Y., "Description of THYDE-P Code (Preliminary Report of Methods and Models)", JAERI-M 7751, 1978.

(2) Asahi, Y., "User's Manual for THYDE-P1", JAERI-M 82-38, 1982.

(3) Asahi, Y. and Hirano, M., "Verification Study of LOCA Analysis Code THYDE-P (Sample Calculation Run 10)", JAERI-M 8560, 1979.

(4) Shimizu, T. and Asahi, Y., "A Through Calculation of 1,100 MWe PWR Large Break LOCA by THYDE-P code 1 (Sample Calculation Run 20)", JAERI-M 9819, 1981.

(5) Hirano, M. and Asahi, Y., "Through Analysis of LOFT L2-2 by THYDE-P Code (1) (Sample Calculation Run 30)", JAERI-M 9535, 1981.

(6) Hirano, M., "Through Analysis of LOFT L2-3 by THYDE-P Code (Sample Calculation Run 40)", JAERI-M 9765, 1981.

(7) Hirano, M. and at al., "Analysis of LOFT Small Break Experiment L3-1 with THYDE-P Code (CSNI International Standard Problem No. 9 and THYDE-P Sample Calculation Run 50)", JAERI-M 82-008, 1982.

(8) Hirano, M., "Analysis of LOFT L3-6/L8-1 with THYDE-P (CSNI International Standard Problem No. 11 and THYDE-P Sample Calculation Run 60)", JAERI-M 82-028, 1982.

(9) Kosugi, S. and Asahi, Y., "Analysis of PKL K9 by THYDE-P Code (CSNI ISP No. 10 and THYDE-P Sample Calculation Run 70)", JAERI-M 82-115, 1982.

(10) Chalton, et al., "RELAP4/MOD5 User's Manual Volume 3 (Checkout Applications)", ANCR-NUREG-1335(Vol. 3), 1976.

(11) Prassions, P. G., "Experimental Data Report for LOFT Power Ascension Test L2-3", NUREG/CR-0792 TREE-1326, July 1979.

(12) Bayless, P. D., et al., "Experimental Data Report for Large Break Loss-of-Coolant Experiment L2-5", NUREG/CR-2826 EGG-2210, August 1982.

(13) Adams, P. J., "Quick-Look Report of LOFT Nuclear Experiment L2-5", EGG-LOFT-5921, June 1982.

(14) Thermal Reactor Safety Group, TRAC-P1 : An Advanced Best-Estimate Computer Program for PWR LOCA Analysis, Los Alamos Scientific Laboratory (undated).

(15) Berenson, P. J., "Film-Boiling Heat Transfer from a horizontal surface", ASME paper 60-WA-147, 1960.

(16) Henry, R. E, "A Correlation for a Minimum Filim Boiling Temperature", AIChE Symposium Series 138, 81-90, 1974.

(17) Fauske, H. K., "Some Aspects of Liquid-Liquid Heat Transfer and Explosive Boiling", Proceedings of Fast Reactor Safety Meeting, Vol. 2, pp. 992-1005, Beverly Hills, CA, 1974.

(18) Bjornard, T. A. and Griffith, P., "PWR Blowdown Heat Transfer", in Thermal and Hydraulic Aspects of Nuclear Reactor Safety, Vol. 1, pp. 17-41, American Society of Mechanical Engineers, New York, 1977.

(19) Moore, K. V., "RELAP4 A Computer Program for Transient Thermal-Hydraulic Analysis", ANCR-1127, December 1973.

(20) Biasi, L. et al., " Studies on Burnout : Part 3", Energia Nucleare, pp 550-536, 1967.

(21) Slifer, B. S. and Hench, J. E., "Loss-of-Coolant and Emergency Core Cooling Models for General Electric Boiling Water Reactors", NEDO-10329, General Electric Company, April 1971.

(22) Gellerstedt, J. S. et al., "Correlation of Critical Heat Flux in a Bundle Cooled by Pressurized Water", pp 63-71 of Two-Phase Flow and Heat Transfer in Rod Bundles, Symposium presented at the Winter Annual Meeting of the American Society of Mechanical Engeneers, Loss Angeles, Calfornia, November 1969.

(23) Barnett, P. G., "A Correlation of Burnout Data for Uniformly Heated Annuli and Its Use for Predicting Burnout in Uniformly Heated Rod Bundles", AEEW-R 463, 1966.

(24) Hughes, E. D., "A Correlation of Rod Bundle Critial Heat Flux for Water in the pressur Range 150 to 725 psia", IN-1421, July 1970.

(25) Zuber, N. et al, " The Hydrodynamic Crisis in Pool Boiling of Saturated and Subcooled Liquids", International Developments in Heat Transfer, Part II, pp 230-236, 1961.

(26) Murao, Y., "An Analytical Study of the Thermal-Hydrodynamic Behavior of the Reflood-Phase Dring a LOCA", KFK-2545, 1977.

Appendix A　Input data list

```
 LARGE BREAK OF 1,100 MWE PWR (2 CHANNELS) * DATA 1 * 82.07.09
/
/  **** DIMENSION DATA ****
BB01
  0  0  9  4  16  49  40  9 2  2  2  2  3  6  5  3 0 2
/
/  **** MINOR EDIT DATA ****
BB02
PRE-08  PRA-12  GLA-23  GLA-29  GLE-35  GLE-36  GLA-37  GLA-38  PRA-26
/
/  **** TIME STEP CONTROL DATA ****
BB03
SB0301
   0.2  0.2  100.
SB0302
   20   3  50   0  1.0E-3  1.0E-6  0.3  0.1
SB0303
   200  3  50   0  8.0E-3  1.0E-6  60.0  0.1
SB0304
   200  3  50   0  16.0E-3  1.0E-6  90.0  0.1
SB0305
   200  3  50   0  32.0E-3  1.0E-6  2000.0  0.1
/
/  **** TRIP CONTROLL DATA ****
BB04
SB0480
  1  0  1  0  1000.0      0.0
SB0481
  5 46  1  0     0.4      0.0
SB0482
  5 47  1  0     0.4      0.0
SB0483
  2  8  1  0     0.01     0.0
SB0484
 2  19  1  0     0.01     0.0
SB0485
  3  0  1  0     0.01     0.0
SB0486
  4  1  1  0    25.01     0.0
SB0487
 -4  1  1  0  1000.0      0.
SB0488
  4  2  1  0    25.01     0.0
SB0489
 -4  2  1  0  1000.0      0.
SB0492
  6  1 -3  1   240.0      0.005
SB0493
  6  2 -3  1   250.0      0.0
SB0494
```

```
----*----1----*----2----*----3----*----4----*----5----*----6----*----7-R--*----8
  6  3 -3  1    360.0       0.0                                          00005100
SB0495                                                                   00005200
 -6  1  3  1    350.0       0.0                                          00005300
SB0496                                                                   00005400
 -6  2  3  1    305.0       0.0                                          00005500
SB0497                                                                   00005600
 -6  3  3  1    380.0       0.00                                         00005700
/                                                                        00005800
/  **** FLOW AJUST DATA ****                                             00005900
BB05                                                                     00006000
  1  9000.0  360.0                                                       00006100
/                                                                        00006200
/  **** NODE DATA ****                                                   00006300
BB06                                                                     00006400
SB0601                                                                   00006500
 1  1 26  1  0  1      158.4538  0.737 0.  5.24  0.0                     00006600
                       0.043 0.084  0.0  0.0                             00006700
SB0602                                                                   00006800
 2  1  1  2  0  1      158.9708  1.92  0.  1.665 1.665                   00006900
                       3.73  1.97   0.0  0.0                             00007000
SB0603                                                                   00007100
 3  7  2  3  1 3265    158.7624  0.0197 0. 5.0   5.0                     00007200
                       0.033 0.048  0.0  0.0                             00007300
SB0604                                                                   00007400
 4  7  3  4  1 3265    158.1581   0.0197 0. 5.46  5.46                   00007500
                       0.0   0.0    0.0   0.0                            00007600
SB0605                                                                   00007700
 5  7  4  5  1 3265    157.4898  0.0197 0. 10.46 -10.46                  00007800
                       0.0   0.0  0.033   0.048                          00007900
SB0606                                                                   00008000
 6  1  5  6  0  1      157.7862  1.92  0.  1.665 -1.665                  00008100
                       0.0   0.0   3.73   1.97                           00008200
SB0607                                                                   00008300
 7  1  6  7  0  1      157.4466  0.787 0.  7.34 -3.54                    00008400
                       0.042 0.077   -1.   -1.                           00008500
SB0608                                                                   00008600
 8  8  7 34  0  1      157.5243  0.737 0.  5.57635  3.54                 00008700
                       -1.   -1.   0.2029  0.2027                        00008800
SB0609                                                                   00008900
 9  1 34  8  0  1      162.0607  0.699 0.  2.825  0.0                    00009000
                       0.0   0.0   0.0   0.0                             00009100
SB0610                                                                   00009200
10  1  8 29  0 1       162.0332   0.699 0.  3.13  0.0                    00009300
                       0.0   0.0   0.0   0.0                             00009400
SB0611                                                                   00009500
11  1 26 27  0 3       158.4538  0.737  0.  2.0 0.                       00009600
                       0.043 0.083  0.0   0.0                            00009700
SB0612                                                                   00009800
12  1 27  9  0 3       158.4334   0.737  0.  3.24 0.                     00009900
                       0.0   0.0   0.0   0.0                             00010000
SB0613                                                                   00010100
13  1  9 10  0 3       158.9528  1.92  0.  1.665  1.665                  00010200
                       3.73  1.97  0.0   0.0                             00010300
SB0614                                                                   00010400
14  7 10 11  1 9795    158.7445  0.0197 0. 5.0  5.0                      00010500
                       0.033 0.048  0.0   0.0                            00010600
SB0615                                                                   00010700
15  7 11 12  1 9795    158.1387   0.0197 0. 5.46 5.46                    00010800
                       0.0   0.0   0.0   0.0                             00010900
```

```
----*----1----*----2----*----3----*----4----*----5----*----6----*----7-R--*----8
SB0616                                                                  00011000
16  7 12 13   1 9795  157.4691  0.0197 0. 10.46 -10.46                  00011100
                      0.0   0.0  0.033  0.048                           00011200
SB0617                                                                  00011300
17  1 13 14   0   3   157.7645   1.92  0.  1.665  -1.665                00011400
                      0.0   0.0   3.73  1.97                            00011500
SB0618                                                                  00011600
18  1 14 15   0   3   157.4249  0.787 0.  7.34 -3.54                    00011700
                      0.042  0.077  -1.   -1.                           00011800
SB0619                                                                  00011900
19  8 15 28   0   3   157.5027  0.737 0.  5.57635  3.54                 00012000
                      -1.   -1.    0.2029  0.2027                       00012100
SB0620                                                                  00012200
20  1 28 29   0 3     162.0373  0.699 0. 5.955    0.                    00012300
                      0.0   0.0    0.0   0.0                            00012400
SB0621                                                                  00012500
21  4 29 16   0 1     162.4638   1.869 0. 7.248 -7.248                  00012600
                      0.0   0.0    0.0   0.0                            00012700
SB0622                                                                  00012800
22  5 16 30   0 1     162.9140  2.487 0. 6.075 1.948                    00012900
                      0.0   0.0    0.0   0.0                            00013000
SB0623                                                                  00013100
23  2 30 17   0 39170 162.6047  1.0   0. 0.23  0.23                     00013200
                      0.74  0.74   0.0   0.0                            00013300
SB0624                                                                  00013400
24  2 17 18   1 39170 162.1173  1.0   0. 0.80  0.80                     00013500
                      0.0   0.0    0.0   0.0                            00013600
SB0625                                                                  00013700
25  2 18 31   1 39170 161.5410  1.0   0. 0.80  0.80                     00013800
                      0.0   0.0    0.0   0.0                            00013900
SB0626                                                                  00014000
26  2 31 19   1 39170 160.9517  1.0   0. 0.80  0.80                     00014100
                      0.0   0.0    0.0   0.0                            00014200
SB0627                                                                  00014300
27  2 19 20   1 39170 160.3296  1.0   0. 0.80  0.80                     00014400
                      0.0   0.0    0.0   0.0                            00014500
SB0628                                                                  00014600
28  2 20 33   0 39170 159.7062  1.0   0. 0.23  0.23                     00014700
                      0.0   0.0    0.0   0.0                            00014800
SB0629                                                                  00014900
29  2 30 21   0 200   162.6047  1.0   0. 0.23  0.23                     00015000
                      1.284  2.482  0.0  0.0                            00015100
SB0630                                                                  00015200
30  2 21 22   1 200   162.1173  1.0   0.  0.80  0.80                    00015300
                      0.0   0.0    0.0   0.0                            00015400
SB0631                                                                  00015500
31  2 22 32   1 200   161.5410  1.0   0.  0.80  0.80                    00015600
                      0.0   0.0    0.0   0.0                            00015700
SB0632                                                                  00015800
32  2 32 23   1 200   160.946155  1.0  0.  0.80  0.80                   00015900
                      0.0   0.0    0.0   0.0                            00016000
SB0633                                                                  00016100
33  2 23 24   1 200   160.3296  1.0   0.  0.80  0.80                    00016200
                      0.0   0.0    0.0   0.0                            00016300
SB0634                                                                  00016400
34  2 24 33   0 200   159.7062  1.0   0.  0.23  0.23                    00016500
                      0.76  0.34   0.0   0.0                            00016600
SB0635                                                                  00016700
35  3 30 33   0  1    162.6047  0.555 0.  3.66  3.66                    00016800
```

```
----*----1----*----2----*----3----*----4----*----5----*----6----*----7-R--*----8
                        0.77  0.83   0.87  0.78                             00016900
SB0636                                                                      00017000
36  1 32 31   0 200    161.029550  0.034 0.  0.1    0.                      00017100
                        0.0   0.0    0.0   0.0                              00017200
SB0637                                                                      00017300
37  1 33 26   0  1     159.17209  3.44  0.  4.341  1.64                     00017400
                        0.0   0.0    0.0   0.0                              00017500
SB0638                                                                      00017600
38 13 26 40   0  1       5.0   2.216 0.  3.658  2.073                       00017700
                         1.491E4  1.491E4  0.0   0.0                        00017800
SB0639                                                                      00017900
39 13 27 25   0  1       5.0   0.29  0.  15.0   1.7                         00018000
                         0.41  0.87   0.0   0.0                             00018100
SB0640                                                                      00018200
40 13 25 35   0  1       5.0   0.29  0.  14.3   1.6                         00018300
                         0.0   0.0    0.0   0.0                             00018400
SB0641                                                                      00018500
41 13 28 37   0  3      10.0   0.305 0.   12.0  0.0                         00018600
                         0.0   0.0    0.0   0.0                             00018700
SB0642                                                                      00018800
42 13 34 38   0  1      10.0   0.305 0.   12.0  0.0                         00018900
                         0.0   0.0    0.0   0.0                             00019000
SB0643                                                                      00019100
43 13 28 36   0  3      10.0   0.222 0.  120.0  0.0                         00019200
                         0.109  0.049  0.0  0.0                             00019300
SB0644                                                                      00019400
44 13 34 39   0  1      10.0   0.222 0.  120.0  0.0                         00019500
                         0.109  0.049  0.0  0.0                             00019600
/                                                                           00019700
/  **** JUNCTION DATA ****                                                  00019800
BB07                                                                        00019900
    1    1    0.0                                                           00020000
    2    1    0.0                                                           00020100
    3    1    0.0                                                           00020200
    4    1    0.0                                                           00020300
    5    1    0.0                                                           00020400
    6    1    0.0                                                           00020500
    7    1    0.0                                                           00020600
    8    1    0.0                                                           00020700
    9    1    0.0                                                           00020800
   10    1    0.0                                                           00020900
   11    1    0.                                                            00021000
   12    1    0.0                                                           00021100
   13    1    0.0                                                           00021200
   14    1    0.0                                                           00021300
   15    1    0.0                                                           00021400
   16    1    0.0                                                           00021500
   17    1    0.0                                                           00021600
   18    1    0.0                                                           00021700
   19    1    0.0                                                           00021800
   20    1    0.0                                                           00021900
   21    1    0.                                                            00022000
   22    1    0.                                                            00022100
   23    1    0.                                                            00022200
   24    1    0.                                                            00022300
   25    1    0.                                                            00022400
   26    2    1.027                                                         00022500
   27    4    0.049                                                         00022600
   28    4    0.351                                                         00022700
```

```
----*----1----*----2----*----3----*----4----*----5----*----6----*----7-R--*----8
   29   3   0.531                                                           00022800
   30   4   0.1                                                             00022900
   31   4   0.01                                                            00023000
   32   4   0.01                                                            00023100
   33   4   0.05                                                            00023200
   34   4   0.117                                                           00023300
   35   6   0.                                                              00023400
   36   5   0.                                                              00023500
   37   7   0.                                                              00023600
   38   7   0.                                                              00023700
   39   5   0.                                                              00023800
   40   8   0.                                                              00023900
/                                                                           00024000
/  **** MIXING JUNCTION DATA ****                                           00024100
BB08                                                                        00024200
SB0801                                                                      00024300
   26   3    1   11   38    0   0.25    0.75     0.     0.                  00024400
SB0802                                                                      00024500
   27   2   12   39    0    0   1.0     0.0      0.     0.                  00024600
SB0803                                                                      00024700
   28   3   20   41   43    0   1.0     0.0      0.0    0.0                 00024800
SB0804                                                                      00024900
   29   1   21    0    0    0   1.0     0.0      0.0    0.0                 00025000
SB0805                                                                      00025100
   30   3   23   29   35    0   0.945   0.005    0.05   0.0                 00025200
SB0806                                                                      00025300
   31   1   26    0    0    0   1.0     0.0       0.     0.                 00025400
SB0807                                                                      00025500
   32   2   32   36    0    0   0.99    0.01     0.     0.                  00025600
SB0808                                                                      00025700
   33   1   37    0    0    0   1.0     0.0      0.0    0.0                 00025800
SB0809                                                                      00025900
   34   3    9   42   44    0   1.0     0.0      0.0    0.0                 00026000
/                                                                           00026100
/  **** PUMPED INJECTION DATA ****                                          00026200
BB09                                                                        00026300
SB0901                                                                      00026400
    1   37     30.0                                                         00026500
   2  1                                                                     00026600
   0.0    666.0  1000.0   666.0                                             00026700
SB0902                                                                      00026800
    2   38     30.0                                                         00026900
   2  1                                                                     00027000
   0.0    222.0  1000.0   222.0                                             00027100
/                                                                           00027200
/  **** PUMP DATA ****                                                      00027300
BB10                                                                        00027400
SB1001                                                                      00027500
   8  1 1 1185.0   5.58   4.33E4   105.0 749.0   1150.0   3460.0   0.5   0.0  00027600
   0.05                                                                     00027700
SB1002                                                                      00027800
  19 1 1 1185.0    5.58   4.33E4   105.0 749.0   1150.0   3460.0   0.5   0.0  00027900
   0.05                                                                     00028000
/                                                                           00028100
/  **** PUMP DATA TABLE ****                                                00028200
BB11                                                                        00028300
SB1101                                                                      00028400
 1                                                                          00028500
 14                                                                         00028600
```

```
----*----1----*----2----*----3----*----4----*----5----*----6----*----7-R--*----8
 -1.0  1.56        -0.85 1.33        -0.80 1.28        -0.72 1.30       00028700
 -0.62 1.35        -0.50 1.36       -0.34 1.34         -0.21 1.29       00028800
 -0.11 1.23         0.0  1.22         0.25 1.16         0.50 1.13       00028900
  0.75 1.07         1.0  0.98                                           00029000
 14                                                                     00029100
 -1.0        0.18  -0.85       0.34  -0.80       0.40  -0.72      0.48  00029200
 -0.62       0.556 -0.50       0.67  -0.34       0.77  -0.21      0.84  00029300
 -0.11       0.89   0.0        0.95   0.25       1.16   0.50      1.35  00029400
  0.75       1.62   1.0        1.94                                     00029500
 11                                                                     00029600
 -1.0  0.18        -0.75 -0.13       -0.50 -0.32       -0.32 -0.40      00029700
 -0.16 -0.42        0.0  -0.39        0.16 -0.28        0.32  0.16      00029800
  0.50  0.01        0.75 0.40         1.0   0.98                        00029900
 11                                                                     00030000
 -1.0        1.56  -0.75       1.12  -0.50       0.90  -0.32       0.82 00030100
 -0.16       0.76   0.0        0.71   0.16       0.71   0.32       0.76 00030200
  0.50       0.90   0.75       1.33   1.0        1.94                   00030300
 14                                                                     00030400
 -1.0  0.70        -0.90 0.70        -0.80 0.68        -0.70 0.63       00030500
 -0.60 0.53        -0.50 0.47        -0.40 0.46        -0.30 0.45       00030600
 -0.20 0.45         0.0  0.48         0.25 0.55         0.50 0.66       00030700
  0.75 0.83         1.0  1.02                                           00030800
 14                                                                     00030900
 -1.0       -1.42  -0.90      -1.32  -0.80      -1.23  -0.70      -1.14 00031000
 -0.60      -1.07  -0.50      -0.99  -0.40      -0.91  -0.30      -0.84 00031100
 -0.20      -0.77   0.0       -0.64   0.25      -0.49   0.50      -0.34 00031200
  0.75      -0.20   1.0       -1.10                                     00031300
   13                                                                   00031400
 -1.0 -1.42      -0.8 -1.12      -0.6 -0.82      -0.5 -0.68             00031500
 -0.4 -0.55      -0.2 -0.28       0.0 -0.08       0.11 0.0              00031600
  0.25 0.12       0.50 0.33       0.75 0.61       0.92 0.82             00031700
  1.0  1.02                                                             00031800
   13                                                                   00031900
 -1.0       0.70 -0.8       0.5 -0.6       0.4 -0.5       0.39          00032000
 -0.4       0.38 -0.2       0.33 0.0       0.28 0.11      0.25          00032100
  0.25      0.22  0.50      0.14 0.75      0.03 0.92      0.01          00032200
  1.0      -0.10                                                        00032300
/  2                                                                    00032400
/ 0.0 1.0  1000.0  0.5                                                  00032500
/ 2                                                                     00032600
/ -1.0  -50.0  1.0  50.0                                                00032700
  12                                                                    00032800
  -1.0   -1.15       -0.9  -1.24       -0.6   -2.8       -0.5  -2.9     00032900
  -0.4   -2.7         0.0   0.0         0.12   0.85       0.2   1.1     00033000
  0.5     1.02        0.7   1.0         0.9    0.95       1.0   1.0     00033100
  4                                                                     00033200
  -1.0    0.0         0.0   0.0         0.5   -0.8        1.0  -1.46    00033300
  7                                                                     00033400
  -1.0    0.0         0.0   0.0         0.1   -0.02       0.2   0.0     00033500
   0.3    0.1         0.9   0.78        1.0    1.0                      00033600
  12                                                                    00033700
  -1.0   -1.15       -0.8  -0.5        -0.6   -0.2       -0.4   0.03    00033800
  -0.2    0.04        0.0   0.1         0.2    0.15       0.4   0.12    00033900
   0.6    0.05        0.8  -0.5         0.9   -0.9        1.0  -1.46    00034000
  0                                                                     00034100
  0                                                                     00034200
  0                                                                     00034300
  0                                                                     00034400
 13                                                                     00034500
```

```
----*----1----*----2----*----3----*----4----*----5----*----6----*----7-R--*----8
  0.0  0.0    0.05 0.0      0.1  0.025     0.15  0.075   0.2  0.18
  0.3    0.475     0.4    0.625     0.5    0.74       0.6     0.82
  0.7    0.87      0.8    0.84      0.9    0.72       1.0     0.08

 11
  0.0    0.0       0.1    0.0       0.20   0.13       0.3     0.24
  0.4    0.31      0.5    0.33      0.6    0.3        0.7     0.23
  0.8    0.16      0.9    0.08      1.0    0.0
  6  6
    0.0  0.2  0.4  0.6  0.8  1.0
  0.0  0.0  0.0  0.0  0.0  0.0  0.0
   0.2  0.0  3.065E-5  7.7239E-5  1.3263E-4  1.946E-4  2.6207E-4
  0.4  0.0  4.866E-5  1.2261E-4  2.1053E-4  3.0996E-4  4.1602E-4
  0.6  0.0  6.376E-5  1.6066E-4  2.7587E-4  4.0485E-4  5.4514E-4
  0.8  0.0  7.7239E-5  1.9463E-4  3.3419E-4  4.9044E-4  6.6037E-4
  1.0  0.0  8.9628E-5  2.2585E-4  3.878E-4  5.691E-4  7.6631E-4
/
/  **** ACCUMLATOR DATA ****
BB12
SB1201
   48   36   70.   30.   30.0   44.
  0.9  3.0
SB1202
   49   39   23.3  10.   30.0   44.
  0.9  1.0
/
/  **** BREAK POINT DATA ****
BB13
   8  0.01  0.4  0.8  0.6  0.6  0.8  0.6  0.6
   6
  0.0 1.0  7.5  2.7  15.  4.0  30.  4.0  60.  4.0  1000. 4.0
/
/  **** PRESSURIZER DATA ****
BB14
   45    35    11  3.58  15.56  9.0  0.99  0.1
         1.7  385.0
   50.0  1.0  0.1  0.0  0.0
   0.915  0.915  0.915  1.525  3.05  4.58
   0.564  0.67  0.619
      2
   0. 1.0  1.0  1.0  1000.  1.0  1.0  1.0
/
/  **** STEAM GENERATOR DATA ****
BB15
SB1501
 46 3265  3  5  3  1
 5.5   18.9  0.7  0.5    3.0E-2  1.0E-2    10.4  4.0  222.1  474.5
 0.1  0.95  62.0
      2.0  11.0
 -40.  -30.  -25.
     0.001    80.  0.5  0.5  0.5
   3
   0.0  1.0  1.0  1.0  1.0  1.0  1.0  1.0  1000.0  1.0  1.0  0.0
SB1502
  47    9795  14  16  3  1
  16.5  18.9   2.1   0.5     3.0E-2  1.0E-2    10.4  4.0  222.1 1423.5
 0.1  0.95  62.0
      2.0  11.0
  -40.0  -30.0  -25.0
     0.003    80.  0.5  0.5  0.5
```

```
----*----1----*----2----*----3----*----4----*----5----*----6----*----7-R--*----8
   3
  0.0 1.0  1.0  1.0  1.0  1.0  1.0  1.0  1000.0  1.0  1.0  0.0
/
/  **** CORE DATA ****
BB16
/    --- AVERAGE  CHANNEL -----
SB1601
  1
 39170  23  28  0  3  1  2  2
  9000.0  5.3658E-3  0.6187E-3   4.6573E-3   1.42E-2     0.6   1.0E-4
  0.0124  0.0212E-02  0.0305  0.1402E-02
  0.111  0.1254E-02  0.301  0.2529E-02
  1.13  0.0736E-02  3.00 0.0269E-02
  5.0   0.6  4.91E-04  3.41E-06  1.2  1.54E03
  0.  156.  234.  234.  156.  0.
  1.6122E-07  6.42E-07  7.56E-07  7.56E-07  6.42E-07  1.622E-07
  1.6122E-07  6.42E-07  7.56E-07  7.56E-07  6.42E-07  1.622E-07
  1.6122E-07  6.42E-07  7.56E-07  7.56E-07  6.42E-07  1.622E-07
  1.6122E-07  6.42E-07  7.56E-07  7.56E-07  6.42E-07  1.622E-07
/       --- HOT CHANNEL ---
SB1602
  2
  200     29  34  0  3  1  2  2
  9000.0  5.3665E-3  0.6187E-3   4.6682E-3   1.42E-2     0.6   1.0E-4
  0.  203.0  304.0  304.0  203.0  0.
  1.6122E-07  6.42E-07  7.56E-07  7.56E-07  6.42E-07  1.622E-07
  1.6122E-07  6.42E-07  7.56E-07  7.56E-07  6.42E-07  1.622E-07
  1.6122E-07  6.42E-07  7.56E-07  7.56E-07  6.42E-07  1.622E-07
  1.6122E-07  6.42E-07  7.56E-07  7.56E-07  6.42E-07  1.622E-07
/
/  **** REACTIVITY DATA ****
BB17
   3
  0.  0.  0.5  -5.  1.  -25.
   5
 18. 3.56E-3   538. 0.   1093. -3.08E-3   1649. -2.7E-3   2760. -2.44E-3
   5
  0.01  0.0  1.0  -0.1  1.5  -0.2  2.0  -3.0  1000. -8.0
/
/   ****METAL WATER REACTION DATA ****
BB18
   1.54E03 0.775E-04 2.29E04
/
/  **** FUEL GAP DATA ****
BB19
 0.0301  0.0  1.235E-5  0.0  0.0  0.0  0.0  0.6  0.6  0.0
 0.9495  0.0157  0.0028  0.0  0.032  0.0  0.0
/
/  **** BURST DATA  ****
BB21
2  2  5.0E7  6.96E-08  2.87E4  2.86E-03  1.15E0  1.528E0
1.49E-07  2.0E-08  1.25E-16  1.85E-01  8.0E09  3.3E-03
       0.1
/
/  **** OTHER DATA ****
BB22
   0. 1.4  1.4  0.
BEND
10
 0  0  0  0  0  15.
  0. 1.0-7 0.  -1.0E+10   0.01     0.01
  0
  0  0.0
  0  0.0
```

```
 LARGE BREAK OF 1,100 MWE PWR (2 CHANNELS) * DATA 2 * 82.07.09
/
/  **** DIMENSION DATA ****
BB01
  0  2  9  4  16  49  40  9 2  2  2  2  3  6  5  3 0 2
/
/  **** MINOR EDIT DATA ****
BB02
PRE-08  PRA-12  GLA-23  GLA-29  GLE-35  GLE-36  GLA-37  GLA-38  PRA-26
/
/  **** TIME STEP CONTROL DATA ****
BB03
SB0301
    0.2  0.2  100.
SB0302
    20  3  50   0  1.0E-3  1.0E-6  0.3  0.1
SB0303
    200 3  50   0  8.0E-3  1.0E-6  60.0  0.1
SB0304
    200 3  50   0  16.0E-3  1.0E-6  90.0  0.1
SB0305
    200 3  50   0  32.0E-3  1.0E-6  2000.0  0.1
/
/  **** TRIP CONTROLL DATA ****
BB04
SB0480
  1  0   1  0  1000.0       0.0
SB0481
  5 46   1  0     0.4       0.0
SB0482
  5 47   1  0     0.4       0.0
SB0483
  2  8   1  0     0.01      0.0
SB0484
  2  19  1  0     0.01      0.0
SB0485
  3  0   1  0     0.01      0.0
SB0486
  4  1   1  0    25.01      0.0
SB0487
 -4  1   1  0  1000.0       0.
SB0488
  4  2   1  0    25.01      0.0
SB0489
 -4  2   1  0  1000.0       0.
SB0492
  6  1 -3   1   240.0       0.005
SB0493
  6  2 -3   1   250.0       0.0
SB0494
```

```
----*----1----*----2----*----3----*----4----*----5----*----6----*----7-R--*----8
  6  3 -3  1    360.0       0.0                                             00005100
SB0495                                                                      00005200
 -6  1  3  1    350.0       0.0                                             00005300
SB0496                                                                      00005400
 -6  2  3  1    305.0       0.0                                             00005500
SB0497                                                                      00005600
 -6  3  3  1    380.0       0.00                                            00005700
BEND                                                                        00005800
10                                                                          00005900
 0  0  0  0  0  30.0                                                        00006000
  0. 1.0-7 0. -1.0E+10      0.01      0.01                                  00006100
  0                                                                         00006200
  11  0.                                                                    00006300
  7     8     9     10     18     19     20     41     42     43            00006400
  4.    4.    4.    4.     4.     4.     4.     4.     4.     4.            00006500
  44                                                                        00006600
  4.                                                                        00006700
  0   4.                                                                    00006800
```

```
 LARGE BREAK OF 1,100 MWE PWR (2 CHANNELS) * DATA 3 * 82.07.09
/
/  **** DIMENSION DATA ****
BB01
  0  2  9  4  16  49  40  9 2  2  2  2  3  6  5  3 0 2
/
/  **** MINOR EDIT DATA ****
BB02
PRE-08  PRA-12  GLA-23  GLA-29  GLE-35  GLE-36  GLA-37  GLA-38  PRA-26
/
/  **** TIME STEP CONTROL DATA ****
BB03
SB0301
    0.2  0.2  100.
SB0302
    20  3  50   0  1.0E-3  1.0E-6  0.3  0.1
SB0303
    200 3  50   0  8.0E-3  1.0E-6  60.0  0.1
SB0304
    200 3  50   0  16.0E-3  1.0E-6  90.0  0.1
SB0305
    200 3  50   0  32.0E-3  1.0E-6  2000.0  0.1
/
/  **** TRIP CONTROLL DATA ****
BB04
SB0480
  1  0  1  0  1000.0       0.0
SB0481
  5 46  1  0     0.4       0.0
SB0482
  5 47  1  0     0.4       0.0
SB0483
  2  8  1  0     0.01      0.0
SB0484
  2  19  1  0     0.01      0.0
SB0485
  3  0  1  0     0.01      0.0
SB0486
  4  1  1  0    25.01      0.0
SB0487
 -4  1  1  0  1000.0       0.
SB0488
  4  2  1  0    25.01      0.0
SB0489
 -4  2  1  0  1000.0       0.
SB0492
  6  1 -3  1   240.0       0.005
SB0493
  6  2 -3  1   250.0       0.0
SB0494
```

```
----*----1----*----2----*----3----*----4----*----5----*----6----*----7-R--*----8
  6  3 -3  1    360.0       0.0                                         00005100
SB0495                                                                  00005200
 -6  1  3  1    350.0       0.0                                         00005300
SB0496                                                                  00005400
 -6  2  3  1    305.0       0.0                                         00005500
SB0497                                                                  00005600
 -6  3  3  1    380.0       0.00                                        00005700
BEND                                                                    00005800
12                                                                      00005900
 0  0  0  0  0  250.                                                    00006000
  0. 1.0-7 0. -1.0E+10      0.01      0.01                              00006100
  0                                                                     00006200
  18  10.                                                               00006300
  21   22   23    24    25    26    27    28    29   30                 00006400
  40.  40.  4.    4.    4.    4.    4.    4.    4.   4.                 00006500
  31   32   33    34    35    36    37    8                             00006600
  4.   4.    4.    4.    4.    4.   40.   40.                           00006700
  0   10.                                                               00006800
```

Appendix B Figures showing results from base calculation

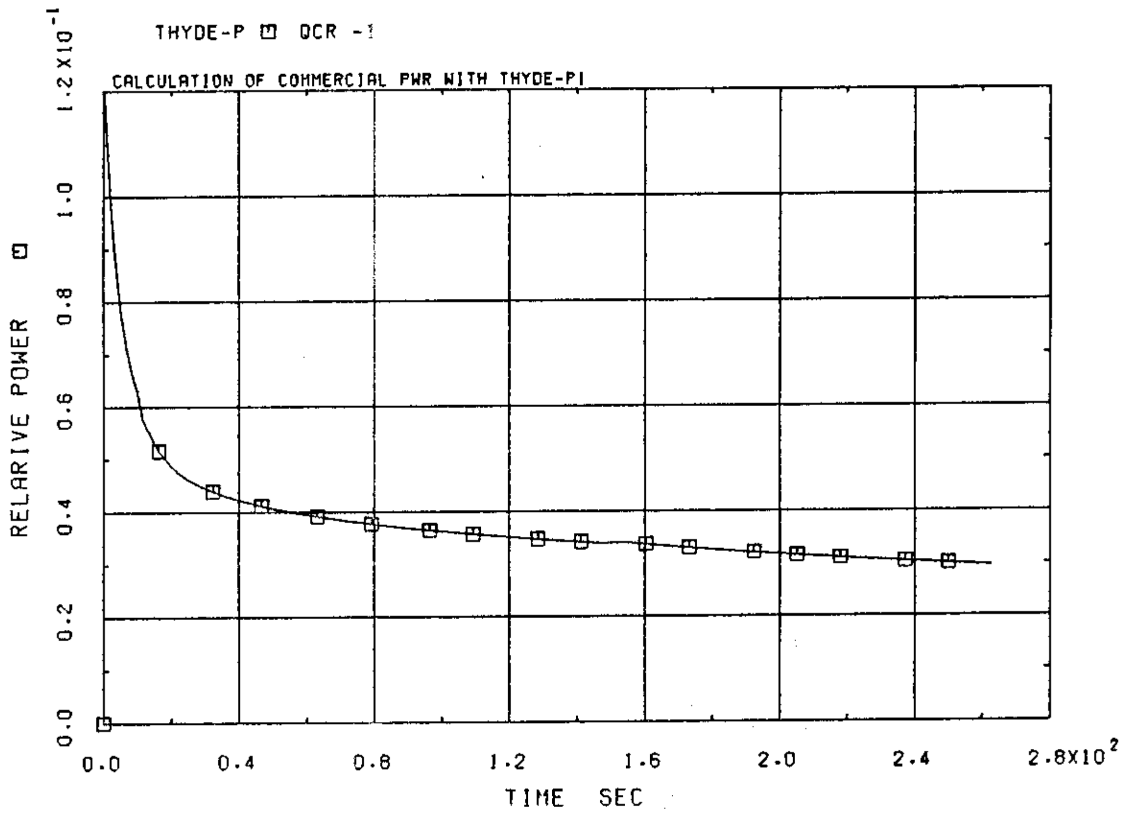

Fig.B-1 Normalized power

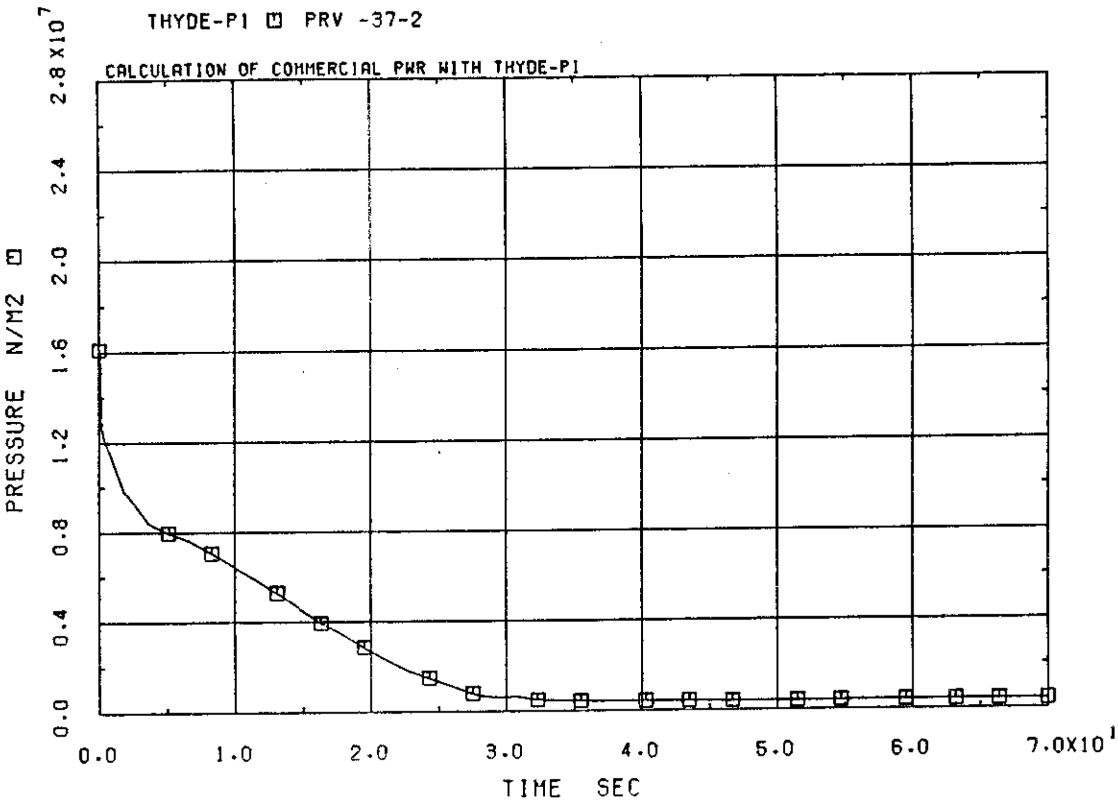

Fig.B-2-1 Upper plenum pressure (short range)

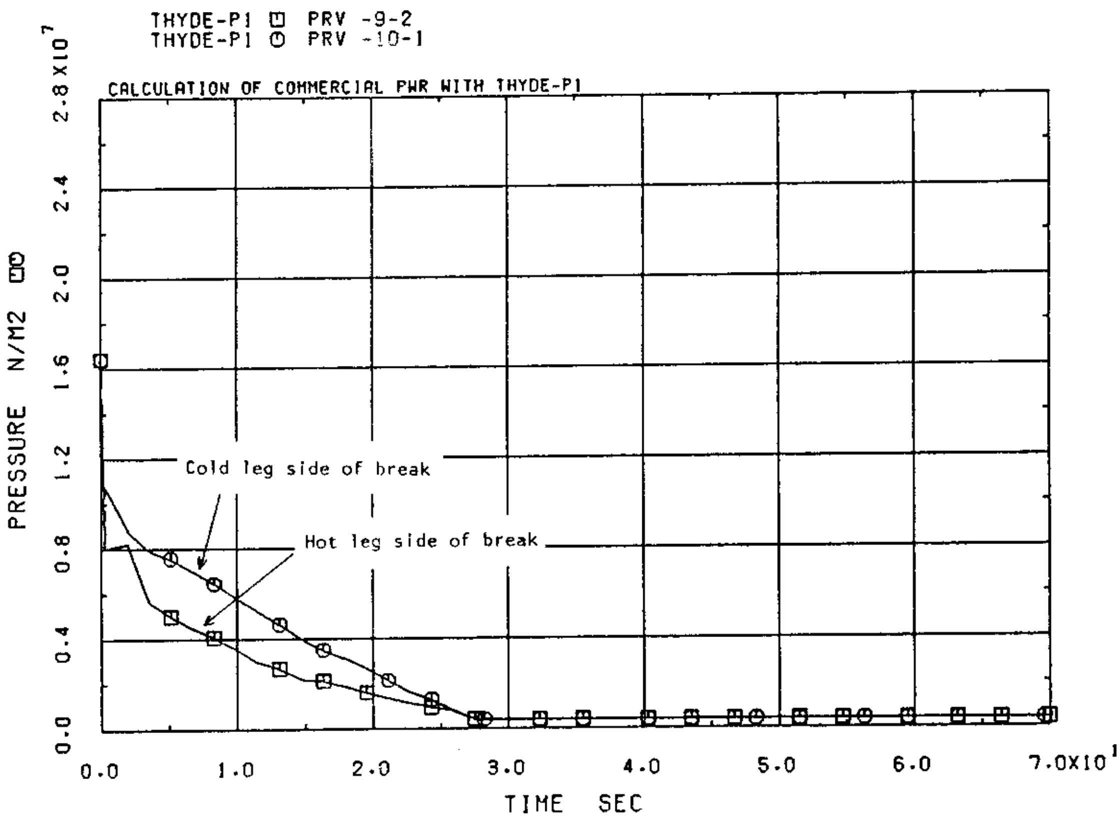

Fig.B-2-2 Break pressures (short range)

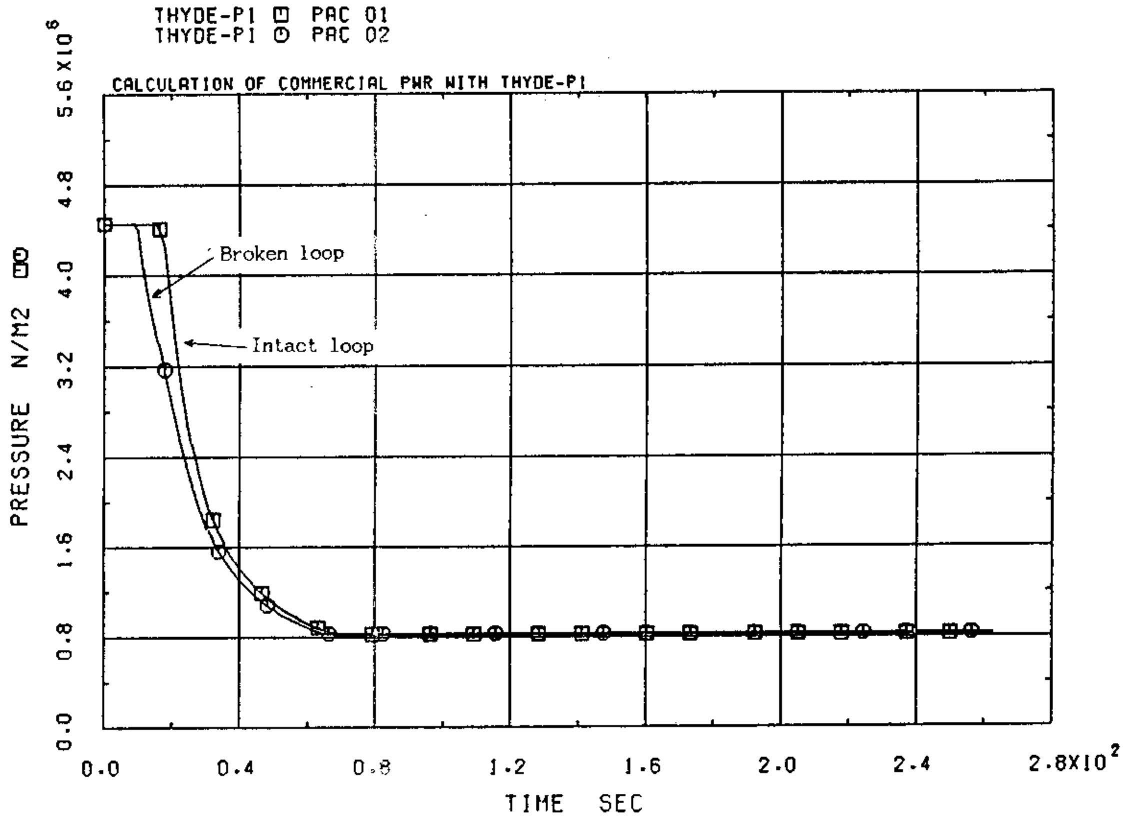

Fig.B-2-3 Accumulator pressures (short range)

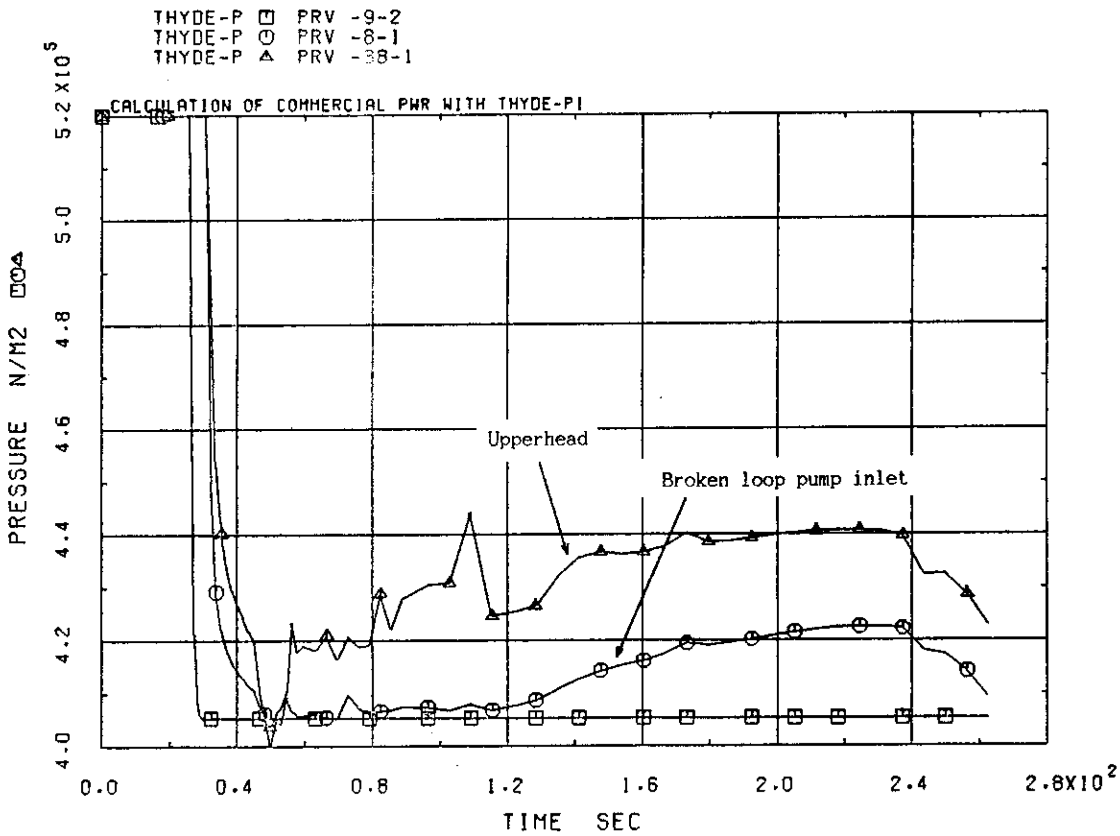

Fig.B-2-4 Pressures during reflooding (broken loop)

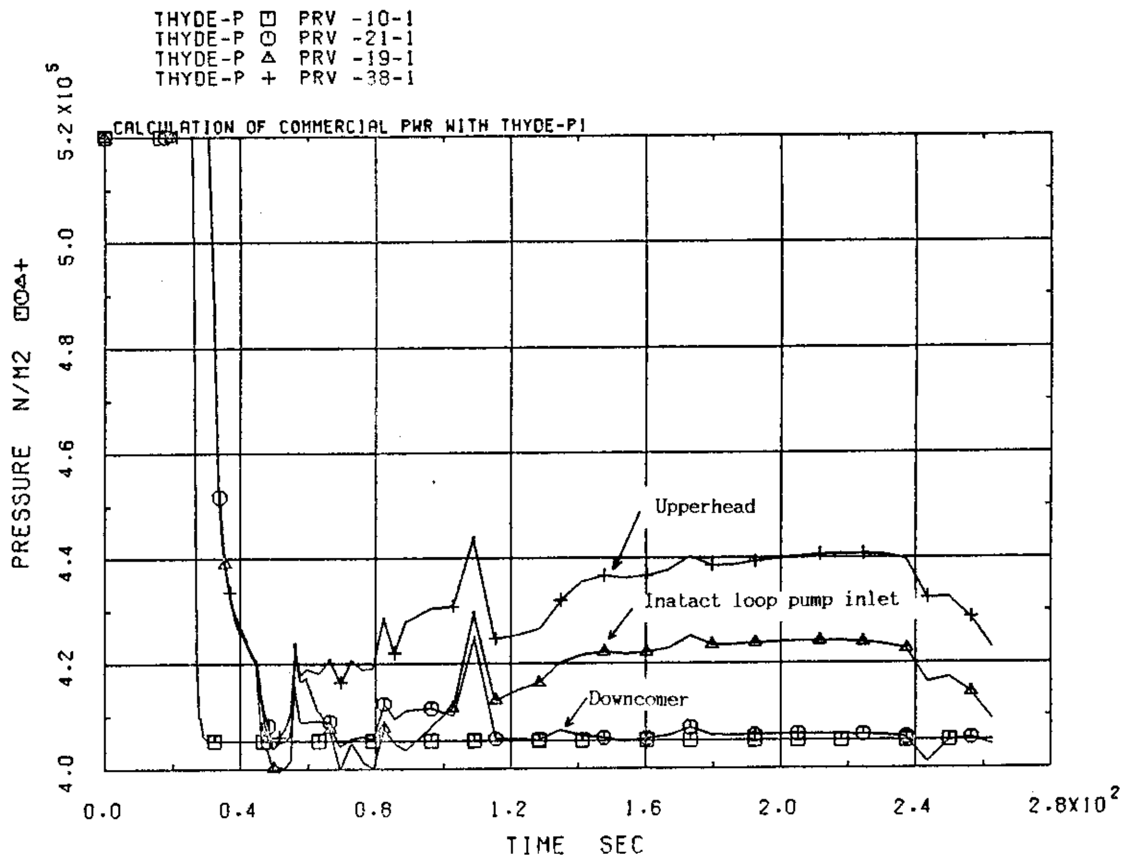

Fig.B-2-5 Pressures during reflooding (intact loop)

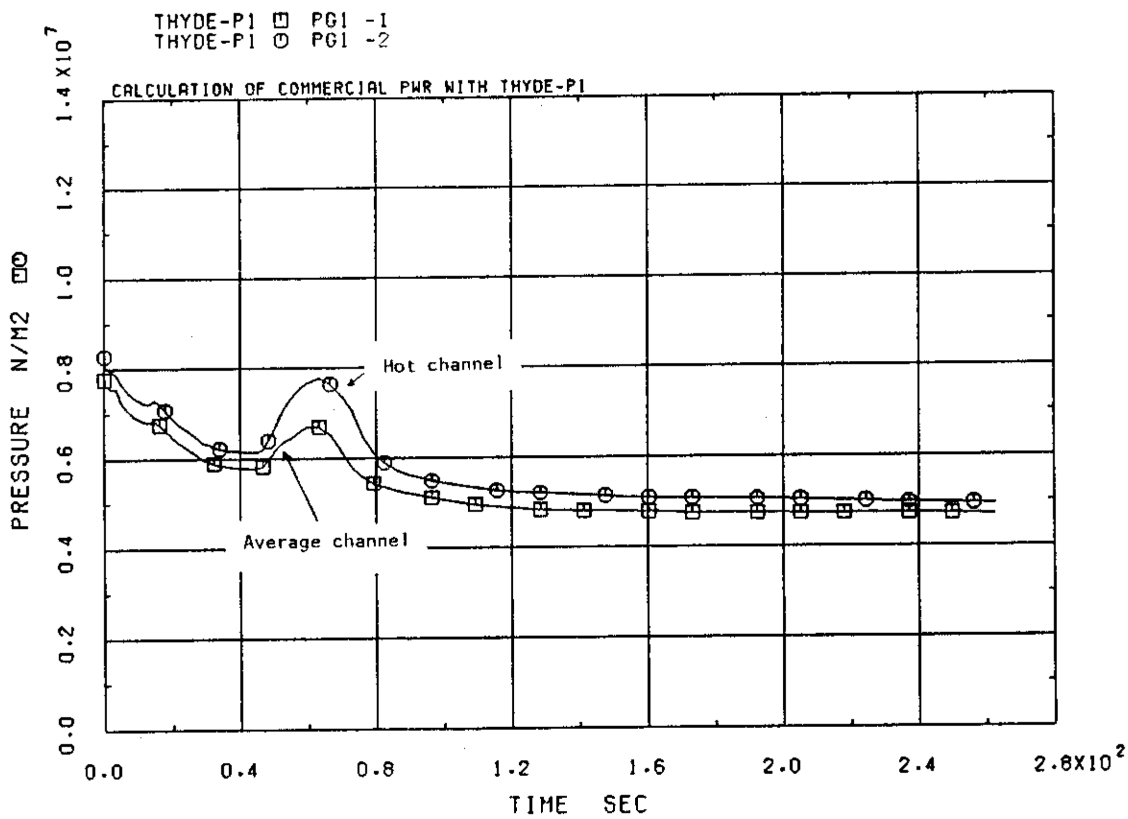

Fig.B-2-6 Gap pressures

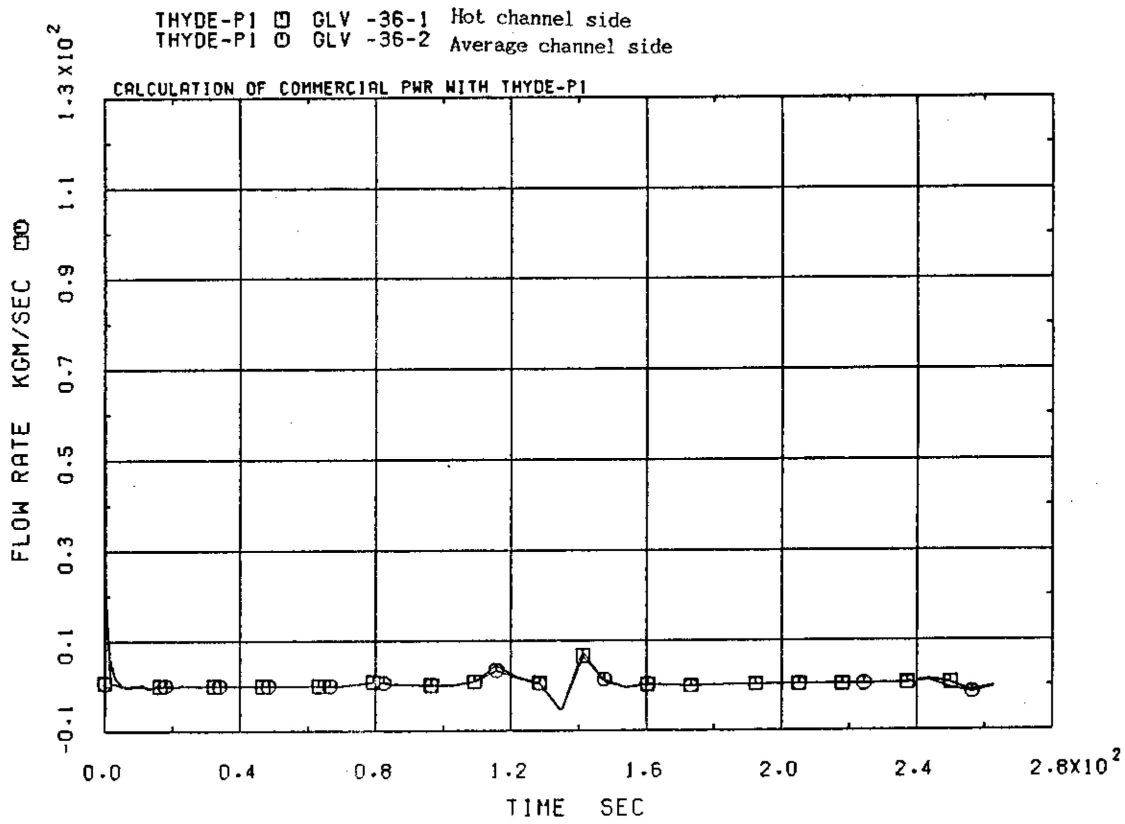

Fig.B-3-1 Mass flow rates at cross flow area

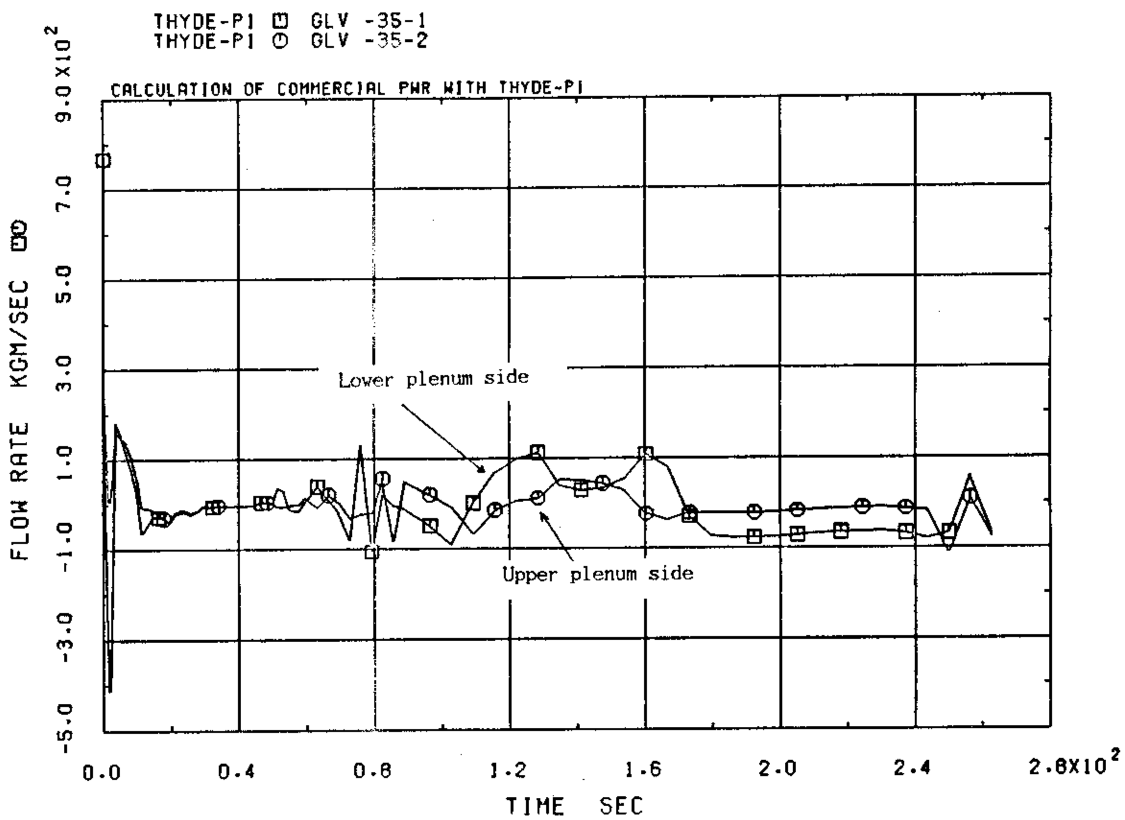

Fig.B-3-2 Mass flow rates at core bypass

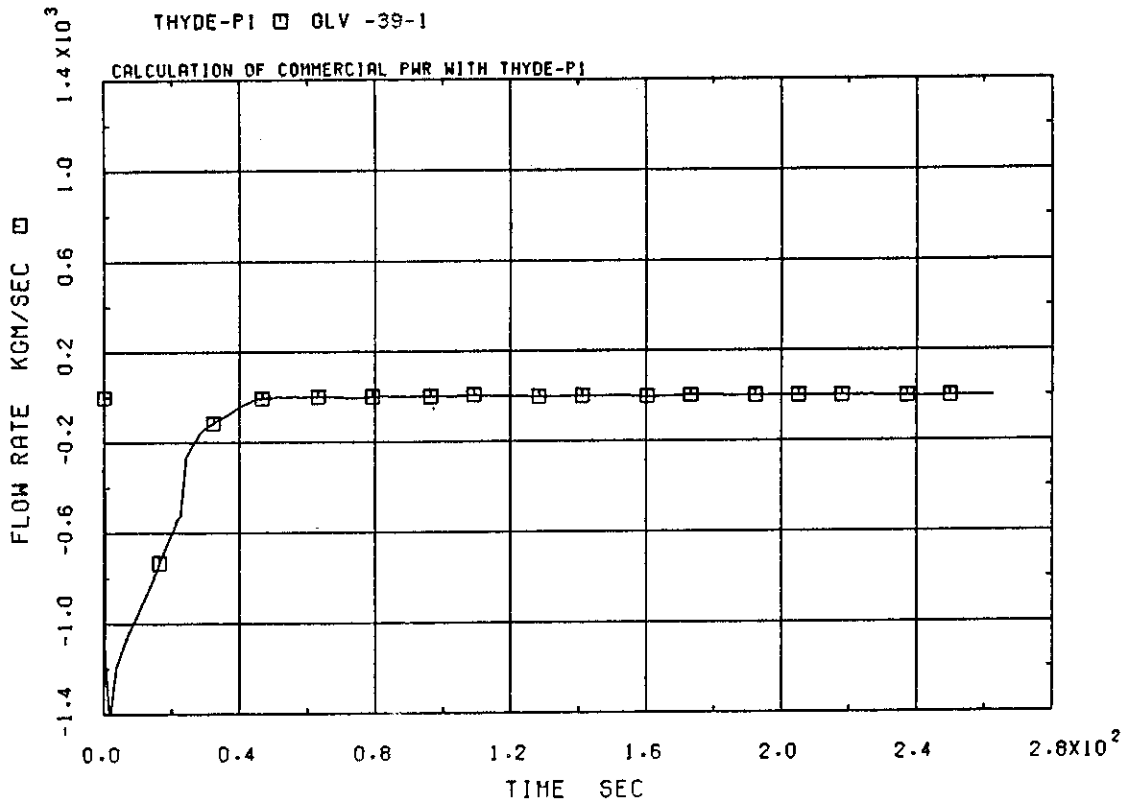

Fig.B-3-3 Mass flow rate at pressurizer surge line

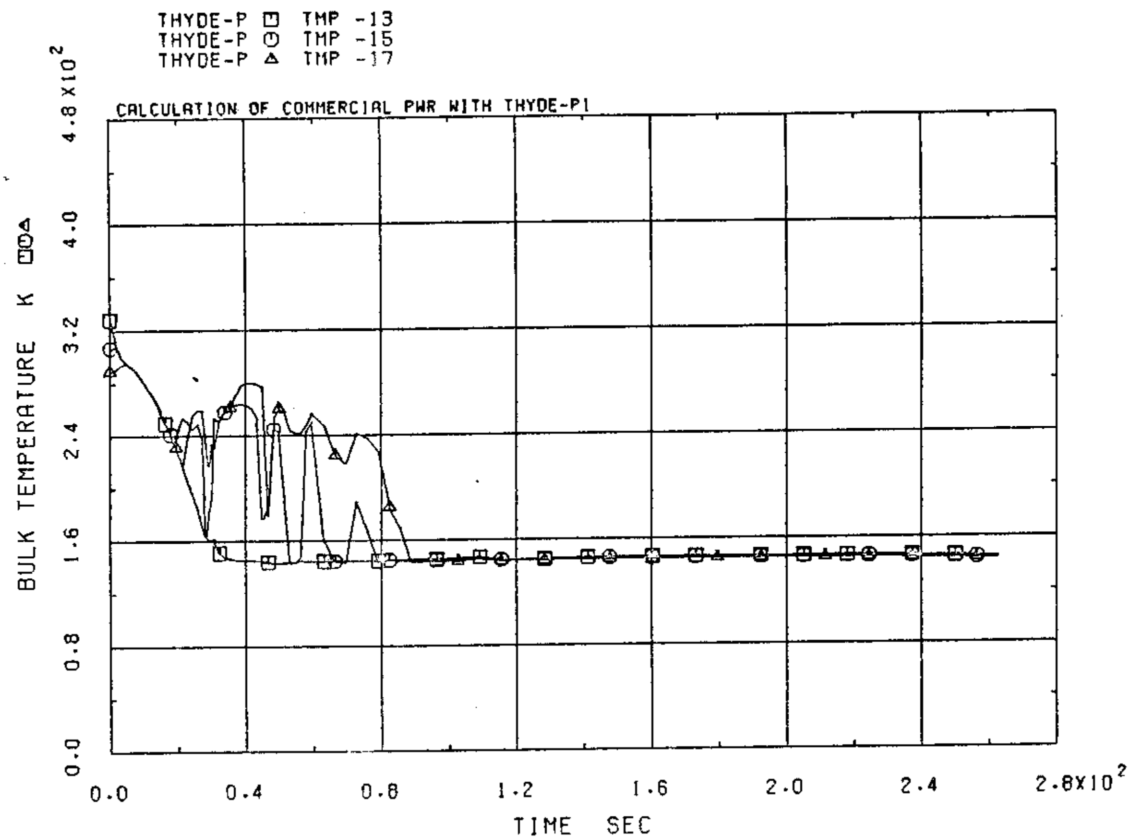

Fig.B-4-1 Coolant temperatures at SG primary system of intact loop

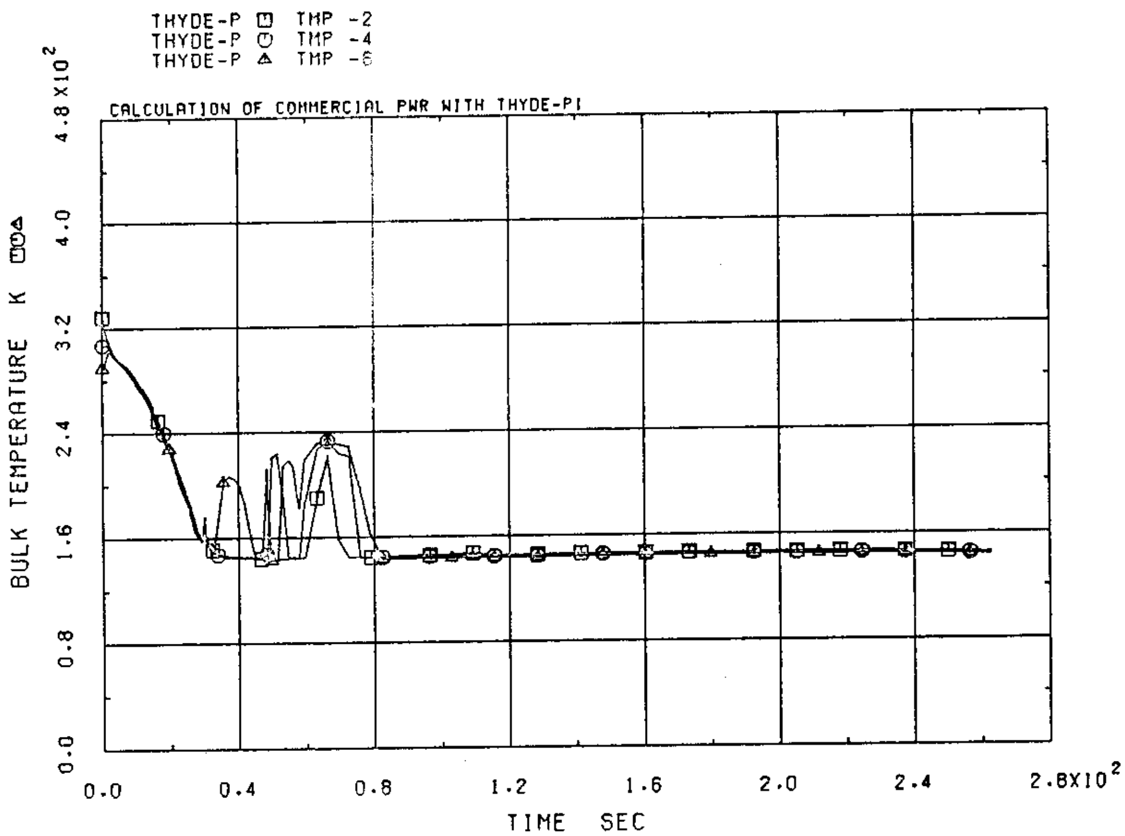

Fig.B-4-2 Coolant temperatures at SG primary system of broken loop

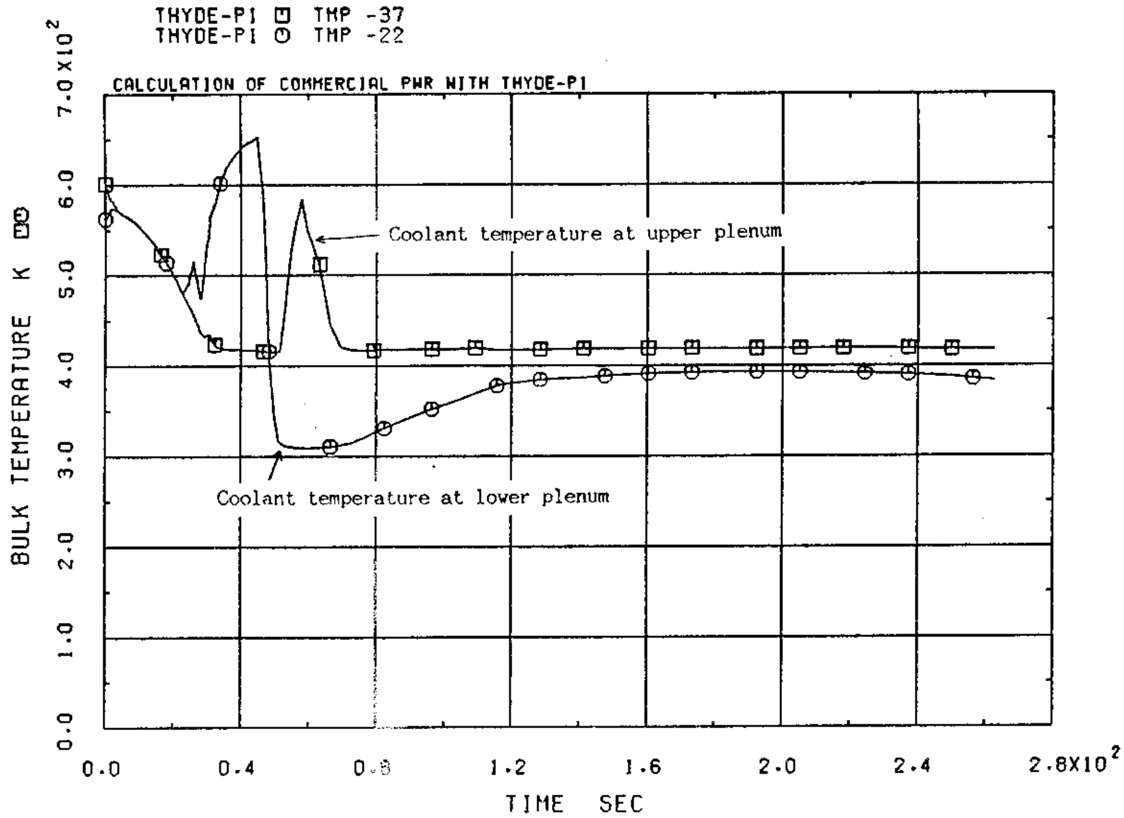

Fig.B-4-3 Coolant temperatures at upper plenum and lower plenum

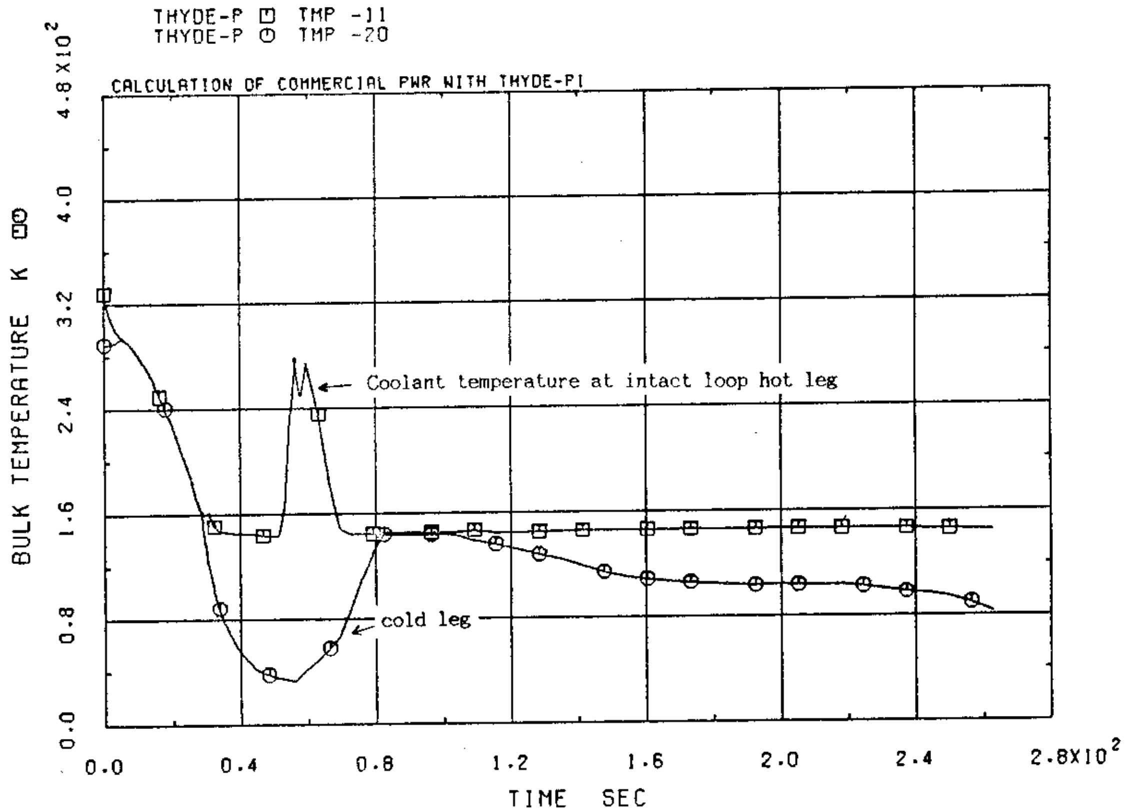

Fig.B-4-4 Coolant temperatures at intact loop hot leg and downcomer

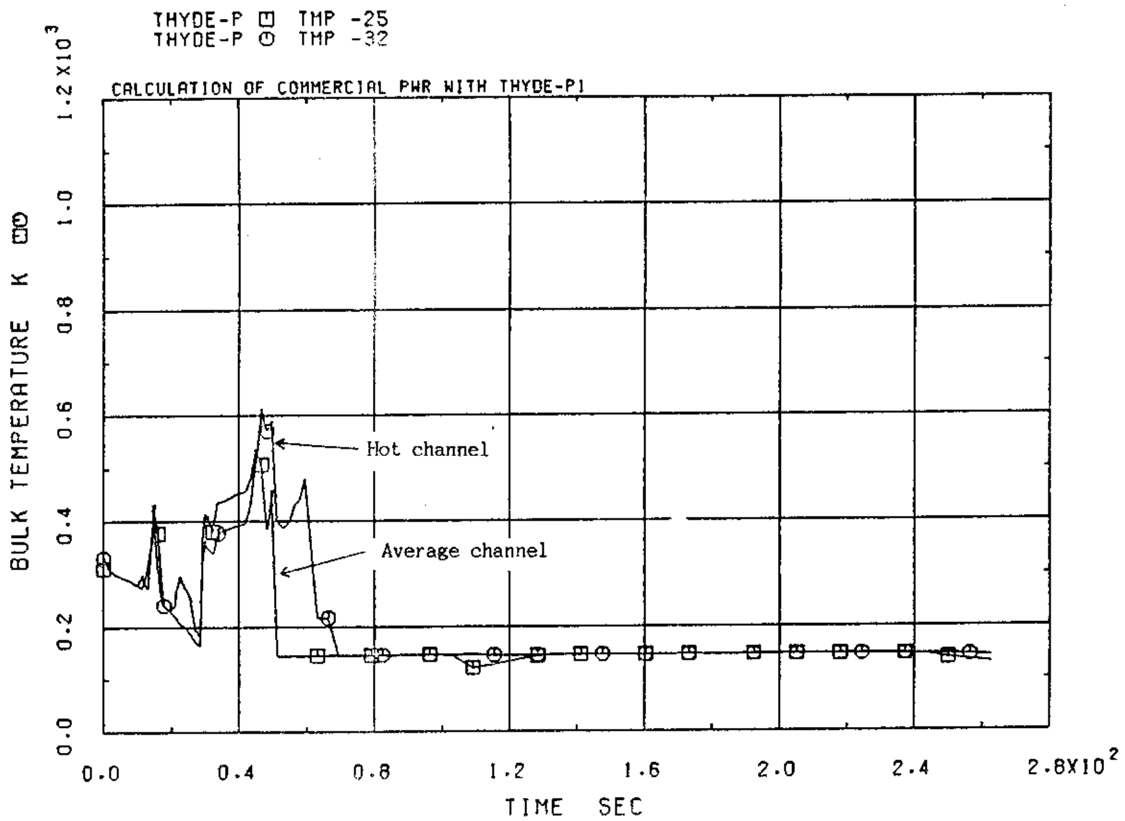

Fig.B-4-5 Coolant temperatures at middle of core

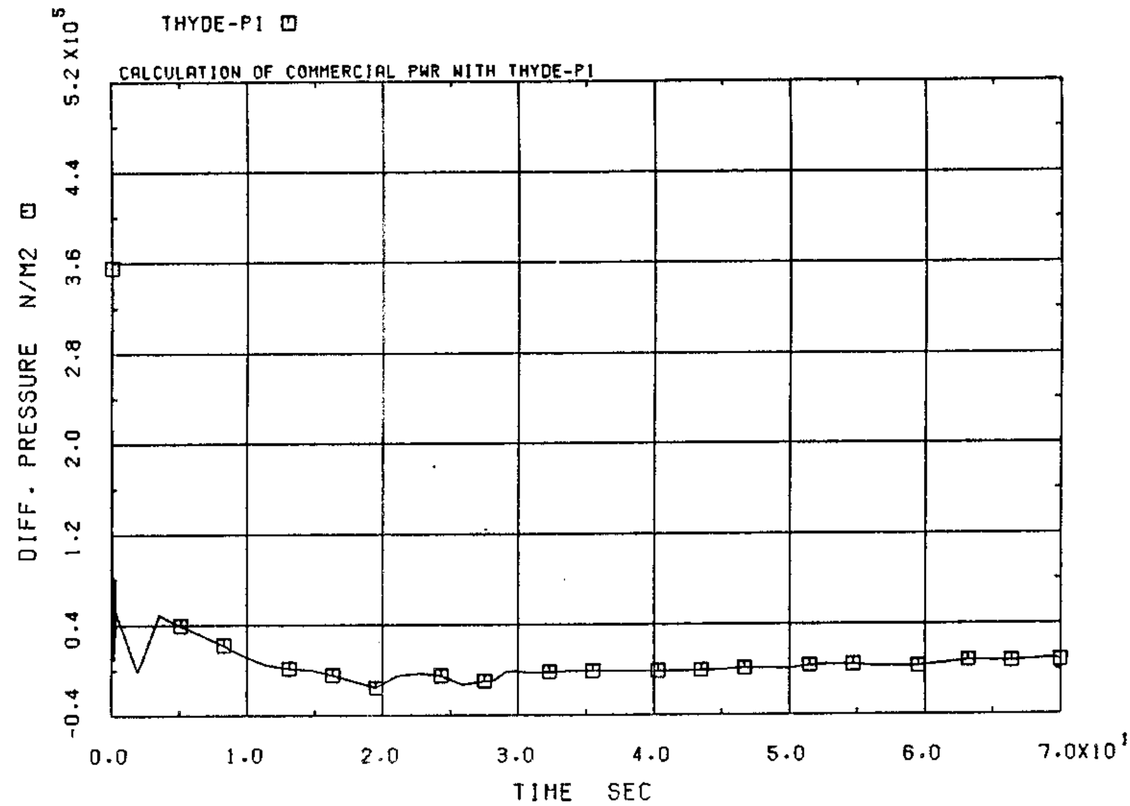

Fig.B-5-1 Differential pressure through core (short range)

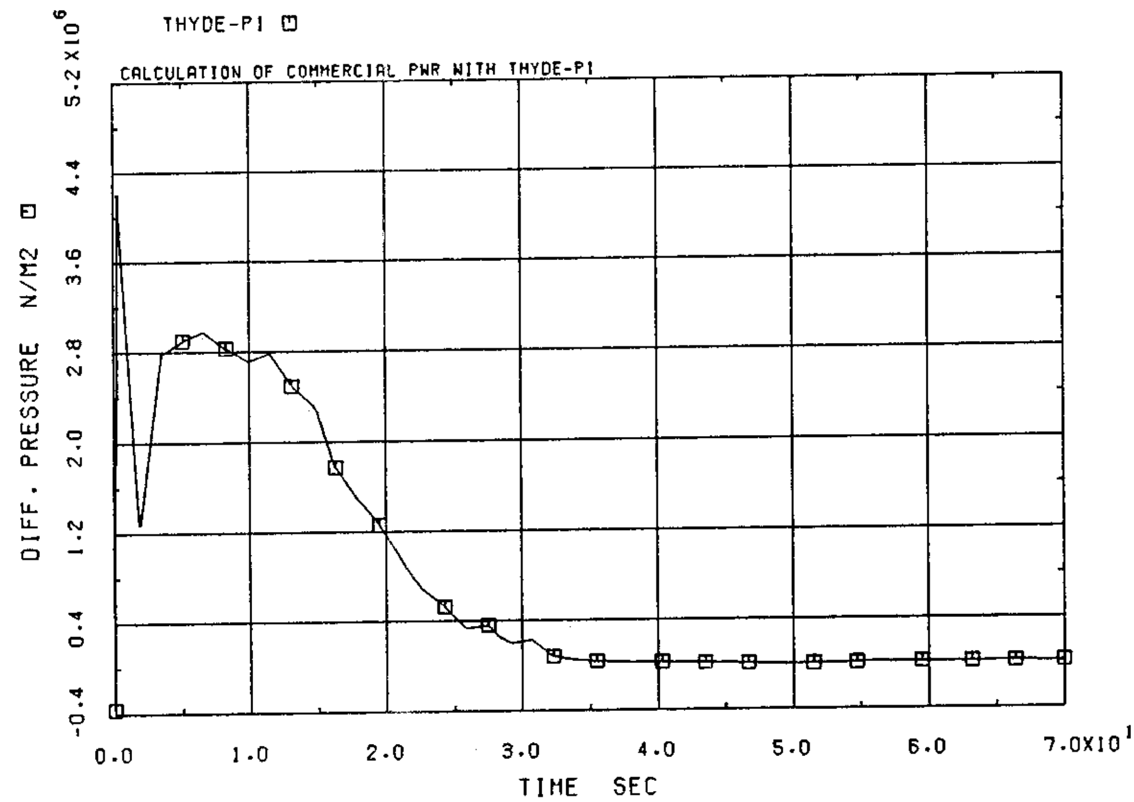

Fig.B-5-2 Differential pressure through broken loop (short range)

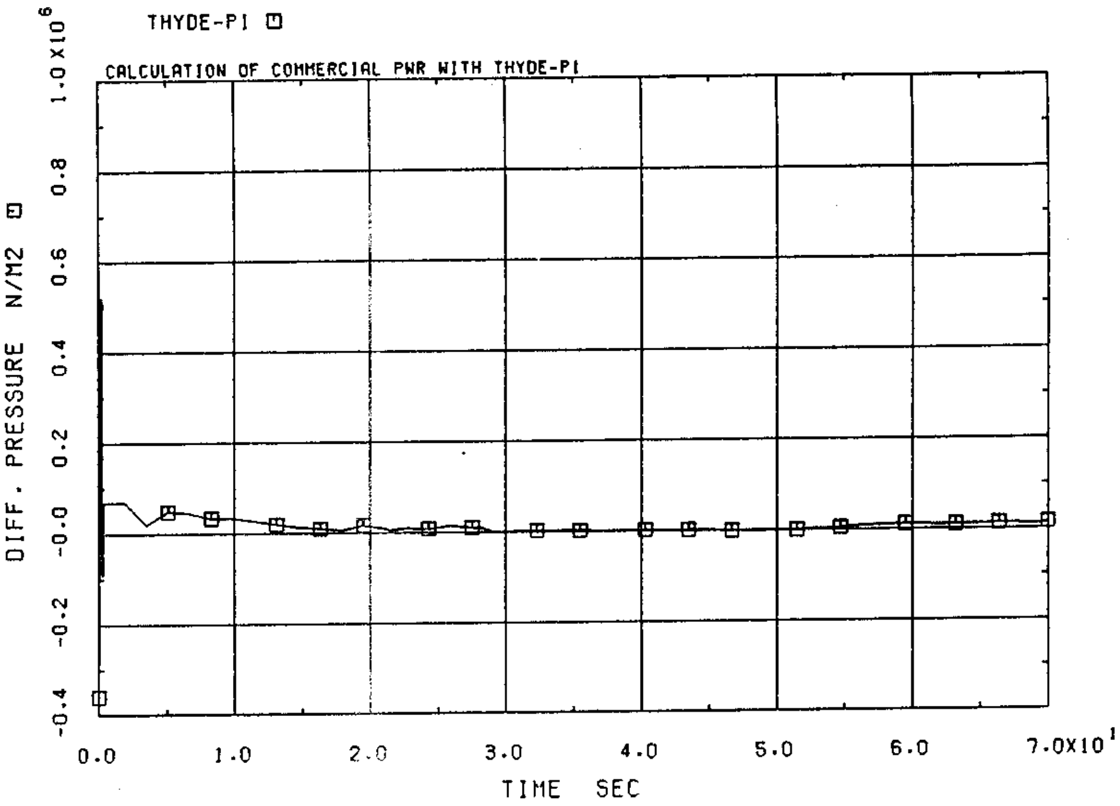

Fig.B-5-3 Differential pressure through intact loop (short range)

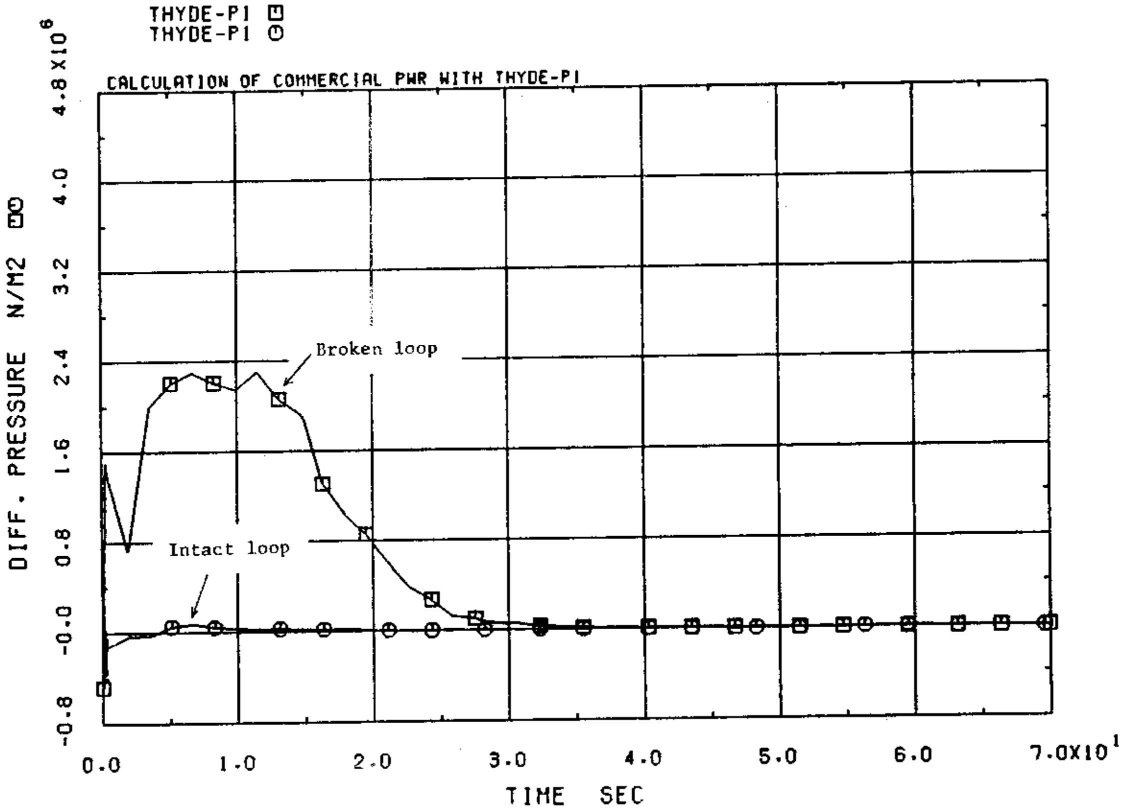

Fig.B-5-4 Differential pressures through pumps (short range)

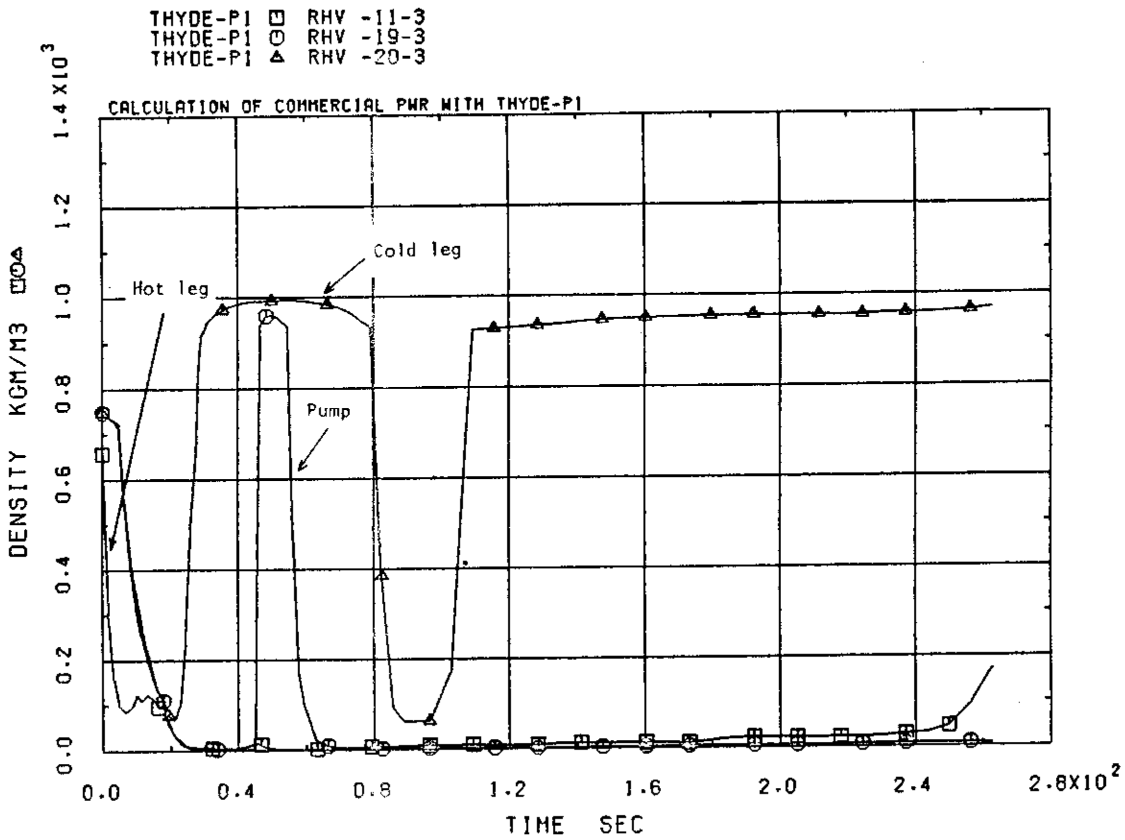

Fig.B-6-1 Equilibrium densities at intact loop

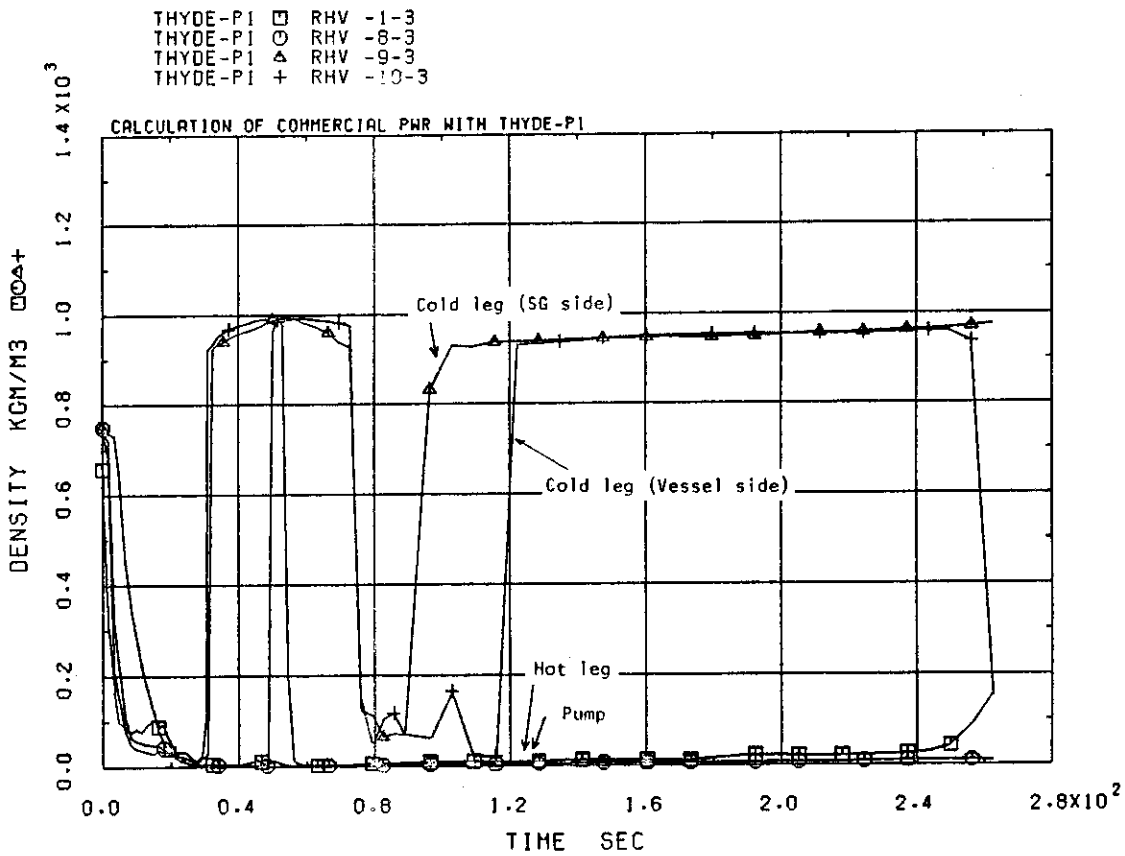

Fig.B-6-2 Equilibrium densities at broken loop

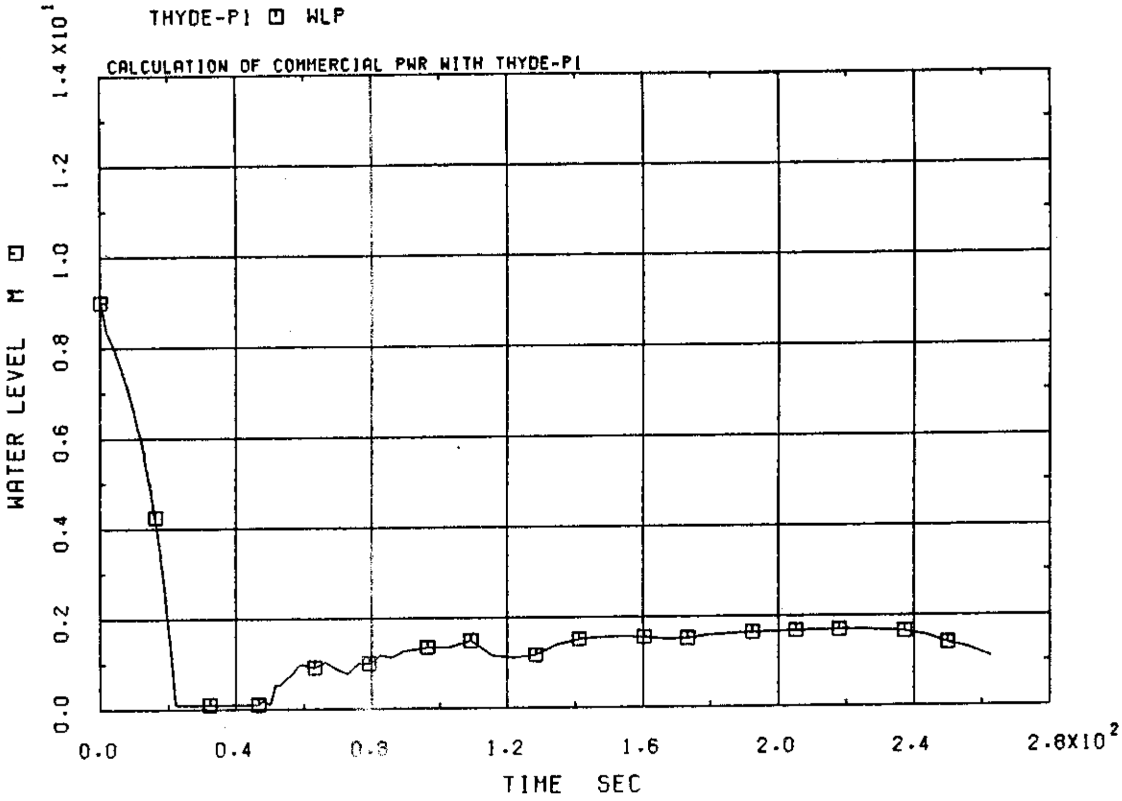

Fig.B-7-1 Pressurizer water level

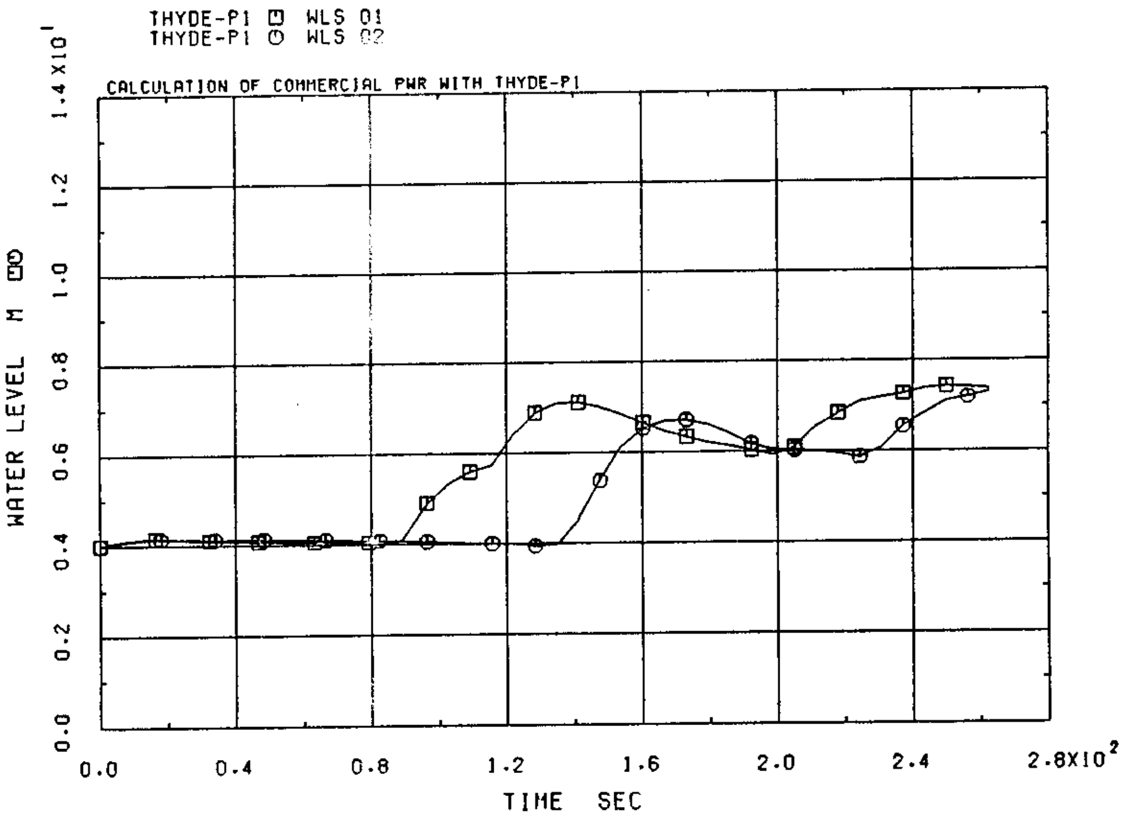

Fig.B-7-2 Water levels at SG secondary systems

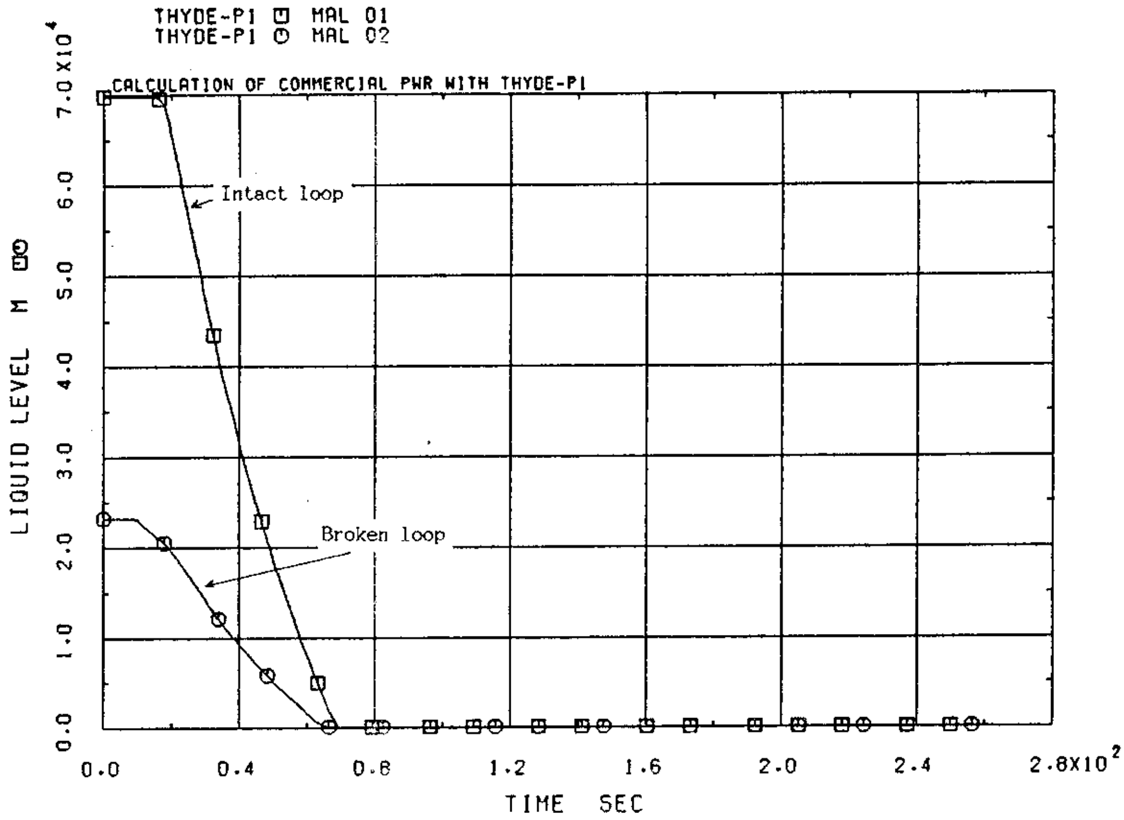

Fig.B-7-3 Accumulator water levels

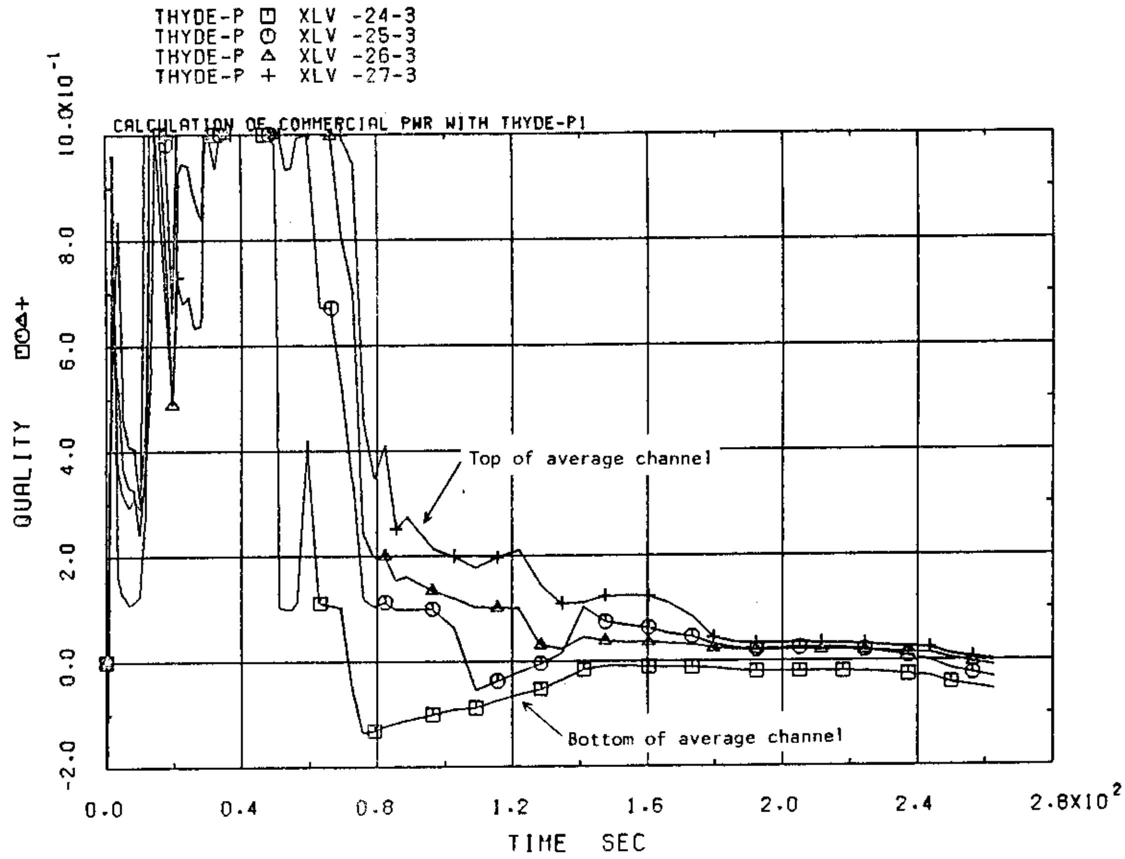

Fig.B-8-1 Equilibrium coolant qualities at average channel

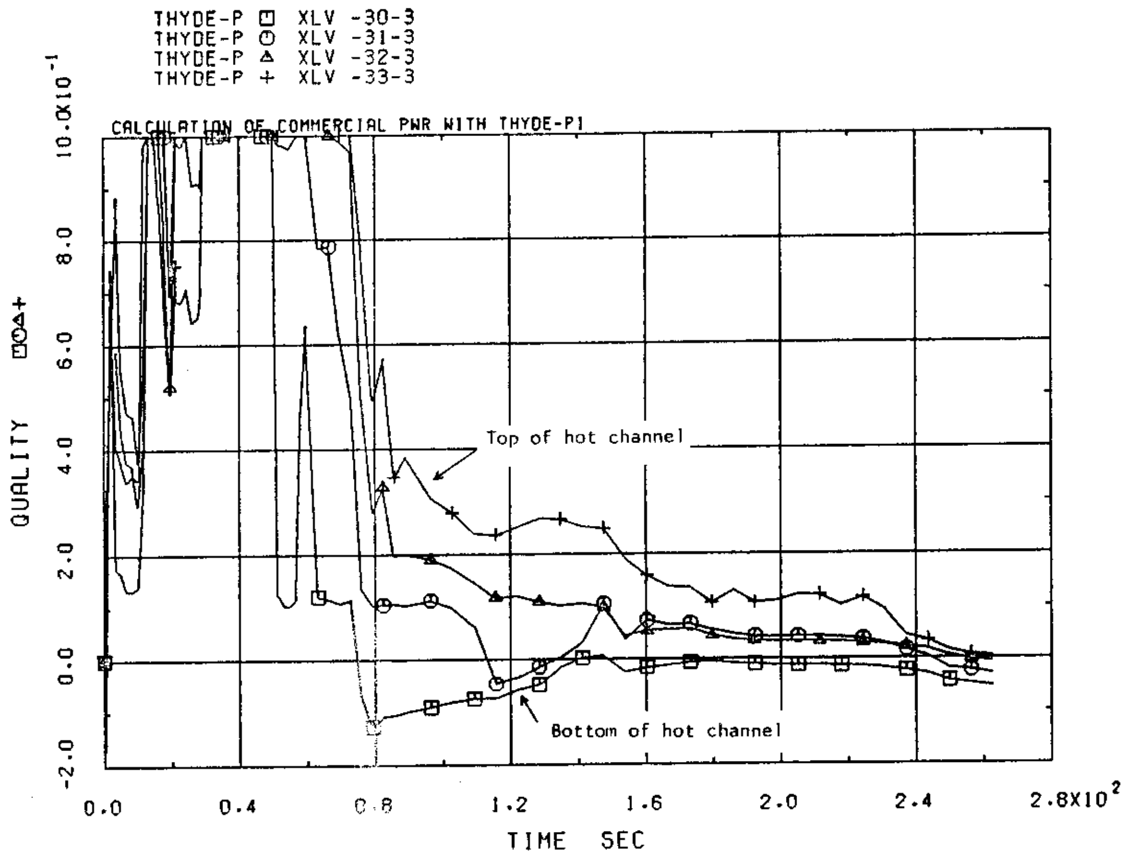

Fig.B-8-2 Equilibrium coolant qualities at hot channel

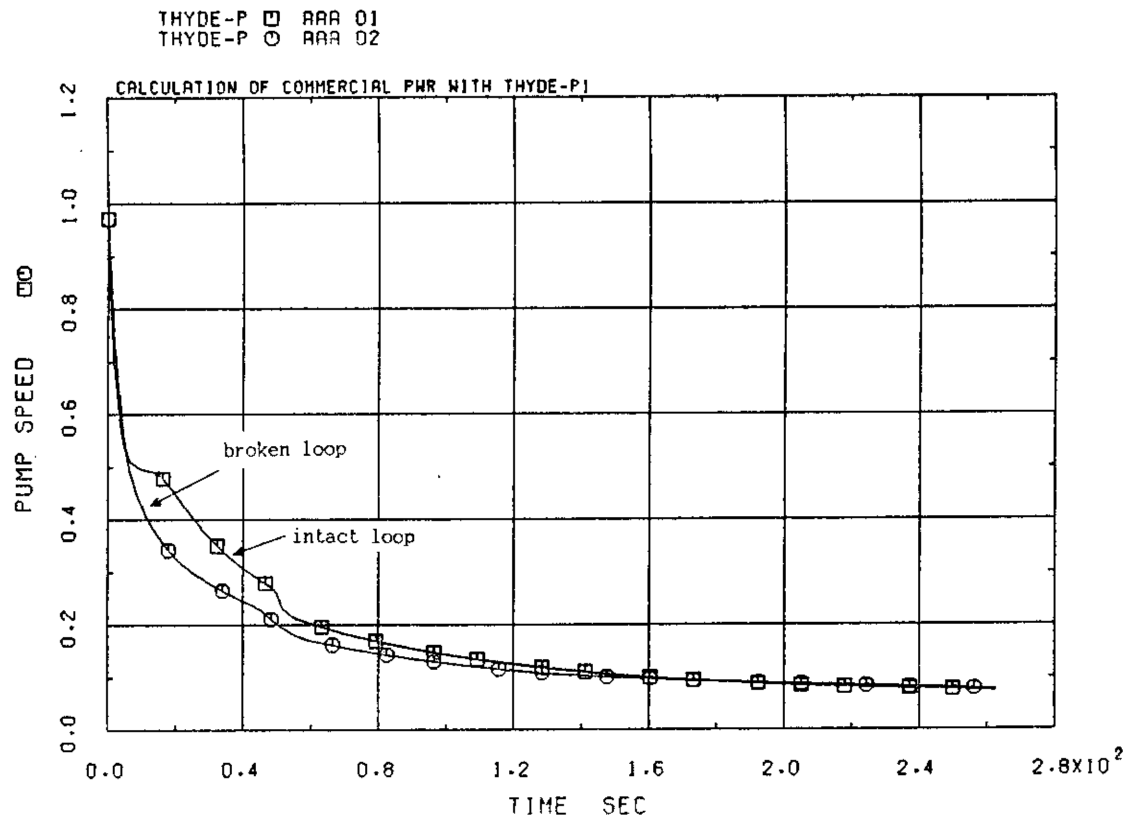

Fig.B-9-1 Normalized pump speeds

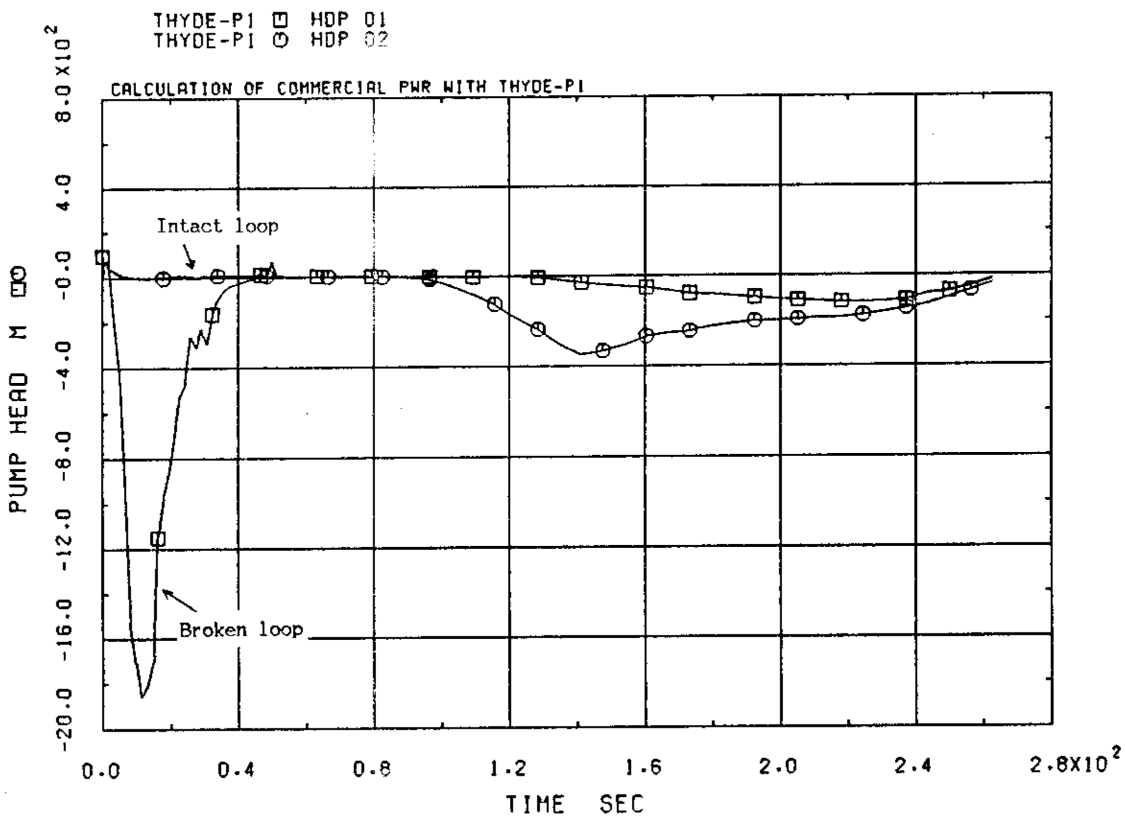

Fig.B-9-2 Pump heads

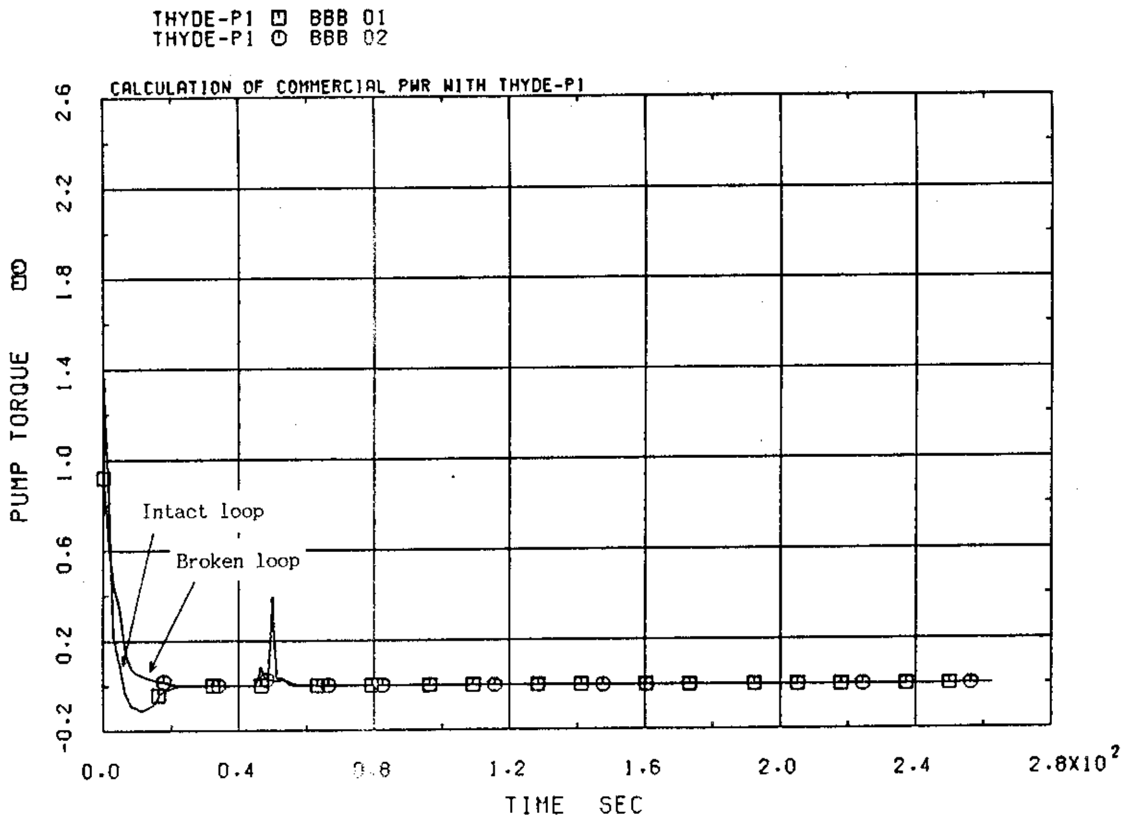

Fig.B-9-3 Normalized pump hydraulic torques

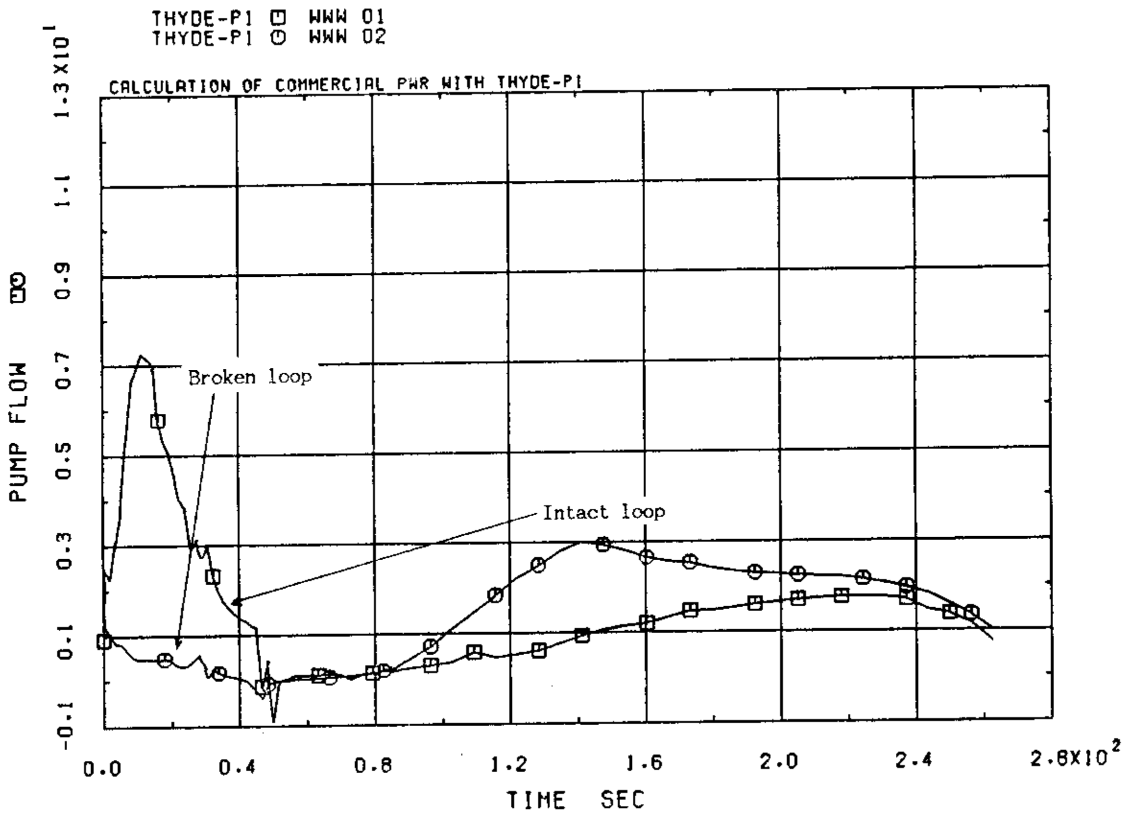

Fig.B-9-4 Normalized pump volumetric flows

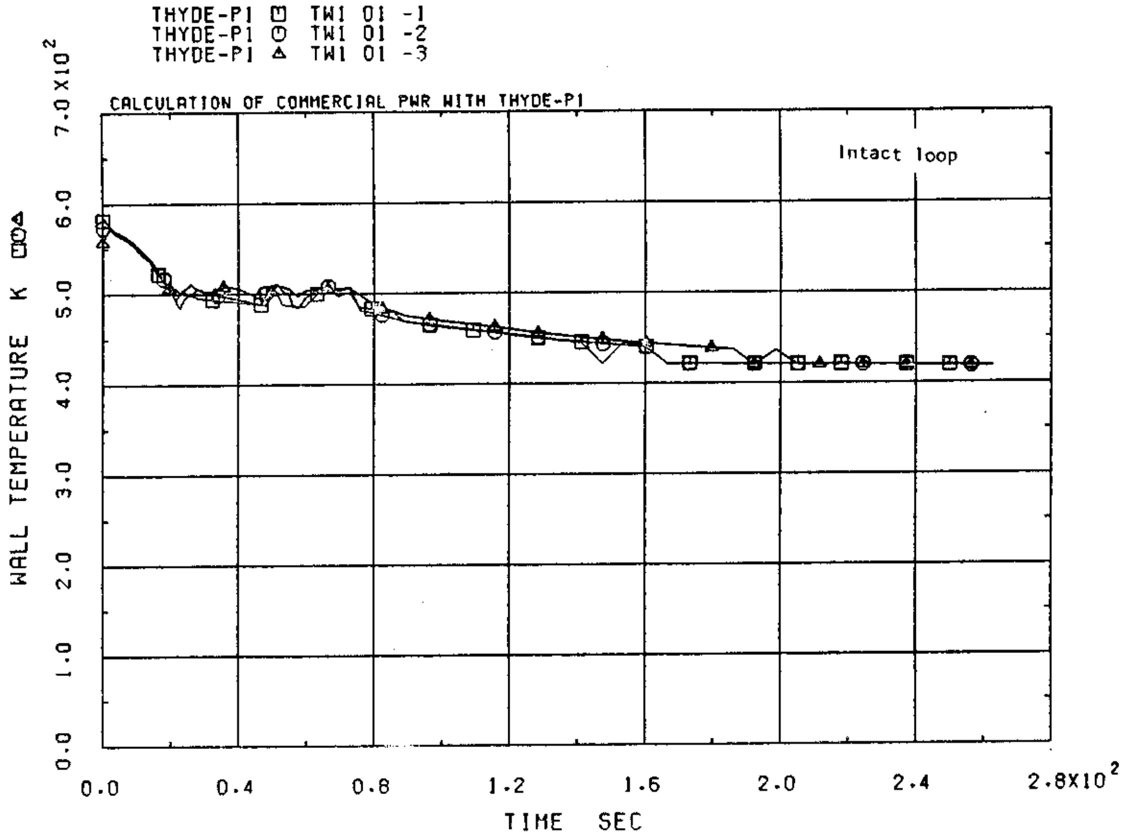

Fig.B-10-1 Wall temperatures at SG primary system of intact loop

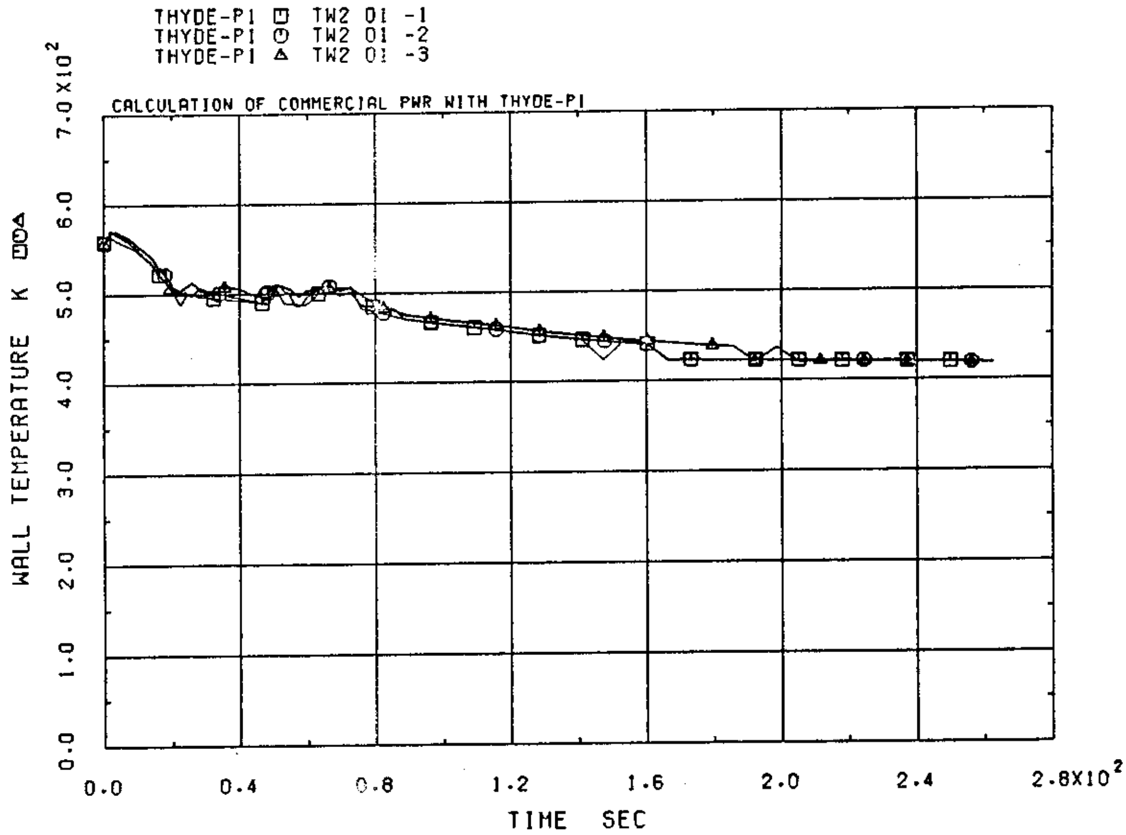

Fig.B-10-2 Wall temperatures at SG secondary system of intact loop

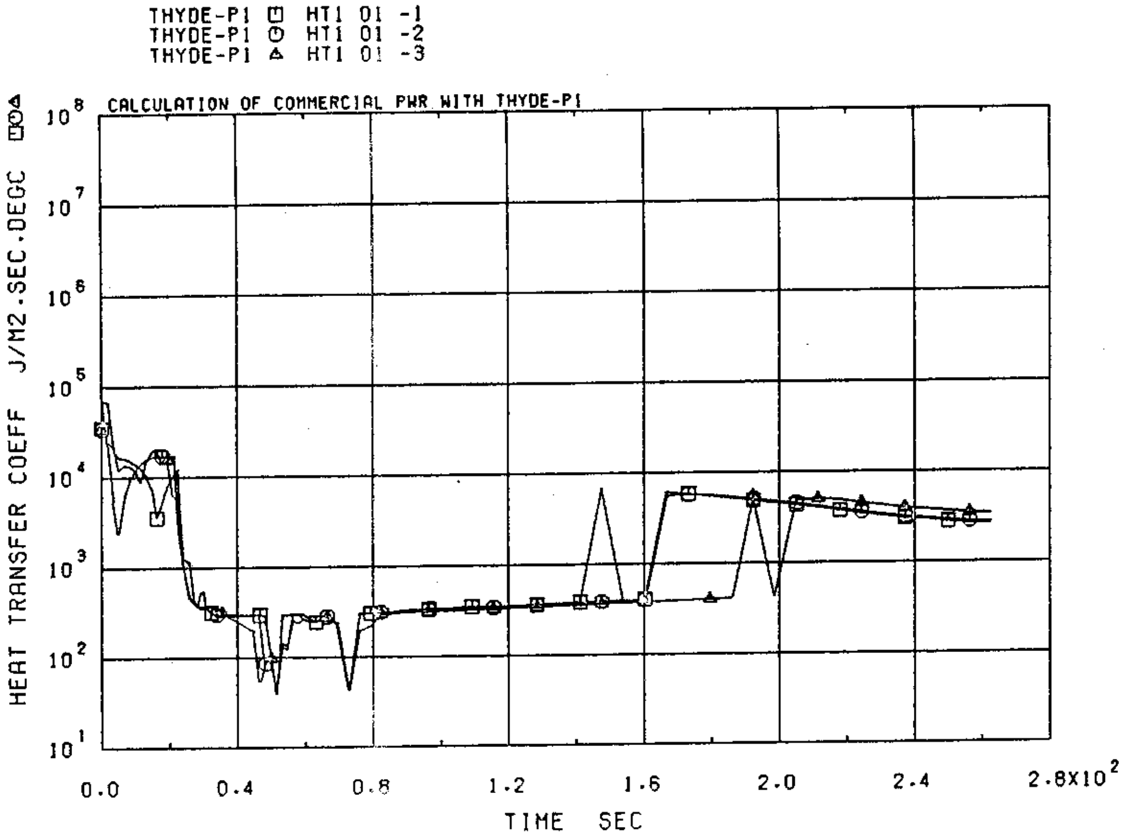

Fig.B-10-3 Heat transfer coefficients at SG primary system of intact loop

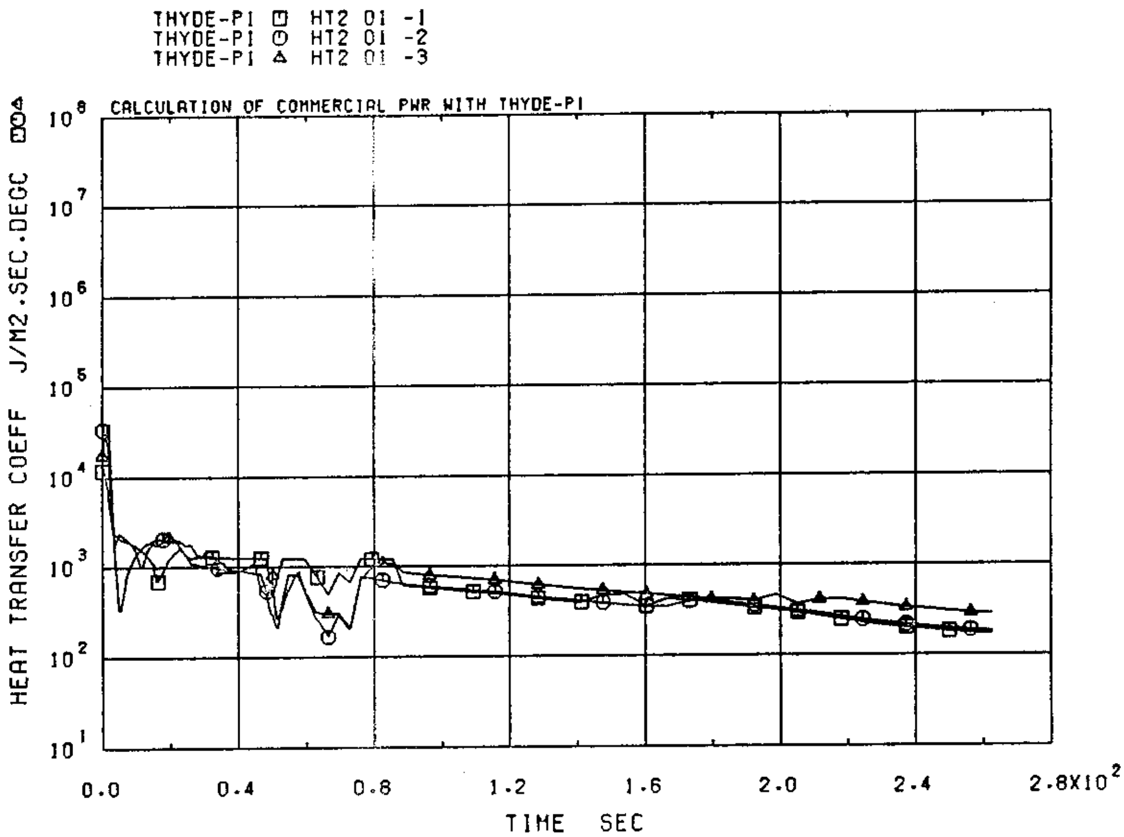

Fig.B-10-4 Heat transfer coefficients at SG secondary system of intact loop

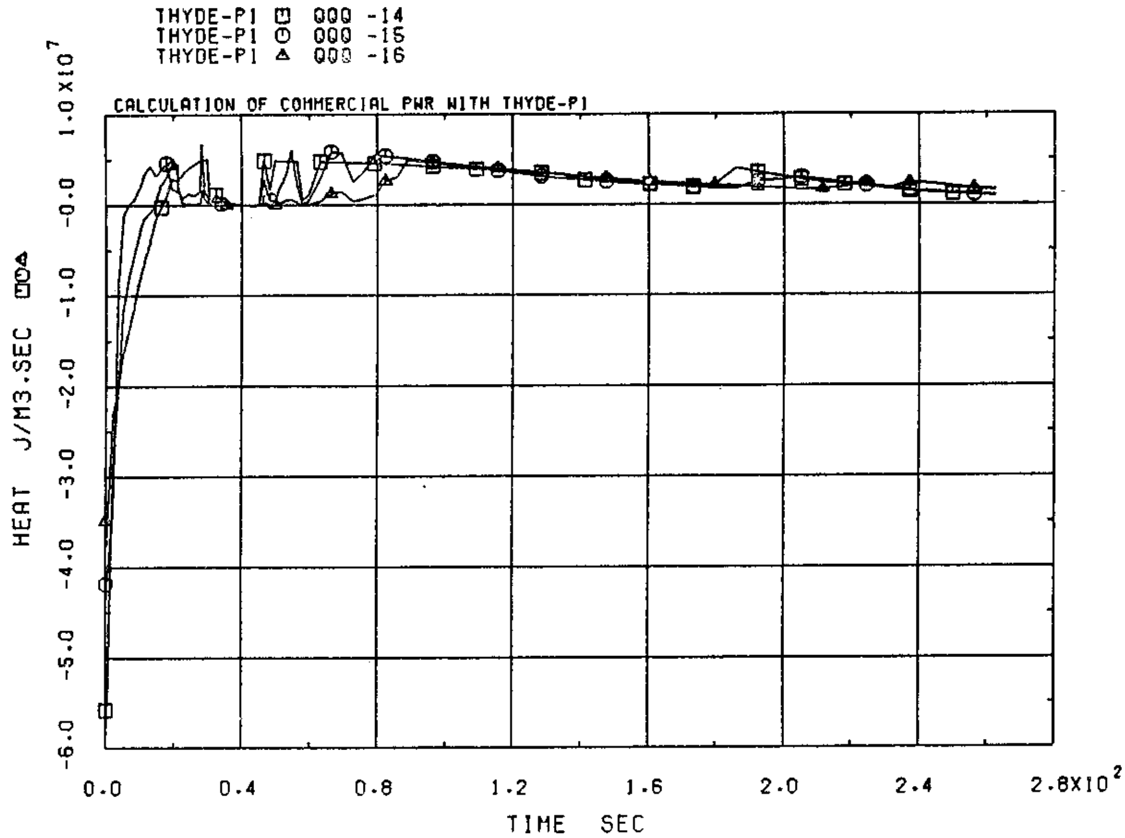

Fig.B-10-5 Heat inputs to coolant per unit volume at SG of intact loop

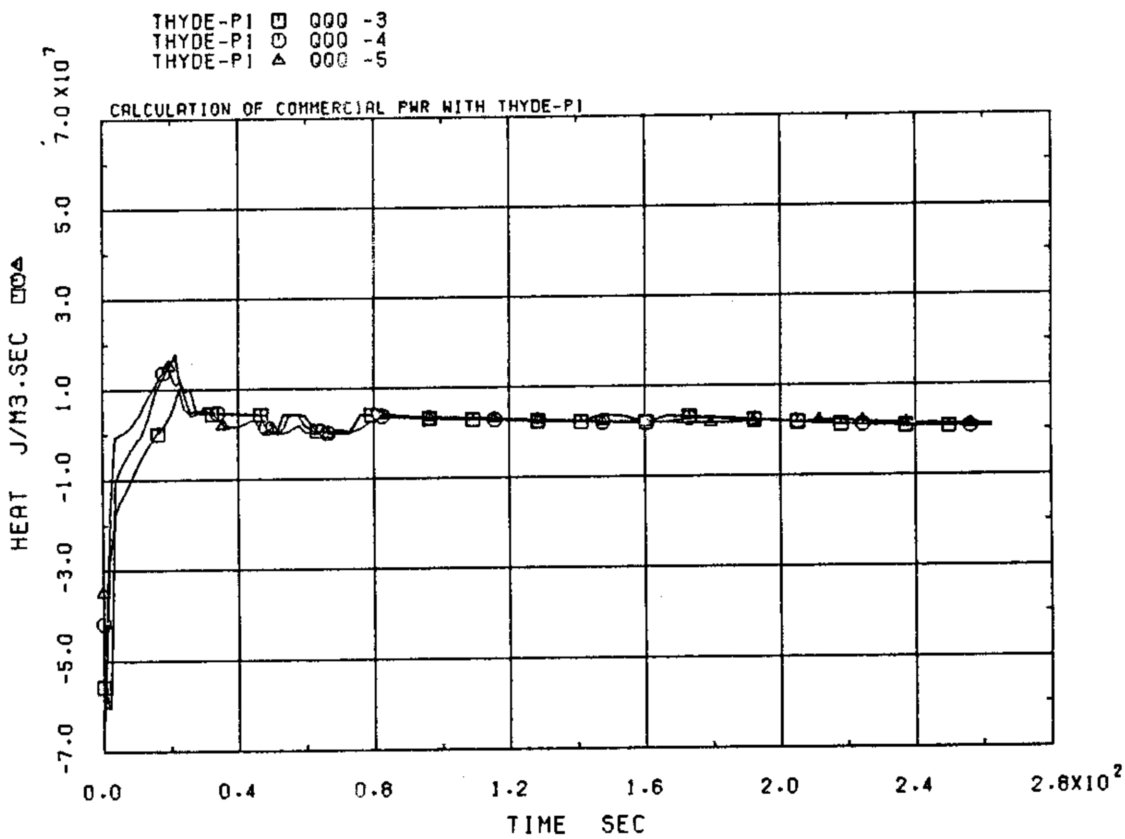

Fig.B-10-6 Heat inputs to coolant per unit volume at SG of broken loop